DOTTORATO DI RICERCA IN CHIMICA

Convenzione tra
UNIVERSITÀ DEGLI STUDI DI TRIESTE
e
UNIVERSITÀ CA' FOSCARI DI VENEZIA

CICLO XXX

Nanostructured electrochemical immunosensors for the identification of egg proteins: Immunoglobulin Y and Ovalbumin – application to cultural heritage and food analysis

Settore scientifico-disciplinare: **CHIM01 (Analytical chemistry)**

DOTTORANDA
Chiara Gaetani

COORDINATORE
Prof. Mauro Stener

SUPERVISORE DI TESI
Prof. Ligia Maria Moretto

CO-SUPERVISORE DI TESI
Prof. Paolo Ugo

ANNO ACCADEMICO 2016/2017

Riassunto

Nonostante i biosensori siano ampiamente utilizzati in diversi campi di ricerca e offrano numerosi vantaggi, quali alta selettività e sensibilità, bassi costi e velocità delle procedure, nel campo dei beni culturali sono stati introdotti solo di recente.

In questo progetto di dottorato sono stati messi a punto due immunosensori elettrochimici che hanno come *target* l'immunoglobulina Y (IgY) e l'ovalbumina (OVA), rispettivamente un anticorpo presente in alta concentrazione nel tuorlo e la principale proteina dell'albume. Per questo motivo, lo sviluppo di sensori in grado di determinare queste proteine consente di ottenere informazioni complete su campioni di dipinti a tempera con l'uovo come legante. Il trasduttore elettrochimico utilizzato per questi sensori è un *ensemble* di nanoelettrodi d'oro (NEE), preparati mediante deposizione electroless di oro nei pori di membrane nano porose *track-etched* di policarbonato. Per la conformazione specifica dei NEE, è possibile sfruttare la grande superficie di policarbonato per catturare le proteine *target*, senza necessità di modificare chimicamente la superficie dell'elettrodo.

In una prima fase del lavoro di tesi, sono stati ottimizzati alcuni parametri relativi alla preparazione ed all'impiego analitico dell'immunosensore per IgY in modo da migliorarne l'applicabilità nel campo dei beni culturali. La richiesta di una bassa quantità di campione è infatti un parametro chiave in questo settore d'indagine. Con questo obiettivo, l'area geometrica globale del sensore è stata ridotta a dimensioni sub-millimetriche ed è stato dimostrato che tale miniaturizzazione non diminuisce le prestazioni analitiche del sensore.

Successivamente l'immunosensore per l'OVA è stato sviluppato *ex-novo*. La procedura analitica è stata ottimizzata, concentrandosi in particolare sulla necessità di ridurre eventuali riconoscimenti nonspecifici di altre proteine. Le capacità di rivelazione del sensore sono state valutate in termini di sensibilità e selettività.

Entrambi i sensori sono stati utilizzati per il riconoscimento di tuorlo e albume in campioni pittorici, preparati appositamente sotto forma di *cross-section* che simulano la presenza di più strati pittorici sovrapposti. In particolare, tali strati erano costituiti da tempera preparate con uovo intero, con tuorlo, con albume eventualmente mescolate con pigmenti, olii siccativi o altri leganti quali colle di origine animale. La

sperimentazione dell'uso degli immunosensori elettrochimici sugli estratti, ottenuti mediante incubazione diretta sulle *cross-sections*, ha dimostrato con successo la possibilità di riconoscere le due proteine target (IgY e/o OVA) nella maggior parte dei campioni.

Con lo scopo di verificare la possibilità di estendere l'applicabilità dei sensori studiati anche ad altri campi d'indagine, si è infine studiata l'applicazione del sensore per IgY alla determinazione della presenza di tuorlo d'uovo in alimenti ed integratori alimentari di vario genere. I dati ottenuti col sensori elettrochimico in tali tipologie di campioni, sono risultati in buon accordo con quelli ricavati mediante analisi elettroforetiche, indicando peraltro una migliore sensibilità analitica del sensore nel caso di campioni contenenti piccole quantità di tuorlo d'uovo.

Abstract

Despite biosensors are widely used in many research fields and offer many advantages, as high selectivity and sensitivity, low costs and fast analytical procedures, they have been introduced in the cultural heritage field only recently.

In this PhD project, two electrochemical immunosensors were developed, with Immunoglobulin Y (IgY) and Ovalbumin (OVA) as the target proteins. IgY is an antibody present in high concentration in egg yolk, while OVA is the main protein in egg white. For these reasons, the development of sensors able to identify these proteins provides complete information about samples from tempera paintings with egg as the organic binder. The electrochemical transducer used for these sensors is an ensemble of gold nanoelectrodes, prepared by electroless deposition of gold in track-etched nanoporous polycarbonate membranes. Thanks to the specific conformation of the NEEs, it is possible to exploit the polycarbonate surface present in large amount to capture the target proteins avoiding the need of the chemical modification of the surface.

In a first phase of this project, some parameters of the IgY-immunosensing procedure were optimised, to improve the applicability of the sensor in the cultural heritage field. Indeed, low amount of samples is a key role parameter in this research field. To this aim, the geometric area of the sensor was reduced to sub-millimetre dimensions, and it has been proved that this miniaturization does not affect the analytical performance of the sensors.

Afterwards, the OVA immunosensor was developed *ex-novo.* The analytical procedure was optimised, focusing in particular on reducing eventual non-specific adsorption of other proteins. The performance of the OVA-immunosensors was evaluated in terms on sensibility and selectivity.

Both the IgY- and OVA-electrochemical immunosensors were applied in the identification of egg yolk and egg white in complex mock-up samples prepared as cross-sections that simulate multilayer painting. In particular, the layers were prepared with whole egg or egg components separately, in a mixture with pigments and other organic binders, as linseed oil or animal glues. Also in this case, the identification of the protein was successful. Measurements carried out on extracts obtained by direct incubation of the cross-sections, successfully demonstrated the ability of the electrochemical

immunosensors to identify the two target proteins (IgY and/or OVA) in most of the samples.

With the aim of extending the applicability of the sensors to other research fields the IgY-immunosensors was applied for the identification of egg yolk in food and food supplements. The results obtained with the electrochemical immunosensor on these particular kind of samples were compared with those obtained by electrophoretic and western blot analysis, indicating a higher sensitivity of the sensor when samples with small amount of egg yolk were analysed.

1_Introduction

Electrochemical immunosensors are interesting analytical tools able to detect a large range of analytes, providing many information and ensuring high specificity and sensitivity. Until now, this promising tool has been applied only in the last few years in the field of cultural heritage.

In this chapter, general information about egg-based tempera for the preparation of a piece of art will be provided; structures and main applications of immunoglobulin, IgY, and ovalbumin, OVA, (the target proteins of the developed immunosensors) will be analysed. Afterwards biosensors will be introduced, with particular attention to immunosensors and electrochemical biosensors and last, theoretical information about gold nanoelectrodes ensemble will be given.

1.1_Egg-based tempera paintings

Binding medium is one of the main constituent of paintings, with the important role to disperse pigments and other materials on a support. The medium must have specific ability to form a film that need to be elastic, adhesive and resistant, in order to be durable and stable against water and room conditions[1]. Artists from the past exploited foods with these characteristics. Eggs, both as the whole egg or in its components, satisfy these requests so they were widely used in Italy and Europe until the fifteenth century, before the introduction of oils. Other food products that were exploited in the past have a high concentration of proteins, such as milk or animal glues, or a high lipid content, as linseed oil[2].

Egg tendency to be a good binding medium is due to the dual composition of the dry yolk: it contains both proteins and lipids. Fast drying and resistance of the media are mainly due to lipids, that form cross-links between the polymeric chains; on the other hand, proteins denature because of the mechanical whipping of the components and loose of the water content by evaporation[1]. For temperas preparation, usually whole egg or egg yolk were used, sometimes in presence of oil (i.e. tempera *mista*), while egg white was less exploited due to the mainly proteinaceous composition that characterise more fragile films.

1.1.1_Analytical techniques in the identification of organic binders

Identification of the materials that constitute a piece of art is an important step to determine a restoration project or to define a conservation strategy. Many analytical techniques have been proposed during the last decades for the identification of the materials that make a piece of art. Fourier Transform Infrared (FTIR) technology is one of the first method introduced in the study of pigments and organic components in an artwork, commonly used since the '80s[3] and exploited also in the last years with some improvements in the detection strategy[4]. A non-invasive approach is provided by imaging techniques, such as multispectral UV/vis imaging[5] or UV/vis spectroscopy[6,7], but the specific distinction of the different organic components has not been optimised yet.

Chromatographic techniques were also exploited in the identification of proteinaceous binders, but they show the disadvantage of a long procedure for the samples preparation[8,9].

In the last decade a great improvement in the field of characterisation of organic materials was provided by the introduction of immunological and immunoenzymatic assays, especially for the specific identification of the different proteins used since the XV century[10]. These techniques offer the great advantage of being highly specific, thanks to the specific recognition of an antigen (Ag) by an antibody (Ab), moreover they are low cost, easy and fast. Among the available immunoenzymatic techniques, ELISA[10] and Dot-ELISA[11] were applied on a large range of mock-up samples.

1.2_Target proteins

Two target proteins were chosen, to provide complementary information about egg-based samples from an artwork or from food products. Immunoglobulin Y (IgY) is an antibody present in egg yolk, while ovalbumin (OVA) is the main protein of egg white. Briefly we report the composition of eggs, that are manly composed by water, present in both its component. Yolk is characterised by a dual composition, lipid and proteins in different concentrations. Egg white is manly constituted by proteins. The general composition of egg is summarized in Tab. 1.1[12].

Tab 1.1: Egg yolk and egg white composition.

	Fresh yolk (%)	**Dry yolk (%)**	**Fresh white (%)**	**Dry white (%)**
Water	50	-	87.6	-
Lipids	35	62.5	/	/
Proteins	14	33.0	10.9	89
Carbohydrates	0.6	1.2	0.7	5.7
Minerals	1.7	3.5	0.8	6.3

1.2.1_ Immunoglobulin Y - IgY

Immunoglobulin Y (IgY) is a glycoprotein, part of water-soluble livetin, present in egg yolk[12]. There are three different livetins and each of them corresponds to a protein of hen serum: α to albumin, β to α-2-glycoprotein and γ to gamma globulins. IgY is the dominant fraction of the γ-livetins; these livetins are present in egg yolk with the following proportion, 2:5:3, respectively[13].

IgY function is similar to mammalian IgG to provide protection to the chicks by antibody transfer from maternal blood to early egg yolk. Concerning the structure, IgY is more similar to mammalian IgE, since the Hinge region is not present in its molecular structure[14]. IgY is composed of two heavy chains (Mw = 65.105 Da) and two light chains (Mw = 18.660 Da), resulting in a molecular weight of around 167.250 Da.

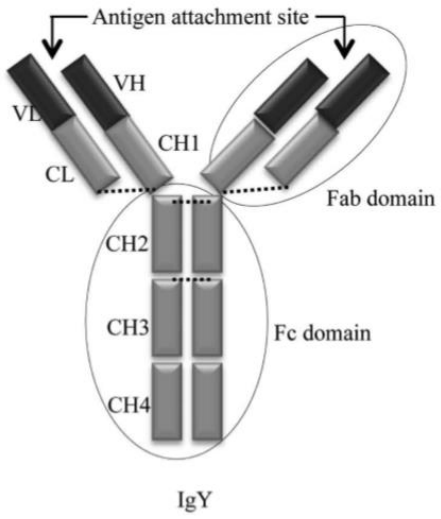

Fig 1.1: Molecular structure of IgY[15].

The concentration of the antibody in hen blood serum is 5–15 mg/mL while in egg yolk is 10–25 mg/mL; for this high concentration and for its complete absence in egg white, IgY is well representative of egg yolk[16]. Recently, it has been demonstrated that IgY has useful applications in many research and application fields. Among them, the most promising use of IgY is in immunotherapy[15,17,18]; for example, IgY can protect humans and mammalians against diseases caused by virus or bacteria attacks. Moreover, isolation of IgY from egg yolk has been widely investigated and its production is economically more advantageous compared to immunoglobulins isolation from

mammalians[14,16]. IgY from hen egg yolk is a great resource in the field of primary and secondary antibodies research and development, especially because the cross-reactivity with mammalian complement system is very low or totally absent.

1.2.2_Ovalbumin - OVA

Ovalbumin (OVA) is the main protein of egg white and represents the 55% of the protein content[12]. OVA is a glycoprotein with a molecular weight is 45 kDa; on the base of its structure, ovalbumin is considered as a serpin (serine proteinase inhibitor), although its real function is still unknown[19]. It is often present in standard solutions for electrophoresis.

Together with lysozyme, ovotransferrin and ovomucin, they represent the 80% of the egg white composition and are the main cause of egg allergies[20]. Due to this property ovalbumin was investigated in food products and egg derivatives, such as pasta[21] or ice-cream and cheese[22].

1.3_Biosensors

IUPAC (International Union of Pure and Applied Chemistry) defines a chemical sensor as a "device that transforms chemical information, ranging from the concentration of a specific sample component to total composition analysis, into an analytically useful signal"[23,24]. The structure of a sensor is shown in Fig. 1.2; sensors are made by two elements: a chemical (molecular) recognition system (Fig. 1.2 – bioelement), called receptor, in direct special contact with a physicochemical transducer (Fig. 1.2 – transducer). If the recognition system of the sensor is based on a biochemical mechanism, then the sensor is named a biosensor (Fig. 1.2).

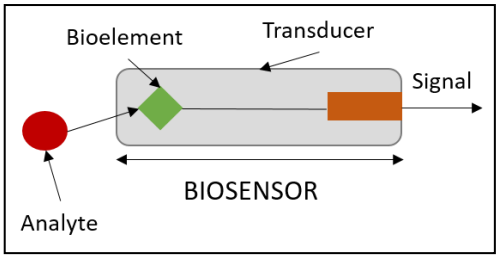

Fig 1.2: Basic scheme of a biosensor.

Biosensors can be classified on the base of the bioreceptors or according to the transducers. The bioreceptor is the part of the device that interacts specifically with the target analyte. In the case where the biomolecule in contact with the transducer is an enzyme, the biosensors are defined catalytic or enzymatic biosensors, while, if the biomolecule is an antigen-antibody complex the biosensors are classified as affinity biosensors. Other affinity biosensors can be based on DNA target recognised by a complementary probe.

It is important to stress that the bioreceptor, or the recognition system between the bioreceptor and the analyte, must be immobilized on the transducer. The interaction between the bioreceptor and the analyte is then transformed through the transducer to a measurable signal. Typical transducing elements are electrochemical, optical[25], piezoelectric[26], thermometric[27], magnetic and acoustic[28].

Nowadays, the most common and successful biosensors are employed in the measurement of glucose in samples[29–31] and many commercial-kits are available. Nevertheless, biosensors find application in many fields[32,33], such as clinical diagnosis[34], food control[35,36] or environmental screening[37,38]. In the last two decades, biosensor technology had a great implement compared to other traditional techniques, mainly because they can ensure fast measurements, low costs and easy equipment. Moreover, biosensors satisfy the following prerequisites[35]:

- Selectivity: the biosensor needs to be highly selective only for the target analyte and show minimum or no cross reactivity with similar compounds or biomolecules;
- Sensitivity: the biosensor should be able to measure in a large range of concentration;
- Linearity of response: the biosensors should ensure a wide linear response in the concentration range of the target analyte;
- Reproducibility of signal response: this is a crucial parameter, when samples with the same concentrations are analysed many times, the biosensors should give the same response.

1.3.1_Immunosensors

Affinity biosensors with the recognition system based on immunochemical reactions, as antigen-antibody interactions, are also called immunosensors[23]. Antibodies are complex biomolecules that fits uniquely one antigen, thanks to their strictly ordered and precise structures. Richard J. Goldberg first introduced the antigen-antibody concept in 1952[39]: an antigen, that is usually a protein, is specifically recognized by one antibody, forming the antigen-antibody complex (Fig. 1.3).

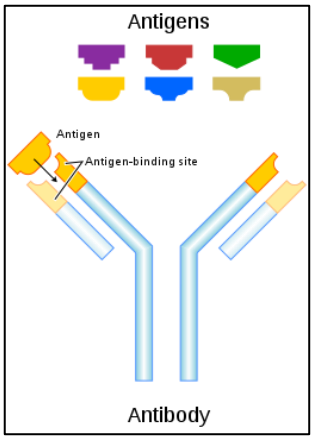

Fig 1.3: Antigen-antibody complex.

The antigen-antibody complex represents the biorecognition system, which needs to be recognised to have an analytically useful signal. To this aim, two kinds of immunosensor can be distinguished: labelled or label free. In case of a label free immunosensor, the analyte immobilised on the transducer is characterised by a detectable properties. Typical techniques exploited for label-free affinity biosensors are surface plasmon resonance[40] or impedance spectroscopy[41].

More often, a label is necessary to detect the formation of the biocomplex. One of the most common methods is represented by the addition of a complementary biocatalytic reaction to the system promoted by an enzyme. Usually the enzyme is labelled to the secondary antibody. The main advantage of using a label is the improvement of the sensitivity of the sensor, even if more steps are required during the analytical procedure[42]. Labelled immunosensors usually operate at the equilibrium and the enzymatic activity is there only to identify the amount of complex produced. These

systems are usually irreversible and can be used only once. Typical techniques exploited for this kind of immunosensors are electrochemical[43].

1.3.2_Electrochemical biosensors

"An electrochemical biosensor is a self-contained integrated device, which is capable of providing specific quantitative or semi-quantitative analytical information using a biological recognition element (biochemical receptor) which is retained in direct spatial contact with an electrochemical transduction element[23]". The distinguish point is the transduction element, that in the case of electrochemical biosensor is an electrode.

The first electrochemical biosensor is dated to 1962, when Clark[44] developed the first device able to detect glucose in blood, with GOx entrapped in a Clark oxygen electrode using dialysis membrane. Biosensors that detect directly the substrate or the product of the enzymatic reaction (as shown in Fig. 1.4A) are considered as first generation biosensors[45]. Some lacks in these detection strategies were supplied with the introduction of a redox mediator in the system[46]. The mediator is required to shuttle electrons between the electrode and the enzyme-substrate complex, as shown in Fig. 1.4B. Typical mediators must react rapidly with the enzyme, have good electrochemical properties and must facilitate the electrons exchange. Molecules that satisfy these requirements and that are widely used in this application are ferrocene derivatives. Biosensors that use mediator are called second generation biosensors. Cyclic voltammetry (CV) is a versatile electrochemical technique that can be exploited for investigation of electrocatalytic systems. In case of a second generation biosensor, when a redox mediator is co-present in the system with the enzyme-substrate complex, CV is often used to study the catalytic reactions and to extract kinetic information, thanks to the development of an electrocatalytic cycle[47,48]. The electrocatalytic cycle generated by the coupling of horseradish peroxidase and hydrogen peroxide as its relevant substrate, and glucose oxidase for the detection of glucose will be extensively described in chapters two and three.

In the third generation biosensors introduced recently, the redox mediator is removed from the system and the electron transfer occurs directly between the protein

and the electrode. Usually the enzyme is directly immobilised on the electrode surface to improve the electron transfer (Fig. 1.4C).

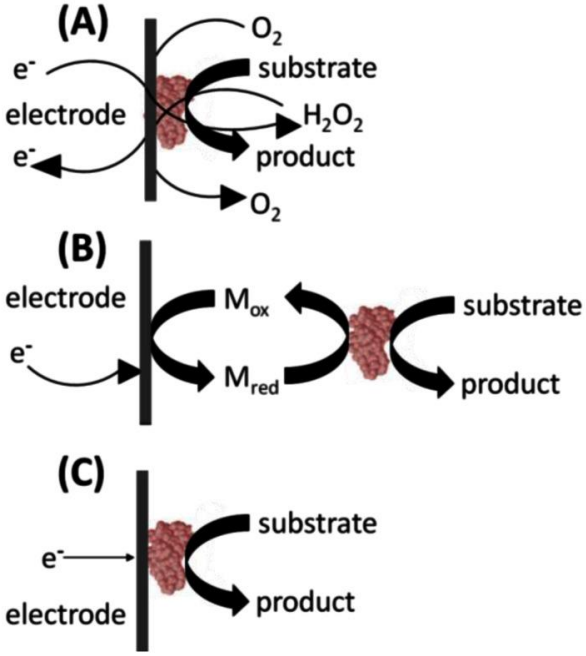

Fig 1.4: Representation of the three generations of electrochemical biosensors: A) first, B) second; C) third generation biosensors[46].

1.4_Nanoelectrodes ensembles

1.4.1_Theoterical approach

In this research, the electrochemical transduction element is represented by an ensemble of gold nanoelectrodes (NEEs). Menon and Martin first developed this electrochemical device in the Colorado State University[49] in 1995; starting from the late 1990s the LSE (Ca' Foscari – Venice) research group guided by Paolo Ugo, acquired this technology widening the application fields[36,50].

An ensemble of nanoelectrodes is an aggregation of nano-sized electrodes randomly disposed on a non-conductive matrix. They are usually obtained by growing nanowires of a conductive material inside the pores of a nanoporous membrane. In this project, the gold nanoelectrodes employed are prepared via electroless deposition of

gold in a nanoporous polycarbonate (PC – Fig1.5) track-etched membrane wetted in polyvinylpyrrolidone.

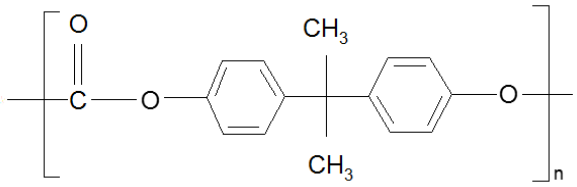

Fig 1.5: Molecular structure of polycarbonate

These electrodes have many advantages compared to bulk electrodes regarding both the electrochemical specificities and the applicability. The main advantage of using NEEs instead of a bulk electrode is related to the diffusive regime that they show performing voltammetric measurements[51]. Depending on the distance between the superficial nanodisks and the scan rate set during the measurements (two parameters that can be controlled and optimised), NEEs can operate in three different diffusional regimes: linear, pure radial and total overlap. Preferably, these parameters are adjusted so that the NEE operate in a total overlap diffusive regime, which allows a high signal to noise ratio that permits to detect analytes in a very low concentration. The total overlap regime occurs when the radius of the diffusion hemispheres is larger than the average hemidistance between the superficial nanodisks (Fig. 1.6) and the scan rate is low.

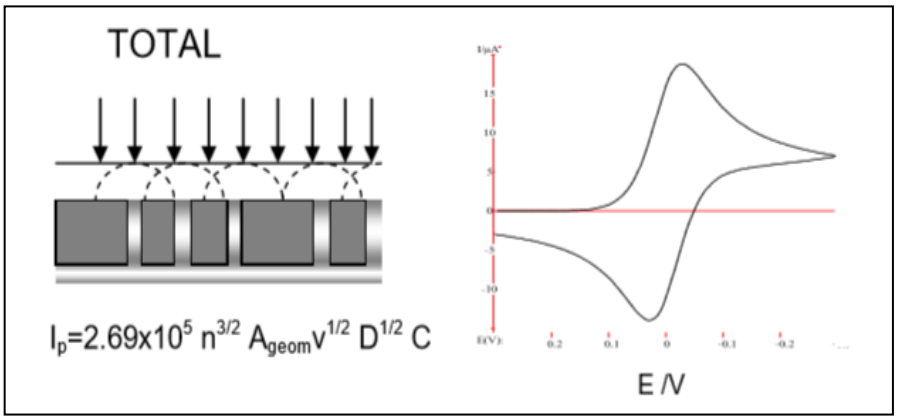

Fig 1.6: Schematic representation of the total overlap diffusive regime.

To show the advantages achieved when NEEs operate in a total overlap diffusive regime, it is necessary to introduce few parameters:

- Total geometric area (A_{geom}): overall area of the electrode, composed by the gold nanodisks and the PC area. This value is decided by the operator during the electrodes assembly, usually goes from 0.008 to 0.580 cm^2 and the surface is circular;
- Active area (A_{act}): summation area of all the gold nanodisks (nanoelectrodes) present on the surface of the electrodes. It is calculated considering the pores density (ρ), the average radius of the pores (r), and the geometric area. The following equation defines A_{act}:

$$A_{act} = \pi r^2 \rho A_{geom} \quad (1)$$

- Fractional electrode area (f): the ratio between A_{act} and A_{geom}:

$$f = \frac{A_{act}}{A_{geom}} \quad (2)$$

The fractional area can also be defined as by Eq. 3, substituting the parameters from Eq.):

$$f = \pi r^2 \rho \quad (3)$$

In the case of a reversible redox system, when NEEs operate in the total overlap diffusional regime, the values of the faradaic peak current (i_F) follows the Randles–Sevcik equation:

$$i_F = 2.69 * 10^5 n^{3/2} A_{geom} D^{1/2} C v^{1/2} \quad (4)$$

i_p is the peak current expressed in Ampere; A_{geom} is the geometric area of the ensemble (cm^2); D is the diffusion coefficient (cm^2/s); C is the concentration of the redox species in bulk, expressed in mol/cm^3; v is the scan rate (V/s).

The double-layer charging current (i_C) is proportional to the active area (Eq. 3) as expressed in Eq. 5:

$$i_C = v C_{dl} A_{act} \quad (5)$$

C_{dl} is the double-layer capacitance of the metal nanodisks of the NEE.

Faradaic-to-capacitive current ratios at NEEs and conventional electrodes with the same geometric area are related by the following equation:

$$\frac{i_F}{i_C} = \left(\frac{i_F}{i_C}\right)_{conv} * \left(\frac{A_{geom}}{A_{act}}\right) \quad (6)$$

This ratio is higher at NEEs than at conventional electrodes by a factor that is the reciprocal of the fractional area (eq 2). At conventional electrodes, where the geometric area coincides with the active area, the faradic current and the capacitive currents depend both on the same parameter. This behaviour is different at NEEs, since the faradic current (signal) is proportional to the geometric area, while the capacitive current of the double layer (background) is proportional to the active area. At NEES the signal (I_F) to background (i_C) ratio can be 2–3 orders of magnitude higher than the ratio at conventional electrodes with the same geometric area. For this reason, detection limits at NEEs are 2–3 orders of magnitude lower than at regular electrodes. This allows to detect elements in trace and to analyse samples with the analyte in a very low concentration.

1.4.2_NEE-based electrochemical immunosensors

In this thesis, ensembles of gold nanoelectrodes (NEEs) are used as the transducer of the immunosensors. NEEs have a dual superficial composition; indeed, gold nanodisks are randomly disposed in a polycarbonate membrane. NEEs offer a good performance as transducer thanks to both its electrochemical behaviour (related to the geometric distribution of the gold nanodisks) and the ability to receive biomolecules (promoted by the superficial PC). The affinity between PC and biomolecules was studied mainly by Henry both in the case of a native PC membrane and in presence of an hydrophilic agent such as polyvinylpyrrolidone[52], demonstrating that the presence of PVP slightly reduces the affinity between the biomolecules and the treated surface[53] (see 2.1.1). Nevertheless, the polycarbonate surface permits biomolecules, such as proteins, to bind the polycarbonate with a stable bound. This property is useful in the field of biosensors because it avoids at least one step in the procedure, that is the

modification of the surface of the electrodes to make it suitable to receive biomolecules.

NEEs were used as platform for biosensors for the first time in 2008 by Ugo's group[54] to identify HER2. After this successful first study, the strategy was proposed also in further applications, such as biosensors for detection of DNA hybridization [55] or, more recently, for the diagnosis of celiac disease[56].

1.5_Aim of the thesis

Biosensors have been introduced in the cultural heritage field only recently. Aim of the thesis was to apply these promising devices in the recognition of proteins from pieces of art, such as egg-based temperas. Immunoenzymatic assays are nowadays commonly used for the identification of biomolecules from artworks, thanks to their selectivity and easy procedures. Electrochemical immunosensors can ensure the selectivity and sensitivity typical of the immunoenzymatic tests, but offering more advantages, such as fast procedures and low costs; moreover, they are simple to handle and assure a good reproducibility of the results.

For these reasons, we have studied two electrochemical immunosensors able to identify egg yolk and egg white, respectively, eventually present as binder in tempera paintings. To this aim, the two sensors have been developed in order to detect specifically: immunoglobulin Y (IgY) from egg yolk and ovalbumin (OVA) from egg white.

The final goal is to provide an analytical tool able to detect the two pictorial binders from samples simulating the different layers of a painting. With the detection of these two biomolecules, valuable information on tempera samples can be obtained, concerning the pictorial technique used, the authenticity of the paint a well as the best methods to be applied for restoration and conservation issues.

With this thesis, we aim to introduce in the cultural heritage field innovative analytical tools with all its advantages. To make the procedure fast and achieve the best results, we used gold nanoelectrodes ensemble that provides high sensitivity and good analytical performances. Note that nanoelectrodes ensembles are more affine to biomaterials than bulk gold or carbon electrodes, and for this reason the immobilization of the biomolecules on the electrochemical transducer is faster and easier.

2_IgY immunosensor

Small amount of sample is a key point in many analytical techniques and defines the applicability of the proposed methods in specific research fields, such as cultural heritage. Among the available analytical techniques, electrochemistry offers the possibility to vary many parameters and allows strong optimisations of the procedures. First goal of this thesis was to optimise the analytical procedure of an electrochemical immunosensor based on gold nanoelectrodes ensemble (NEEs) with egg yolk IgY as the target protein, previously developed in the research group where this work of thesis was carried out. To this aim, the geometric area of the electrode-platform used to capture the analyte was minimised compared to the conventional dimensions previously used. The decrease of this parameter should not affect negatively the performance and should maintain high sensitivity and well resolved results. An ensemble of gold nanoelectrodes is used as platform for the immunosensor and its behaviour with different geometric area is investigated in this chapter, both with direct electrochemistry of two electroactive species with a well-known voltammetric behaviour, and either with the application of the mini-NEEs obtained as platform for the IgY-electrochemical immunosensor. A comparison with gold conventional electrodes is also carried out.

After the optimisation of the procedure, the IgY-electrochemical immunosensor was applied to identify the protein in egg yolk in different pH conditions.

2.1_Nanoelectrodes ensemble preparation

2.1.1_Experimentals

Polycarbonate membrane SPI-PORE (6 µm thick, nominal pore dimension of 30 nm, pore density $6*10^8$ pore/cm^2; the membranes are covered with a thin film of polyvinylpyrrolidone (PVP) to increase the hydrophilicity), $Na_3[Au(SO_3)_2]$ was a commercial gold electroless plating solution Oromerse Part B, Technic Inc. All other reagents $SnCl_2$, trifluoroacetic acid (TFA), $AgNO_3$, NH_4, methanol (MeOH) and CH_2O were of analytical grade and used as received. All solutions were prepared in MilliQ water.

SEM measurements were carried out in a TM3000 Hitachi table top scanning electron microscope coupled with a Swift ED3000 X-ray microanalysis system.

Electrochemical characterization of NEEs was studied in a conventional three electrodes cell, platinum wire as counter electrode, Ag/AgCl (KCl saturated) as reference electrode and NEEs as working electrodes. CHI1000a instrument was used for cyclic voltammetry measurements. Two electroactive molecules with a well known redox behaviour were used to test the electrochemical behaviour of the NEEs: (ferrocenylmethyl)trimethylammonium hexafluorophosphate ($FA^+PF_6^-$) and methylene blue (MB). The molecular structures of the probes are shown in Fig. 2.1.

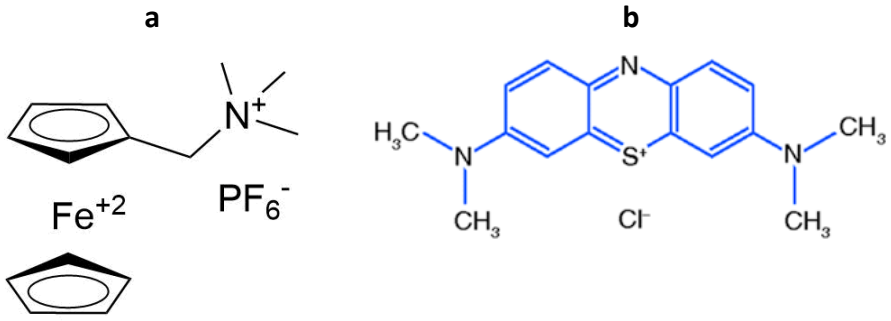

Fig 2.1: Molecular structure of $FA^+PF_6^-$ (a) and methylene blue (b).

2.1.1.1_NEEs synthesis and assembly

The template synthesis of NEEs is a well known electroless procedure, developed first by Martin and Menon[49], then optimised and studied by Ugo and

Moretto[51,57]. NEES are prepared by electroless deposition of gold inside the pores of a nanoporous polycarbonate membrane with three subsequent steps, resumed in Fig. 2.2.

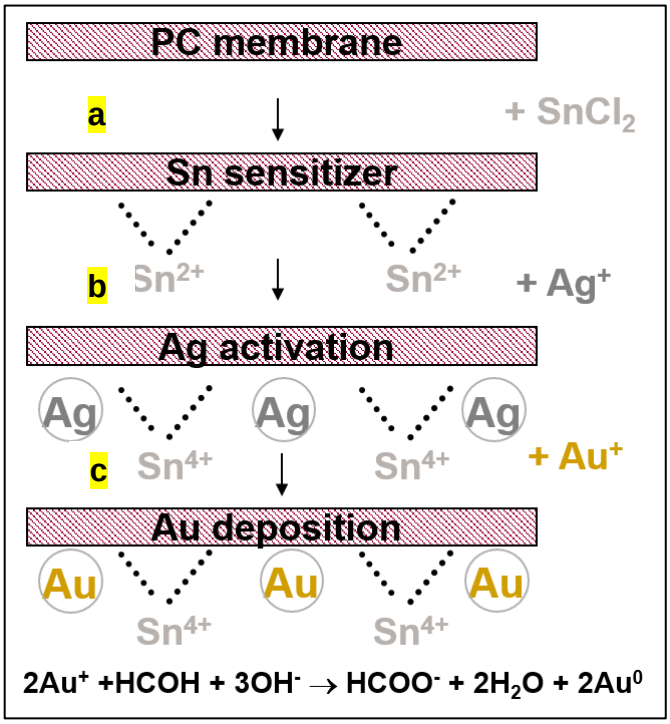

Fig 2.2: Scheme of the NEEs synthesis.

The first step of the electroless procedure (Fig. 2.2a) is sensitisation of the membrane (previously wetted with methanol for few hours) with 0.026 M $SnCl_2$ and 0.07 M TFA in 50/50 methanol/water solution for 45 minutes. This step is required to get the membrane ready to receive the metal. Indeed Sn^{2+} ions are complexed by the amine and carbonyl groups present on the surface of the membrane thanks to the layer of PVP.

In the second step (Fig. 2.2b), the membrane is activated in an aqueous 0.029 M ammonia $AgNO_3$ solution ($Ag[(NH_3)_2]NO_3$) by immersion for 10 minutes. During this step Sn^{2+} previously present on the surface of the membrane is oxidized to Sn^{4+}, while Ag^+ is reduced to elemental Ag, and the membrane pores as well as the membrane surface are covered with Ag nanoparticles, according to the following reaction:

$$Sn^{2+} + 2Ag^+ \rightarrow Sn^{4+} + 2Ag^0$$

In the last step of the procedure (Fig. 2.2c), the activated membrane is immersed in the $Na_3[Au(SO_3)_2]$ gold solution and the Ag nanoparticles are galvanically displaced by gold nanoparticles, according to the reaction:

$$Au^{+} + Ag^{0} \rightarrow Au^{0} + Ag^{+}$$

In this step, kinetic and temperature have a key role: a temperature of 0°C ensure a slow growth of the gold nanowires, indeed at the beginning gold nucleates in contact with the walls of the nanopores and on the two faces of the membrane. To further catalyse the reduction of Au^{+} both in the pores and on the surfaces of the membrane, formaldehyde is added as reducing agent according with the following reaction:

$$2Au^{+} + CH_2O + 3OH^{-} \rightarrow 2Au^{0} + HCOO^{-} + H_2O$$

24 hours are required to complete the gilding procedure and to completely fill the pores. A not complete filling of the pores involves a different electrochemical behaviour of the NEE. At the end of the 24 hours procedure, the membrane is immersed in a HNO_3 /water solution for 6 hours, to remove Sn^{+4} and part of the superficial PVP.

After the complete gold electroless deposition on the nanoporous membrane, NEEs are assembled, in order to be manageable. Briefly, the membrane is former peeled on one side to remove gold excess and to expose the gold nanodisks, and latter cut into small pieces. A synthetic scheme of the assembly procedure is shown in Fig. 2.3. The membrane is placed mid-way with the non-peeled surface on a copper conductive tape that will be the electrical contact between the membrane and the potentiostat, and an aluminum non-conductive tape responsible for the mechanical resistance of the ensemble. A non-conductive polymer is used to insulate the NEEs. A circular hole is created on the polymer with a puncher to define the geometric area of the electrode. Before the utilization, NEEs are heated to 150°C for 30 minutes in order to completely seal the membrane around the nanodisks.

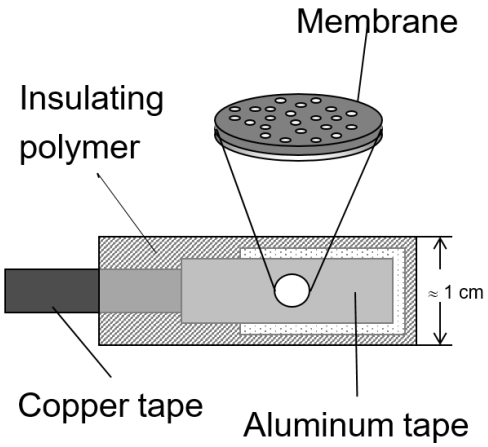

Fig 2.3: scheme of the NEEs assembly procedure[51].

Normally, the diameter of the hole used is 3 mm[54,58,59]; nevertheless voltammetric behaviour of NEEs with different geometric area was previously studied for the identification of analyte in trace concentration[60] and in a biosensing application[61]. In the present work, a nominal diameter of 1.7 mm was used, approximately 57% smaller than the conventionally used 3 mm diameter. Considering that this immunosensor exploits the polycarbonate area of the ensemble, a smaller geometric area can be functionalized with a lower amount of sample. NEEs obtained with 1.7 mm puncher diameter are named as “mini-NEEs”, while NEEs prepared with a 3 mm diameter are called “macro-NEEs”. Previously, a study of NEEs performance with smaller geometrical area (800 µm) were carried out by Habtamu [61].

2.1.2_Results and discussion

2.1.2.1_SEM characterization and determination of the geometric area

Scanning electrode microscopy was used to determine the geometric area of the mini-NEEs and to characterize the superficial composition.

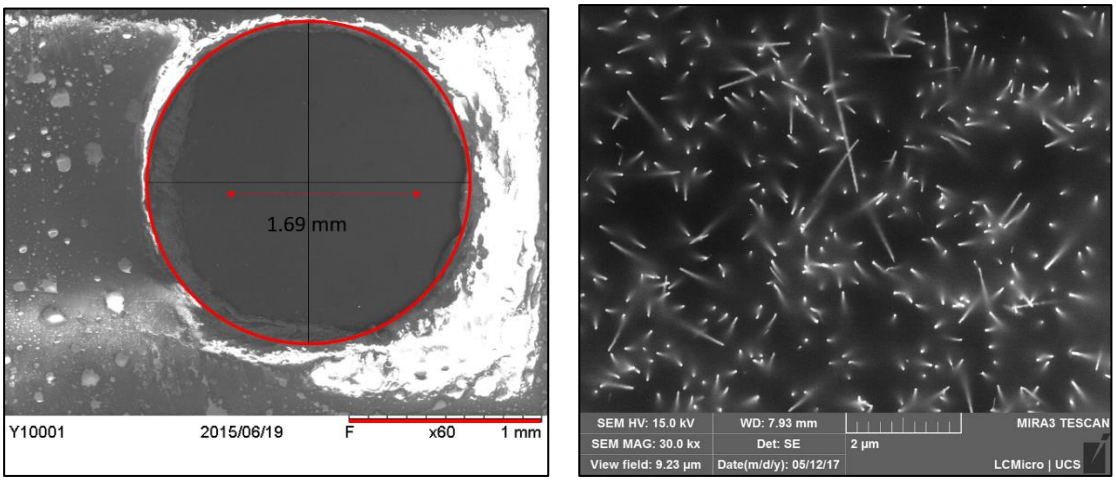

Fig 2.4: a) SEM image of the geometric area of mini-NEEs used to determine the area; b) SEM image of a portion of the NEEs.

Measurements carried out with SEM (Fig. 2.4a) indicate that the diameter of the typical mini-NEE is 1.69 mm, value close to the nominal diameter of the puncher (1.7 mm). The calculated geometric area of the mini-NEE is 0.0224 cm^2, three times smaller than the area of conventional macro-NEEs used (0.07 cm^2). Elemental characterization carried with EDS (spectrum Fig. 2.5), identifies the presence of gold on the surface of the electrode, carbon and oxygen signals represent the PC insulating membrane.

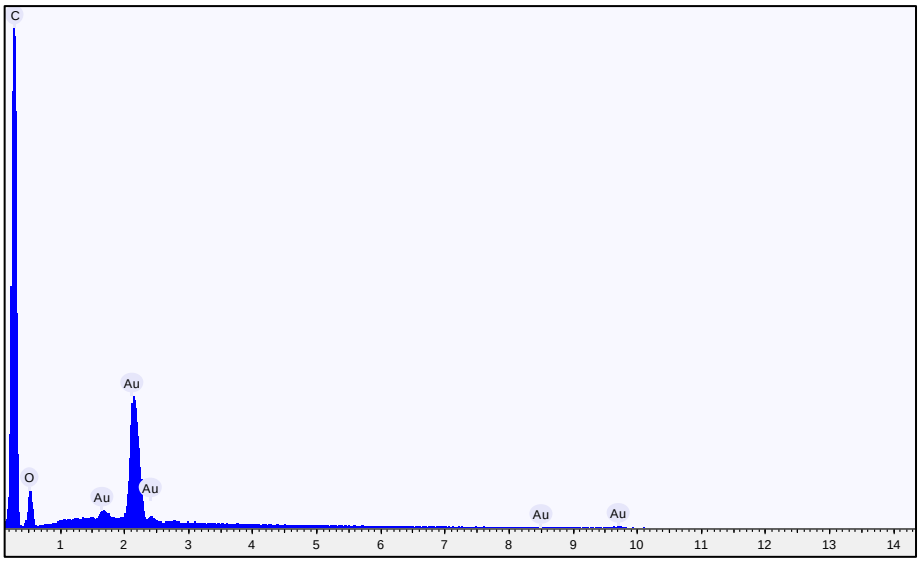

Fig 2.5: SEM-EDS spectrum of a portion of NEE.

2.2.1.2_EC characterization and determination of the geometric area

Two probes were used to characterize mini-NEEs electrochemical properties: FA^+ and MB. The voltammetric behaviour of both the electroactive molecules is well known[54,60,62–65] and, for this reason, suitable to characterize mini-NEEs performance. Fig. 2.6 shows the CV of both the electroactive species recorded at mini-NEEs.

CVs of FA^+ (Fig. 2.6a) shows the typical voltammetric behaviour of the reversible one electron transfer process with $E_{1/2}$ = 0.43 V:

$$FA^+ + e^- \rightleftharpoons FA^{2+}$$

CV of MB is characterized by a different reversible process with $E_{1/2}$ = -0.18 V, corresponding to the reaction:

$$MB + 2e^- + H^+ \rightleftharpoons LB$$

where LB is blue leuco, the reduced form of MB. As showed in the above equation, the redox process is bielectronic and pH dependent. The shape of the voltammogram indicates a diffusive reduction process and a reoxidation characterised by a almost Gaussian peak suggesting a superficial effect.

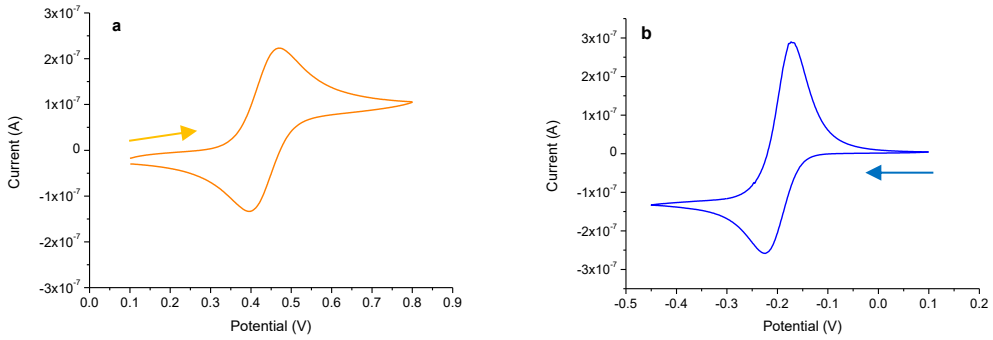

Fig 2.6: CVs of 0.1 mM FA^+ (a) and MB (b) recorded at the mini-NEEs. Scan rate: 10 mV/s.

As introduced in chapter 1.4, in the case of a reversible redox system, when NEEs operate in the total overlap diffusiive regime, the values of the faradaic peak current (I_F) follows the Randles–Sevcik equation.

This behaviour indicates that the faradic current is proportional to the geometric area of the NEEs. To calculate the geometric area of the electrodes, measurements of 0.1 mM FA^+ at different scan rate (from 5 mV/s to 500 mV/s) were performed on the same electrodes. The faradic anodic current values were plotted vs the square root of the scan rate, as shown in Fig. 2.7, and a linear trend observed.

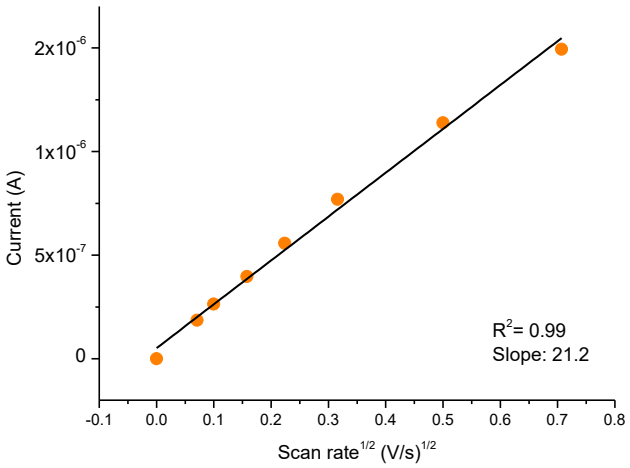

Fig 2.7: Faradic anodic current of 0.1 mM FA^+ recorded at different scan rate (5, 10, 25, 50, 100, 250 and 500 mV/s) plotted vs the square root of the scan rate.

With the slope of the best-fit straight line, it was possible to calculate the geometric area of the electrodes: 0.021 cm^2 ± 0.001. This value is in agreement with the one calculated by the SEM image data.

2.1.2.3_Comparison between macro and mini-NEEs

The decrease of the geometric area should not modify the voltammetric behaviour of the NEEs and the information obtained *via* electrochemistry have to be comparable. Fig. 2.8a compares the CVs of 0.1 mM FA^+ recorded at a NEE with geometric area of 0.07 cm^2 (red line) and a NEE with geometric area of 0.022 cm^2 (blue line). Both the CVs are well resolved, with $E_{1/2}$ = 0.43 V. Capacitive and faradic current decrease with the decrease of the geometric area. To better evaluate the efficiency of the mini-NEEs and the macro-NEEs it is necessary to compare the current density, the current calculated *per* unit area:

$$j = \frac{I}{A_{geom}}$$

where *j* is the current density and *A* is the geometric area of the electrode. Fig. 2.8b shows the current density calculated on the same NEEs.

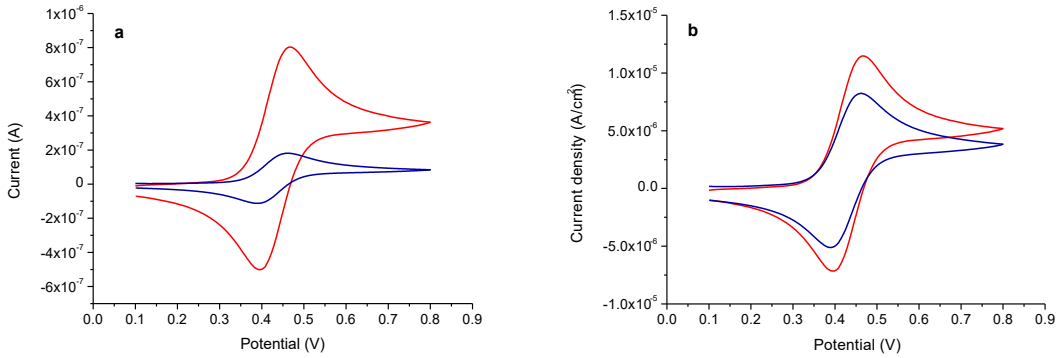

Fig 2.8: a) CVs of 10 mM FA^+ recorded at two different NEEs with different geometric area: red line, 0.07 and blue line 0.022 cm^2. Scan rate: 10 mV/s. b) Current density.

Tab. 2.1 shows capacitive (I_{cap}) and faradic anodic (I_{pa}) peak current values. Ratio I_{pa}/I_{cap} and current density are calculated at two NEEs with different geometric areas and presented in Tab. 2.1 column 4 and 5.

Tab 2.1: Capacitive current, anodic peak current, ratio between faradic and capacitive current and current density recorded at NEEs with different geometric area. 10 mM FA^+. Scan rate 10 mV/s.

Area (cm^2)	I_{cap} (A)	I_{pa} (A)	I_{pa}/I_{cap}	I_{pa}/A (A/cm^{-2})
0.022	$2*10^{-7}$	$2.11*10^{-7}$	1.06 ± 0.05	94.2 ± 4.7
0.07	$0.8*10^{-7}$	$6.82*10^{-7}$	1.17 ± 0.06	97.4 ± 4.9

Calculated current density for the mini-NEEs is $94.2*10^{-6}$ A/cm^2 and the same values for macro-NEEs is $97.4*10^{-6}$ A/cm^2. Values are similar and this result proves that the voltammetric behaviour of the NEEs is not affected by the geometric area. Calculated ratio I_{pa}/I_{cap} at the mini-NEEs (1.06) has a comparable value of the same ratio calculated at the macro-NEEs. High sensitivity of the NEEs does not decrease with the decrease of the geometric area. These results indicate that the mini-NEEs can be

employed for the development of the IgY immunosensor requiring a smaller amount of the sample and reagents.

2.1.3.4_Reproducibility of the measurements

Different NEEs even when prepared from different membranes ensure a good reproducibility when the same measurement is performed[57]. In any case, for the immunosensing procedure described in the next chapters (chapter 2.2 and 3.1), NEEs that show similar CVs were used, to operate with the best reproducibility. To select best working NEEs, CVs of FA^+ and MB were recorded in the same solution. Fig. 2.9 shows the CVs recorded of the probes/mediator at three different NEEs. Potential and current peak values are presented in Tab. 2.2; in case of FA^+ the parameter considered is the anodic peak, while for MB, the cathodic one, for both cases is considered the forward scan.

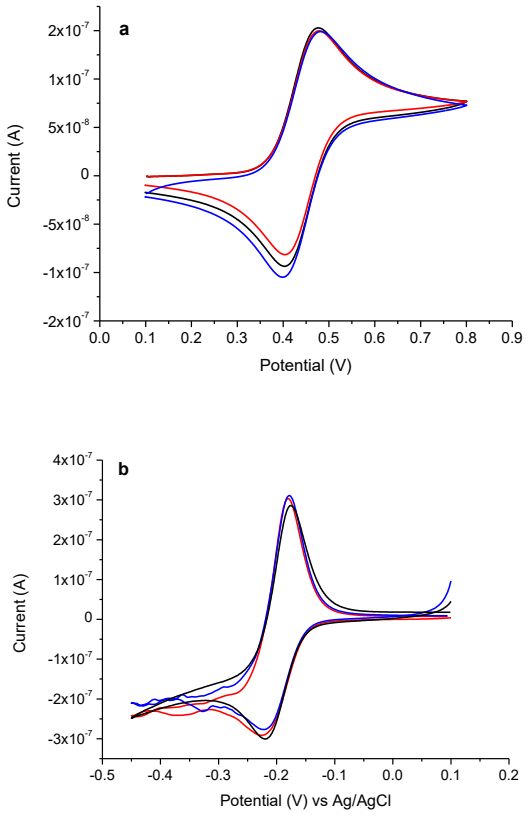

Fig 2.9: CVs of 0.1 mM FA^+ (a) and MB (b) recorded at three different bare NEEs in 10mM PBS pH 7. Scan rate: 10mV/s

Tab 2.2: potential and current values recorded at three different bare NEEs for FA^+PF_6 and MB.

	FA^+		**MB**	
NEE	**E_{an} (V)**	**ip_{an} (A - 10^{-7})**	**E_{cat} (V)**	**ip_{cat} (A - 10^{-7})**
1	0.478	1.245	-0.220	-2.823
2	0,474	1.216	-0.226	-2.685
3	0.474	1.250	-0.232	-2.875
AV ± st.dev.	0.475 ± 0.002	1.237 ± 0.018	-0.226 ± 0.006	-2794 ± 0.098

From Fig. 2.9 and Tab. 2.2, it is possible to observe that good reproducibility can be obtained when measurements are performed both with FA^+ and MB.

2.2_IgY-immunosensor

2.2.1_Introduction

IgY is a promising protein that can be applicable in many research fields and therapeutic veterinary and human medicine[18]. Moreover, it is available in high quantity in egg yolk and can be obtained without expensive instrumentations or effort; methods developed to purify the protein range from electrophoresis[66] to PEG extraction[67].

Despite its multi-functionality and wide range of application, mainly traditional methods such as SDS-PAGE or ELISA[68] have been used for IgY identification in eggs or eggs derivatives. Few papers are present in literature that exploit electrochemical methods for its detection, usually combined with other techniques, as fluorescence[69]. On the other hand, a large number of biosensors and immunosensors were developed for the detection of virus, bacteria or humans and animals diseases with IgY as the primary antibody[70–72]

As a confirmation that electrochemical methods and immunosensors can be reliable tools for the identification of IgY, many studies can be cited that involve the investigation of other kind of immunoglobulins from human serum: IgE was monitored with a sensor based on screen-printed electrodes functionalised with aptamers[73], IgG was detected *via* differential pulse voltammetry immunoassay[74].

2.2.2_NEE-based IgY-immunosensor

The IgY-immunosensor, developed by Bottari[59] follows the scheme of a direct approach, so that the captured antigen is recognized by a specific antibody (labelled with an enzyme). IgY from the sample is directly immobilized on the surface of the NEEs, preferably attaching to the PC component of the electrodes. A following blocking step is required, to ensure the reliability of the sensor and avoid nonspecific interactions. The blocking agent is usually a large protein that cannot be recognized by the specific antibody that binds the antigen. In the present work, bovine serum albumin (BSA), one of the most common proteins used to this aim, is chosen[75–77]. IgY is then recognized by a specific anti-IgY secondary antibody, labelled with the enzyme horseradish peroxidase (HRP). Fig. 2.10 shows the structure of the NEE based IgY-immunosensor.

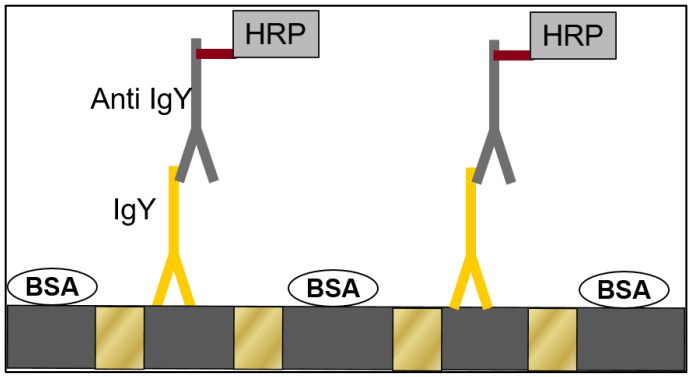

Fig 2.10: Scheme of the IgY-immunosensor. IgY is immobilized on the PC part of the NEEs, BSA (Bovine Serum Albumin) is the blocking agent added after the capture of the antigen. The secondary antibody anti-IgY labelled with the enzyme HRP is then added in order to recognise IgY.

In the presence of its substrate, hydrogen peroxide, HRP promotes an electrocatalytic cycle in the reduction direction of the potential window, so that a redox mediator that can be reduced by the enzyme is required. Methylene blue ($E_{1/2}$ of -0.2 V) was used to this aim. A schematic representation of the reactions that occurs during the catalytic cycle is shown in Fig. 2.11.

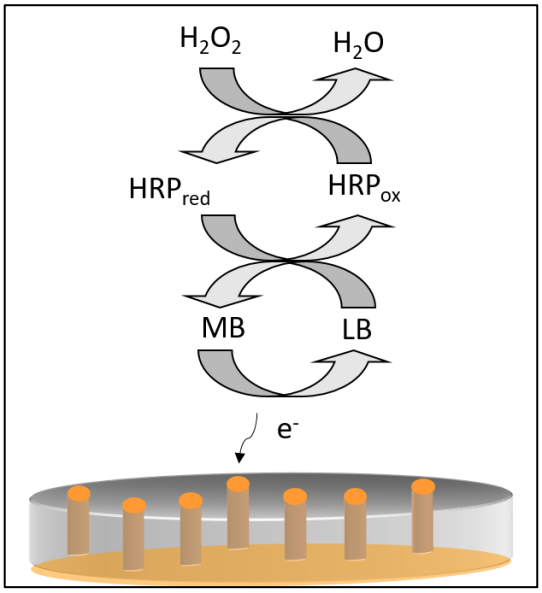

Fig 2.11: Schematic representation of the reactions that occur during the catalytic cycle. MB is the redox mediator; HRP is the enzyme and hydrogen peroxide the substrate.

Bottari performed the IgY detection using macro-NEEs; in the present work, an optimisation of the procedure and a comparison of the results obtained with macro and mini-NEEs is proposed. The decrease of the geometric area allows analysing samples in smaller amount than those used before[59].

2.2.2_Experimental

2.2.2.1_Materials

NEEs (prepared as previously shown), MB, PBS 10mM, TWEEN 20, BSA, H_2O_2. Pure IgY was from Jackson Immunoresearch Laboratories, at a concentration of 5.6 mg/mL. The secondary antibody goat anti-IgY (HRP conjugated) was from Immunology Consultants Laboratory (USA), diluted 1:10 for the immunosensing procedure. Eggs were achieved from a local supermarket.

Measurements were carried in a typical thee electrodes cell, NEE as working electrodes, Ag/AgCl KCl saturated reference electrode and Pt wire as counter electrode. CH1000a instrument was used as potentiostat.

2.2.2.2_Immunosensing procedure – starting point

Bottari[59] applied this IgY-immunosensor in 2014 for the identification of egg yolk in egg temperas. In Tab. 2.3 procedure proposed by Bottari is shown.

Tab 2.3: Immunosensor procedure and electrochemical parameters proposed by Bottari[59].

NEEs Geometric area	**0.07 cm^2**
Capture of IgY	10µL 30 min
Washing step	3 rinsing with PBS
Blocking step	Blocking solution, 1% BSA, 30 min
Washing step	3 rinsing with PBS
Incubation II ab	10µL of 0.05 mg/mL 1 Anti-IgY HRP, 30 min
EC parameters	Supporting electrolyte: PBS 0.1 M pH 7; substrate: 8 µL of 1.2 mM H_2O_2; scan rate: 50 mV/s.

In this thesis, the analytical procedure of the immunosensor was improved and optimized. The structure of the immunosensor performed capturing IgY with the mini-NEEs is unchanged, but few critical parameters were modified, not only to reduce the sample-request, but also mainly to improve the reliability of the system.

2.2.2.3_Sample preparation

To identify IgY from fresh eggs with the optimised analytical procedure, it is necessary to separate the water-soluble proteins (including IgY) from the water-insoluble lipid and lipoprotein part of egg yolk. In the literature, several methods are proposed for the extraction and purification of IgY. Two different buffer were used to extract IgY from egg yolk: 10 mM PBS pH 7 and 0.2 M acetate buffer pH 5. After mechanical separation of yolk and egg white, a known amount of yolk is dissolved in the buffer.

Samples analysed at neutral condition were prepared as shown in Tab. 2.4.

Tab 2.4: Concentration of egg white in the samples prepared for the analysis with the immunosensor.

Egg sample	Concentration
Egg white	0.1 µL/mL
White/Yolk 1:1	0.05/0.05 µL/mL
Egg yolk	0.1 µL/mL

Sample analysed at pH 5, were prepared as shown in Tab. 2.5.

Tab 2.5: Description of the samples analysed at pH 5.

Sample	Egg yolk g/mL
Egg yolk	0.002
	0.005
	0.01
	0.02
	0.05
	0.1

	0.25
	0.5

2.2.3_Results and discussion

2.2.3.1_Cyclic voltammetric results

Cyclic voltammetry is one of the most common electrochemical techniques and it was chosen to monitor the electrochemical behaviour of the immunosensor during different steps of the procedure. First, a cyclic voltammogram (CV) of the mediator (MB) was recorded at the bare NEE, a second CV of the redox mediator was recorded after the complete immunosensing procedure. Finally, a CV was recorded after the addition of the substrate, 0.5 mM H_2O_2 in the electrochemical solution. Fig. 2.12 shows a typical example of the three mentioned CVs, all recorded in 10 mM MB solution. The black dotted line CV of the redox mediator is recorded at the NEE not incubated with IgY. It shows the typical cathodic and anodic peaks of MB, with $E_{1/2}$ of -0.20 V. Black full line CV of MB is recorded after the completion of the procedure of preparation of the immunosensor. Minor changes in the CV can be observed, indeed the current of anodic peak is a bit lower than the current peak recorded before the functionalization procedure. This small decrease of the current can be related to adsorption of the biological materials on the electrode surface. A completely different pattern can be observed in the red CV, when the CV shape evolves to a sigmoidal shape. This change is due to the addition to the substrate to the electrochemical solution that reacts with the enzyme and the mediator, and follows a typical electrocatalytic cycle[54], where the cathodic peak current increases and the anodic peak disappears.

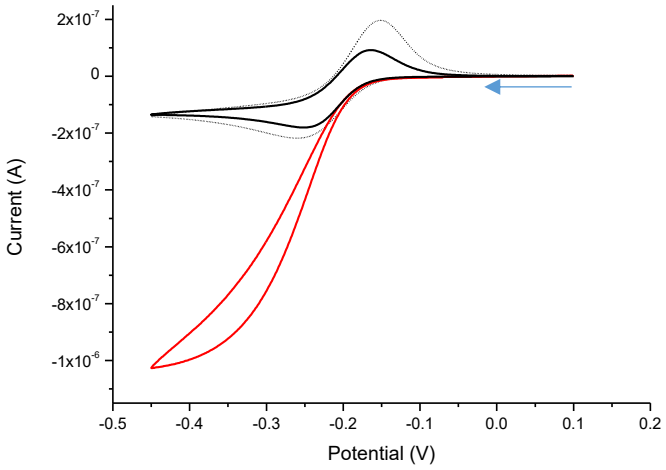

Fig 2.12: CV of 0.1mM MB recorded at the bare electrode (black dotted line) and before (black full line) and after (red line) addition of 0.5mM substrate.

The reactions that occur during the electrocatalytic cycles are the following (2.1-2.3):

$$HRP_{red} + H_2O_2 \rightarrow HRP_{ox} + H_2O \qquad 2.1$$

$$MB + 2e^- + H^+ \rightarrow LB \qquad 2.2$$

$$HRP_{ox} + LB \rightarrow HRP_{red} + MB \qquad 2.3$$

In step 2.1 the enzyme (HRP) reacts chemically with its substrate (H_2O_2), reducing it. The mediator is electrochemically reduced in step 2.2 to the leuco form (LB). Finally, in step 2.3, the oxidized form of the enzyme reacts chemically with the reduced form of the mediator, regenerating its starting condition. “Being a cycle”, both the mediator and the reduced form of the enzyme are regenerated during the last chemical step of the cycle.

To test possible nonspecific interactions, a sample not containing IgY was incubated on the electrode. The procedure of functionalization of the immunosensor was performed and the electrochemical parameters of figure were applied Fig. 2.13 shows the recorded CVs. It can be observed that no electrocatalytic cycle occurs when the substrate is added to the electrochemical solution; indeed minor changes can be observed, as in the previous case (red line CV). The black line corresponds to the CV

recorded at the bare electrode; the CV-red line was recorded after the complete procedure made with a sample not containing the analyte IgY and the CV-blue line was recorded after the addition of the substrate. Even if some modification of the pattern is evident, the electrocatalytic cycle is completely absent: both the cathodic and the anodic peaks are present. This result indicates the high selectivity of the immunosensor.

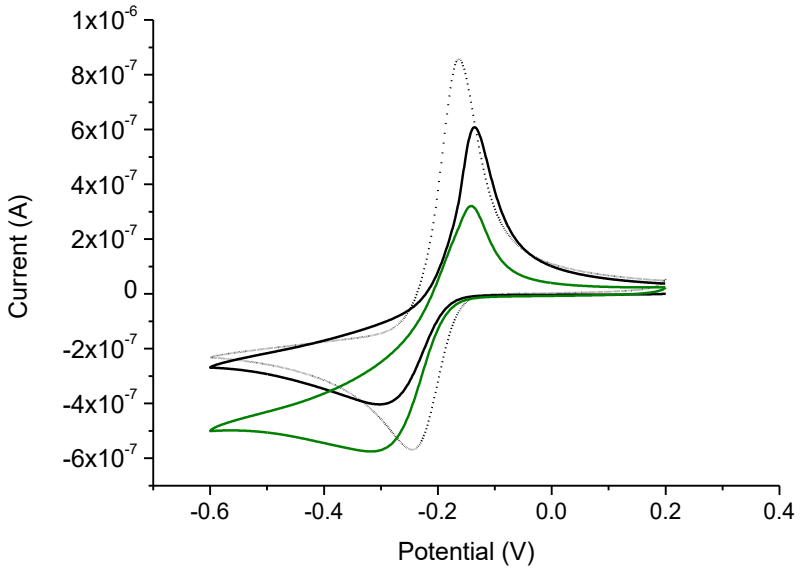

Fig 2.13: Cyclic voltammograms of MB 0.1 mM in PBS 0.01 M before the functionalization (dotted black line), after the complete functionalization of the NEE (full black line) and after add of 0.5 mM substrate (H_2O_2) (green line). Scan rate: 10mV/s.

2.2.3.2_Effect of a smaller geometric area

To investigate the efficiency of the immunosensing procedure and to check the electrocatalytic response of the systems, tests on NEEs with different geometric areas were performed. To this aim, 0.01 mg/mL secondary antibody labelled with HRP was directly immobilised on the NEEs surface, to ensure a high capture level; the secondary antibody was captured by the PC part of the NEEs surface, as for the analyte when present. 10 µL and 5 µL were immobilised on electrodes with 0.07 and 0.022 cm^2 area, respectively. Results are shown in Fig. 2.14; the electrocatalytic cycle was entirely developed in both cases and they are both well resolved. Order of magnitude reached with the electrocatalytic current is 10^{-6} for both the geometric areas, values are $5.5*10^{-}$

^{6} A and 1.25 10^{-6} A for the macro and mini-NEE respectively. To evaluate if the electrocatalytic cycles evolution has the same behaviour, ratio I_{cat}/I_{pc} (where I_{cat} is electrocatalytic current and I_{pc} is cathodic peak current) was calculated and the results are shown in Tab. 2.6.

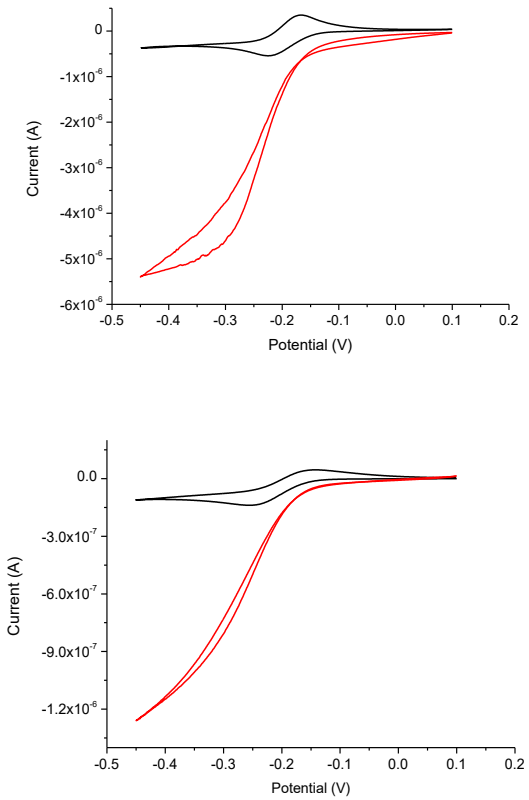

Fig 2.14: CVs of 0.1 mM MB in 10 mM PBS before and after addition of 0.5 mM H_2O_2 at NEEs with different geometric areas: a) 0.07 and b) 0.022 cm^2.

Tab 2.6: Current values recorded before and after the addition of substrate in presence of the redox mediator. Current is recorded at NEEs with different geometric areas.

NEE diameter	0.07 cm^2	0.022 cm^2
I_{pc} MB post	5.09*10^{-7} A	1.36*10^{-7} A
I_{cat} 0.5mM	5.5*10^{-6} A	1.25 10^{-6} A
I_{pc}/I_{cat}	0.92	1.08

The values of I_{cat}/I_{pc} are 0.92 for macro-NEEs and 1.08 for mini-NEEs. This result suggests that the evolution of the electrocatalytic cycle is similar when different geometric areas are used and mini-NEEs have similar efficiency of the macro-NEEs.

After this test, other parameters of the immunosensing procedure can be optimised, from the amount of analyte immobilised on the electrodes to the secondary antibody concentration.

2.2.3.3_Optimisation of the substrate concentration

The optimal concentration of the relevant substrate (H_2O_2) was investigated to ensure the complete catalytic activity of the enzyme. To this aim, the secondary antibody anti-IgY labelled with HRP was directly immobilised on the NEEs surface for 30 minutes. The concentration of the secondary antibody was 0.01 mg/mL. CVs of the redox mediator in presence of the enzyme captured by the electrode were recorded for additional concentrations of the substrate, i.e. 0.05, 0.1, 0.5, 1 and 1.5 mM H_2O_2 and are shown in Fig. 2.15. From the observation of these CVs, it can be noticed that the electrocatalytic current increases from 0.01 to 0.5 mM concentration of H_2O_2, (a, b and c CVs in Fig. 2.15). Further addition of 1 mM H_2O_2 causes a small decrease of the electrocatalytic current, indicating that the activity of the enzyme reaches the maximum at 0.5 mM.

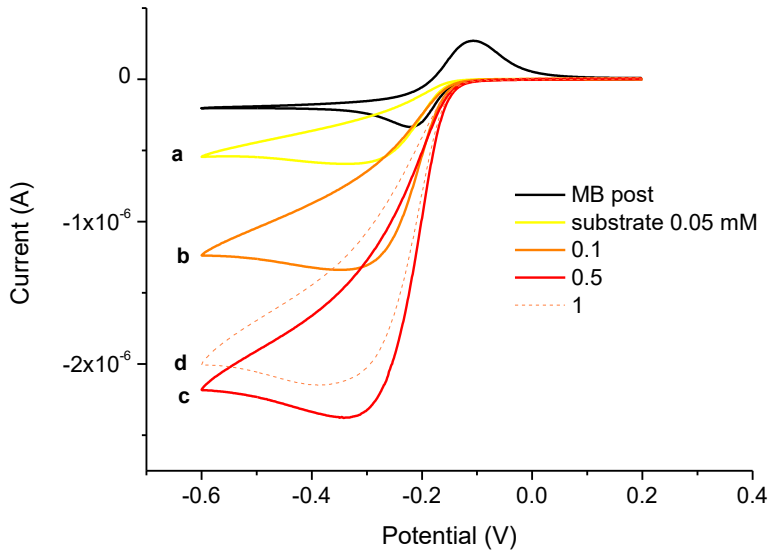

Fig 2.15: CVs of 0.1 mM MB in 10 mM PBS on modified NEE with secondary antibody anti-IgY. Black line is recorded before the addition of the substrate, from yellow to red full lines, the concentration of substrate increases from 0.01 to 0.5 mM. Dashed line is CV recorded with higher concentrations of H_2O_2, but after reaching the complete activity of the enzyme. Scan rate: 10mV/s.

The electrocatalytic currents presents an almost linear trend with the increase of H_2O_2 from 0.01 to 0.5 mM and decreases for higher values, as shown in Fig. 2.16. On the bases of these results, 0.5 mM concentration of the substrate was used for all the measurements.

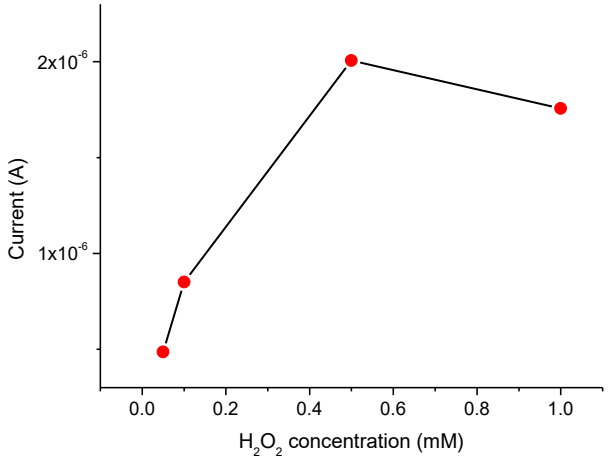

Fig 2.16: Plot of the electrocatalytic current values as a function of the substrate concentration.

2.2.3.4_Incubation of smaller amount of sample

The decreasing of the NEEs geometric area allowed using of smaller amount of immobilised sample. Test with 5 µL (instead of 10 µL) of IgY at different concentration were performed. A wide range of concentration was chosen to verify the development of the electrocatalytic cycle for all the concentration tested, in order to avoid a decrement in the sensitivity of the sensor.

Fig. 2.17 shows the resulting CVs of 0.1 mM MB after the addition of 0.5 mM H_2O_2 to the PBS solution. Electrocatalytic current increases with the increasing of the analyte concentration, from 1.1 µg/mL, to 0.11 mg/mL. When 1.1 µg/mL of IgY was captured by the electrode (Fig. 1.17a), the electrocatalytic cycle is well developed, the anodic peak disappears and the plateau typical of the cycle is reached at $6.2*10^{-7}$ A. This

current value is lower compared to the current values recorded when higher concentration of the analyte were tested. The highest value of the electrocatalytic current was reached when 0.11 mg/mL IgY was immobilised on the electrode surface and a catalytic current of $1.5*10^{-6}$ A was recorded (Fig. 1.17e).

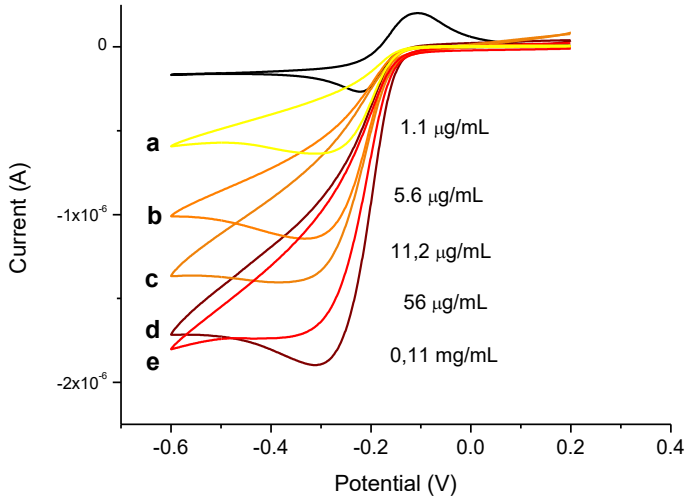

Fig 2.17: CVs of 0.1 mM MB recorded in presence of the relevant substrate for samples of IgY at different concentrations: 1.1 µg/mL, 5.6 µg/mL, 11.2 µg/mL, 56 µg/mL and 0.11 mg/mL. Black line is the CV of 0.1 mM MB recorded after the complete immunosensing procedure, before the addition of the substrate.

The electrocatalytic current values are peaked at -0.40 V potential where the plateau is achieved and calculated as shown in the following equation:

$$I_{net} = I_{cat} - I_{pc}$$

where I_{cat} is the electrocatalytic current, and I_{pc} is the cathodic current recorded before the addition of the substrate.

Observing the evolution of the trend of the electrocatalytic current vs IgY concentration, as plotted in Fig. 2.18, a linear trend can be defined from the lower concentration, 1.1 µg/mL to 11.2 µg/mL. For higher concentration a plateau is reached, indicating the saturation of the saturation of the NEEs surface at a concentration of 0.11 µg/mL of the analyte

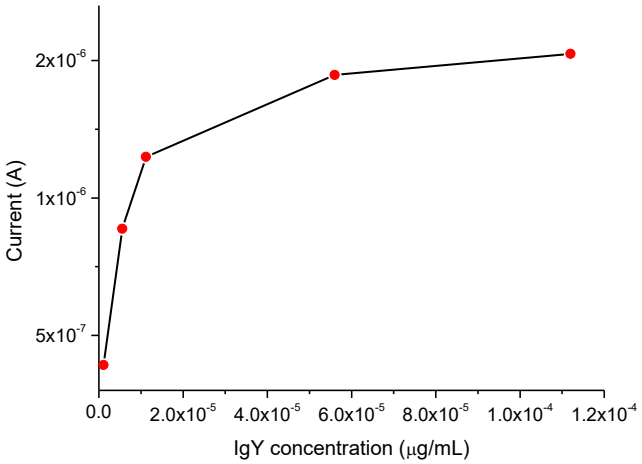

Fig 2.18: Electrocatalytic current values plotted vs the concentration of the analyte.

It was demonstrated that with a lower amount of sample, i.e. 5 µL of the extract, is was possible to detect both low concentration of the analyte and high concentration. The decrement of the volume does not affect the performance of the sensor that maintains its characteristic high sensitivity.

2.2.3.5_Optimised procedure

The decrease of the geometric area from 0.07 to 0.022 cm^2 allowed to decrease chemicals and amount of sample for the immunosensing procedure. The concentration of the substrate was optimised for the mini-NEEs to 0.5 mM H_2O_2; the amount of sample immobilised on the NEEs was reduced from 10 to 5 µL, without losing sensitivity of the sensor, the concentration of the secondary antibody was also reduced from 0.05 mg/mL to 0.01 mg/mL. Washing step efficiency was improved introducing 1% TWEEN 20 to the washing buffer, to reduce the possibility of nonspecific absorption on the NEEs surface. Tab. 2.7 summarises the immunosensing procedure with all the critical parameter optimised.

Tab 2.7: Optimised immunosensing procedure.

NEEs Geometric area	**0.022 cm^2**
Capture of IgY	5 µL 30 min
Washing step	4 rinsing with 1% TWEEN 20 in 10 mM PBS

Blocking step	Blocking solution, BSA 1%, 30 min
Washing step	4 rinsing with 1% TWEEN 20 in 10 mM PBS
Incubation II ab	5 µL of 0.01 mg mL Anti-IgY HRP 30 min
EC parameters	Supporting electrolyte: PBS 10 mM pH 7; substrate: 0.5 mM H_2O_2, scan rate: 10 mV/s

2.2.3.6_Determination of IgY in Eggs

With the optimised immunosensing procedure presented in Tab. 2.7, qualitative and quantitative tests were carried out on fresh eggs samples in two different pH conditions. First, presence or absence of the target protein was investigated in samples described in Tab. 2.4 in a neutral pH, performing a slight extraction of the analyte (IgY) with 10 mM PBS at pH 7. Following, the correlation between the electrocatalytic current and the IgY concentration (related to the concentration of yolk) was investigated; in this case, egg yolk was diluted in acidic conditions, with 0.2 M acetic buffer at pH 5.

Fig. 2.19 shows the results achieved when egg samples were tested at neutral pH. The electrocatalytic current increases with the increment of egg yolk concentration in the sample. When egg white was analysed with the immunosensing procedure, the electrocatalytic current obtained was much lower than the electrocatalytic current obtained in egg yolk. The 1:1 mixture causes an electrocatalytic cycle with an intermediate entity. The trend of the increment of the electrocatalytic current, calculated as $I_{net} = I_{cat} - I_{pc}$, and presented in the inset of Fig. 2.19, is almost linear. The electrocatalytic current was peaked at −0.40 V, where it achieves a plateau. .

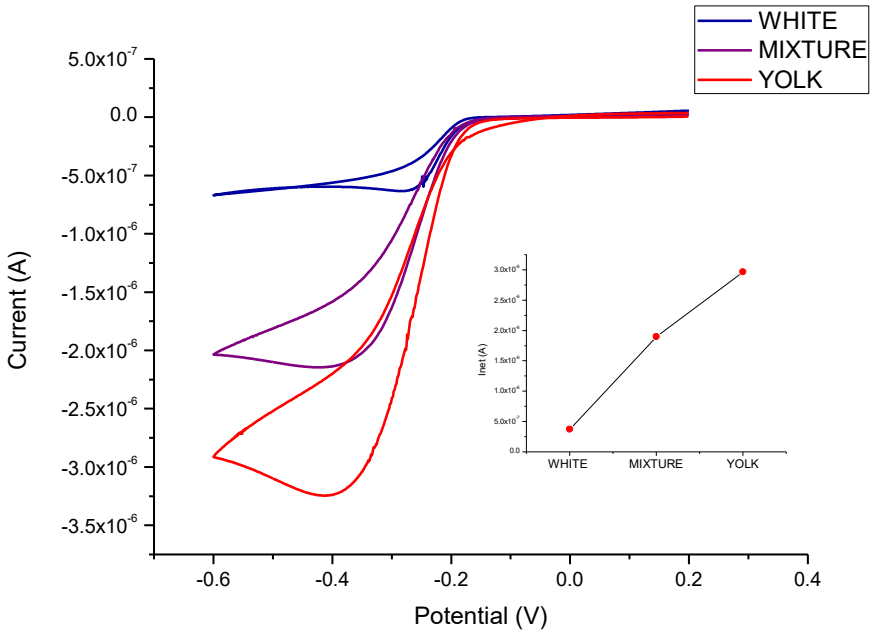

Fig 2.19: CVs of 0.1 mM MB in 10 mM PBS recorded after the addition of the substrate for three egg containing samples: egg white: blue line, 1:1 mixture purple line and egg yolk red line. Inset: trend of the increment of the electrocatalytic cycle as a function of the samples.

Following, the samples described in Tab. 2.5 were analysed with the optimised immunosensing procedure; in this case IgY was slightly extracted from egg yolk with 0.2 M acetic buffer at pH 5. Most representative CVs from the eight samples analysed are shown in Fig. 2.20. The black dotted line CV corresponds to the typical pattern of the mediator MB (at a NEE treated with the immunosensing procedure with egg yolk, BSA and HRP-anti-IgY, see Fig. 2.11) before addition of the substrate. The solid lines CVs, from yellow to red, were recorded in the presence of H_2O_2 at NEEs incubated in samples containing an increasing amount of IgY. A different NEE was used for each sample.

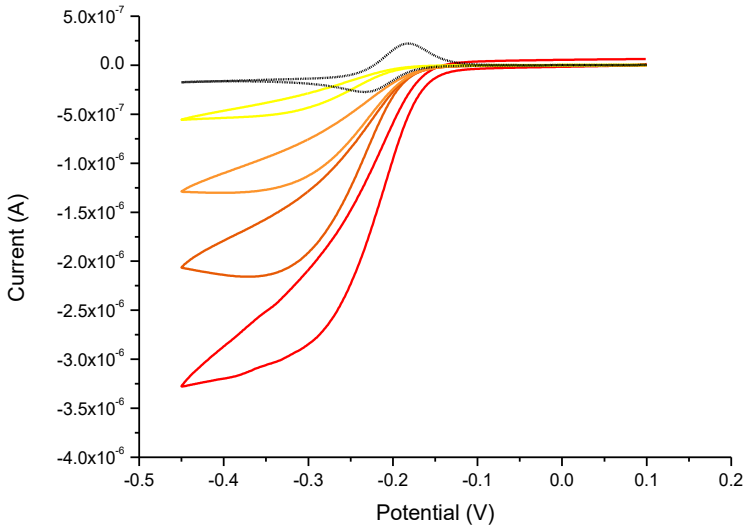

Fig 2.20: CVs of 0.1 mM MB in 0.01 M PBS in the absence (dashed-blue line) and in the presence of 0.5 mM H_2O_2 at NEEs incubated with egg yolk at a concentration from 0.002 g/mL to 0.5 g/mL of yolk (solid-lines from light yellow to red). Scan rate 10 mV/s.

It is possible to observe that the electrocatalytic current increases with an increasing content of IgY in the samples: indeed the dependence of the catalytic current is a function of the egg yolk content; the trend in shown in Fig. 2.21. Also in this case I_{net}, was calculated as: $I_{net} = I_{cat} - I_{pc}$. The pattern of the electrocatalytic current increment vs the amount of yolk fits a saturation-like curve, following equation:

$$y = \frac{ax}{b + x} + c$$

where the fitting parameters are a = 2.25 µA; b = 0.06 g/mL; c = 0.49 µA, with an R^2 value of 0.991. From this curve, it is also possible to define a linear range from 0.002 to 0.05 g/mL of yolk.

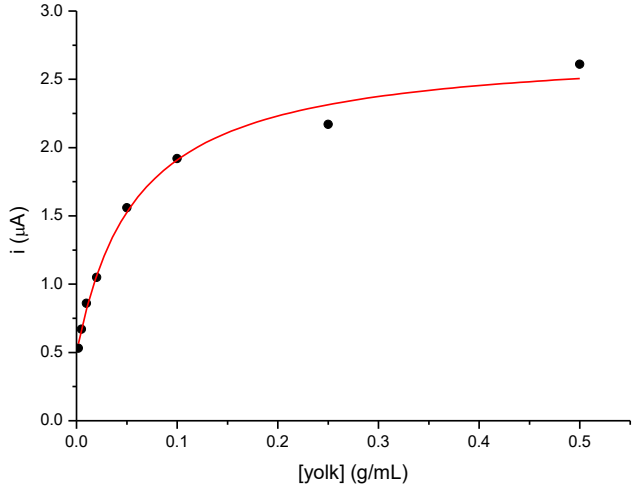

Fig 2.21. Electrocatalytic current vs. the concentration of yolk (lower x-axis) and versus the relevant estimated IgY concentration (upper x-axis), and best fitting curve. The curve can be used to quantify the IgY concentration.

2.3_Conclusion

The analytical procedure of an NEE-base IgY-electrochemical immunosensor was successfully optimised, starting from Bottari[59] procedure. Geometric area of the NEEs, used as the immunosensor platform was reduced 3 times compared with the conventional one. It was demonstrated that the decrease of the geometric area does not affect the performance of the electrodes, both when electroactive probes are investigated, both when the immunosensing procedure is performed. Decrease of the geometric area allows us to decrease, as a consequence, the amount of sample immobilised on the electrodes, and the concentration of the chemical and antibody used. The immunosensor was then successfully applied on eggs samples in different pH conditions and the trend of the increment of the electrocatalytic current as a function of the yolk concentration was determined.

3_OVA immunosensor

Ovalbumin is the main protein of chicken egg white, constituting the 55% of the protein content. Due to its abundance, OVA was chosen as target biomolecule for the electrochemical immunosensor developed to identify egg white in samples. The OVA-immunosensor was designed during the stage spent at the University of Antwerp, following the scheme of an indirect assay. Primary and secondary labelled antibodies are required for the identification of the protein. The immunosensor procedure and few critical parameters (i.e. the blocking agent) were optimised before the application of the sensor on eggs samples. In this chapter the general construction of the sensor, the analytical procedure and the results on real samples are proposed.

3.1_Introduction

Ovalbumin (OVA) is the main protein of egg white, representing the 55% of the total protein content. It was demonstrated that OVA, as lysozyme, is one of the egg proteins that causes egg allergy in children and adults[78]. Eggs are widely used in the production of food, beverage and food supplements, transferring their allergenic proteins to the finished food. For this reason, it is important to identify OVA (or some residual parts) in egg-derived products.

As an alternative to traditional immunoenzymatic assays, such as ELISA[79–81], biosensors have been lately proposed for the investigation of OVA in food derivatives[78]. The allergenic protein was detected in cakes with a graphene based electrochemical immunosensor[82] or in wine with a SPR biosensor[83]. Due to its abundance, OVA was also exploited as the target protein for the development of innovative detection methods such as magnetic beads as capture platform[84–87] or for electrochemical immunoassays.

3.1.2_NEE-based OVA-immunosensor

In this affinity biosensor the target protein, ovalbumin (antigen) is directly immobilized on the electrodes surface. In the application of NEEs as platform for the fabrication of the immunosensor, the target protein is mainly captured by the polycarbonate part of the NEEs. A blocking step is performed with soymilk to avoid nonspecific interactions and then, a primary anti-OVA antibody is employed to recognize the protein. A polyclonal anti-OVA primary antibody was chosen to promote the recognition of the protein also in complex or degraded samples. Following, a secondary antibody anti-anti-OVA labelled with glucose oxidase is incubated to detect the antigen-antibody complex. A scheme of the immunosensor is presented in Fig. 3.1.

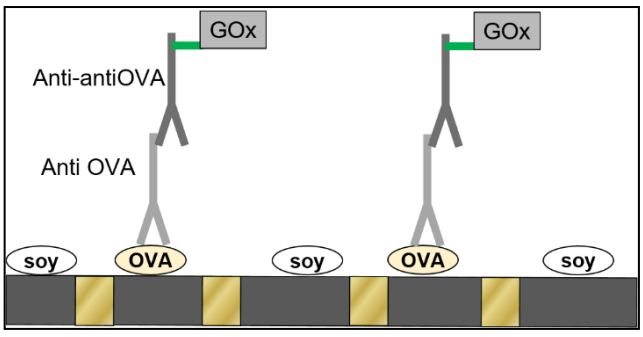

Fig 3.1: Structure of the NEE-based OVA-immunosensor.

The enzyme glucose oxidase was accurately chosen to distinguish the electrochemical outcome of the OVA-immunosensor from the IgY-immunosensor. Indeed, a different redox mediator is used for the electrochemical detection of the system: FA^+ (a ferrocene derivative with $E_{1/2}$ = 0.43 V) that promotes the development of an electrocatalytic cycle in the oxidation direction in a different potential window well separated from that of MB used for IgY (2.2.3). Interaction between the enzyme, its substrate and the redox mediator with the gold nanodisks on the electrode surface is schematised in Fig. 3.2.

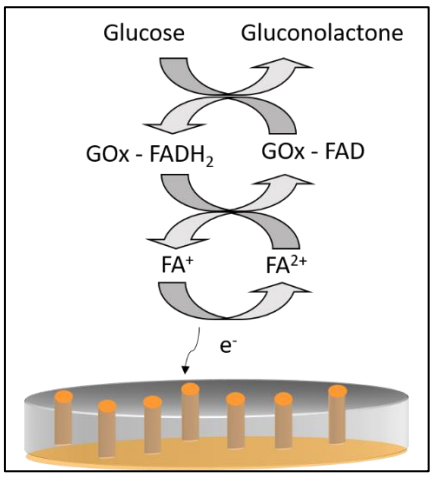

Fig 3.2: Schematic representation of the reactions that occur during the catalytic cycle. FA^+ is the redox mediator; GOx is the enzyme and glucose the substrate.

The idea behind this part of the thesis is that the combined application of both the IgY- and OVA- immunosensors can provide complete information about the composition of egg-based samples, which is detecting the presence of egg white and/or egg yolk in the same sample.

3.2_Experimental

3.2.1_Materials

NEEs (prepared as described in chapter 2.1), FA^+. PBS, TWEEN 20, BSA, PVA and glucose were from Sigma Aldrich. Primary antibody: affinity purified rabbit anti-chicken Ovalbumin from Immunology Consultants Laboratory Inc. diluted 1:10 in 10 mM PBS as

suggest by the producer; secondary antibody: goat-anti Rabbit IgG H&L (Glucose Oxidase) from Abcam diluted 1:50 in 10mM PBS as suggested by the producer. Eggs and soymilk were achieved from a local supermarket.

Measurements were carried in a typical thee electrodes cell, NEEs as working electrodes, Ag/AgCl KCl saturated reference electrode and Pt wire as counter electrode. Autolab pgstat 101 controlled with the software NOVA 1.1 was used for electrochemical measurements.

3.2.2_Immunosensing procedure

The analytical methodology developed for detection of OVA with the NEE-based immunosensor is summarised in Tab. 3.1. The polyclonal nature of the primary antibody required a particular attention in the optimization of the blocking step, to avoid a partial recognition of BSA (used in the IgY immunosensor) by the polyclonal anti-OVA primary antibody. The procedure was carried out in a wet chamber (100% humidity).

Tab 3.1: Steps of the functionalization procedure of the NEEs.

NEEs Geometric area	**0.022 cm^2**
Capture of OVA	5 µL, 30 min
Washing step	4 rinsing with 1% TWEEN 20 in 10 mM PBS
Blocking step	Blocking solution, soymilk 5%, 30 min
Washing step	4 rinsing with 1% TWEEN 20 in 10 mM PBS
Incubation I ab	5 µL of Anti-OVA (diluted 1:10), 30 min
Washing step	4 rinsing with 1% TWEEN 20 in 10 mM PBS
Incubation II ab	5 µL of II ab (diluted 1:50), 30 min
Washing step	4 rinsing with 1% TWEEN 20 in 10 mM PBS
EC parameters	Supporting electrolyte: 10 mM PBS pH 7; substrate: 0.1 M glucose; scan rate: 10 mV/s.

3.2.3_Sample preparation

To optimise the procedure and to test the selectivity of the OVA-immunosensor, different blocking agents and different egg samples were tested. Three different

blocking agents at different concentrations were prepared as described in Tab. 3.2. PVA, BSA and soymilk were diluted in 10 mM PBS.

Tab 3.2: Concentration of the blocking agents tested.

Blocking agent	Concentration
PVA	2.5%
Soy milk	5%
BSA	5%*

*concentration of BSA was increased to have a % comparable with soymilk.

The composition of egg samples containing different concentration of egg yolk, egg white and whole egg is listed in Tab. 3.3. All the samples were diluted in 10 mM PBS. The concentration of OVA in the samples was estimated considering that OVA is the 55% of the protein content of egg white. Egg white density from literature[88] is 1.04 g/mL. For the negative test, a sample containing 0.05 g of rabbit glue diluted in 10 mL 10 mM PBS was analysed.

Tab 3.3: Concentration of egg white in the samples prepared for the analysis with the immunosensor.

Egg sample	Concentration	Amount of OVA
Egg white	0.1 µL/mL	10 ng/mL
Mixture white/yolk	0.05/0.05 µL/mL	5 ng/mL
Egg yolk	0.1 µL/mL	//

3.3_Results and discussion

3.3.1_Cyclic voltammetric results

The electrochemical technique used to monitor the outcome of the measurements is cyclic voltammetry (as for the IgY-immunosensor). Three CVs of the redox mediator (0.1 mM FA^+ in 10 mM PBS) were recorded at the NEE for each of sample analysed, two in absence of the substrate (before and after the functionalization

procedure) and one in presence of the substrate. The typical recorded CVs are shown in Fig. 3.3. The dotted-black CV was recorded at the bare NEE and shows the reversible voltammetric behaviour of the mediator, with $E_{1/2}$ =+0.43 V (see Chapter 2.1). The full line black CV was recorded at the NEE after the complete procedure of preparation of the immunosensor (capture of the analyte on the PC surface of the NEEs, addition of blocking agent, incubation of primary and the secondary antibody); it is still evident the reversible behaviour of the mediator, only a small decrease of the anodic current can be appreciated. This electrochemical response can support the hypothesis that the biomolecules preferably bind on the PC part of the electrode surface, and the superficial gold nanodisks can freely exchange electrons with the solution. A remarkable change in the CV and the current value can be observed when the substrate (glucose) is added to the solution. Blue CV in Fig. 3.3 was recorded after the addition of the substrate. The CV presents a sigmoidal shape, where the cathodic peak is disappeared and the anodic peak increases, typical of an electrocatalytic process, analogous to the one observed for IgY sensor previously discussed. The limit current is almost 10 times higher than the peak current recorded at the bare NEE and after the preparation of the sensor. This current value is proportional to the amount of analyte immobilized on the electrode surface. This electrocatalytic cycle is observed in the oxidation direction by the interaction between the enzyme present in the labelled secondary antibody and its substrate, revealed by the redox mediator.

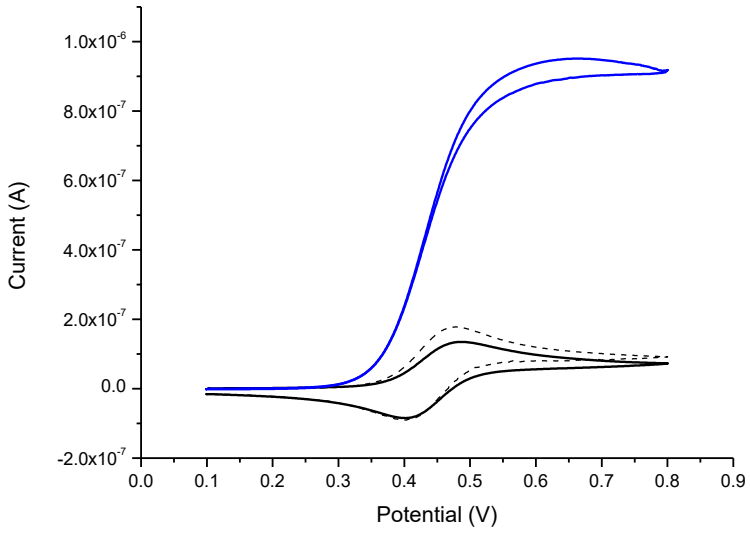

Fig 3.3: CVs of 0.1 mM FA^+ in 10 mM PBS recorded at the NEE at different times of the procedure: before the capture of OVA (dotted black line), after the incubation of a sample of egg white (full black line) and after the addition of the substrate, 0.1 M glucose (blue line). Scan rate 10mV/s.

The reactions that occur in the electrocatalytic cycle are the following[29] (2.1-2.3):

$$GOx(FAD) + \text{D-glucose} \rightarrow GOx(FADH_2) + \text{D-glucono 1,5-lactone} \qquad 3.1$$

$$FA^+ \leftrightarrows FA^{2+} + e^- \qquad 3.2$$

$$GOx(FADH_2) + 2FA^{2+} \leftrightarrows GOx(FAD) + 2FA^+ \qquad 3.3$$

First, the enzyme reacts chemically with its substrate (reaction 3.1), FAD (flavin-adenine dinucleotide, a component of the glucose oxidase enzyme) oxidises the glucose molecule and is reduced to $FADH_2$. The redox mediator FA^+ is oxidised at the electrode generating its oxidized form FA^{2+} (reaction 3.2) that regenerates the enzyme by the chemical reaction (3.3). The mediator is regenerated at the NEE, but this reaction cannot be appreciated via electrochemistry. The anodic peak current value depends on the amount of enzyme, which is directly related to the amount of the analyte captured by electrodes surface.

In the absence of egg white or ovalbumin on the sensor surface, the electrocatalytic cycle is not active. Fig. 3.4 shows the CVs recorded in the negative test, where rabbit glue was captured by the NEE instead of egg white. It is possible to observe that some differences occur after the addition of 0.1 M glucose, but the anodic and the cathodic peaks can still be identified. The presence of the two characteristic peaks indicate that some modifications of the surface occur, but the electrocatalytic cycle is not developed.

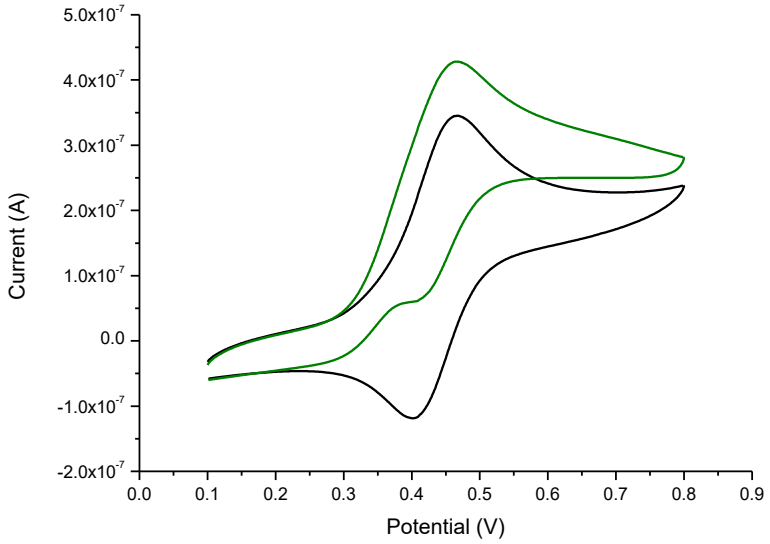

Fig 3.4: CVs of the redox mediator FA^+ in absence (black line) and presence (green line) of 0.1 M glucose at a NEE incubated in a sample containing rabbit glue. Electrolyte: 10 mM PBS, scan rate: 10 mV/s.

3.3.2_Optimisation of the substrate concentration

One of the critical parameters in the development of an immunosensor is the determination of the optimal substrate (glucose) concentration that ensure the complete activation of the electrocatalytic cycle. This is also important in order to quantify the amount of analyte captured on the electrodes (proportional to the catalytic current). To this aim, the secondary antibody labelled with GOx (diluted 1:50 as suggested by the producer) was directly immobilized for 30 minutes on the bare NEE, to guarantee the highest grade of functionalization of the bare surface with the label. The NEEs were then incubated with secondary antibody anti-antiOVA labelled with Gox. Fig. 3.5 shows the CVs recorded at the NEEs after addition of its substrate (glucose) at increasing concentrations, namely 0.01 M, 0.05 M, 0.1 M, 0.2 M and 0.3 M. From the analysis of these voltammograms, it can be noticed that for glucose concentration of 0.01 M and 0.05 M (Fig. 3.5 CVs a and b) there is an increase of the anodic signal and a decrease on the cathodic one, but the shape of the CVs is not fully sigmoidal. At glucose concentration 0.1 M (Fig. 3.5 CV c) the shape of the CV is completely sigmoidal and a further increase in glucose concentration results in a decrease of the maximum current (Fig. 3.5 CVs d and e). This decrement can be associated to the complete consumption

of the activity of the enzyme immobilized on the electrode and a loose of activity and reactivity because of its saturation [89,90].

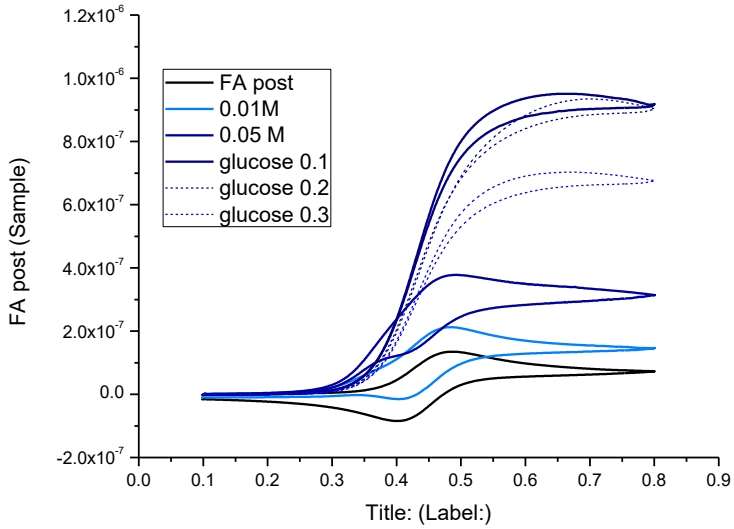

Fig 3.5: CVs of FA in 10 mM PBS on modified NEE with secondary antibody anti-antiOVA. Black line is recorded before the addition of the substrate, different blue full line CVs are recorded at increasing concentration glucose. Dashed lines are CV recorded with higher concentrations, but after reaching the saturation of the signal. The concentration of glucose is show in the legend. Scan rate: 10mV/s.

Fig. 3.6 shows the trend of the current values with the increment of the substrate concentration. At first (0.01 to 0.1 M glucose), there is a linear increment and the system reaches a plateau (0.1 to 0.2 M) and finally decreases (0.3 M). Considering the evolution of the data in Fig. 3.6, 0.1 M glucose concentration was chosen for the operation of the immunosensor since it ensures the development of a fully electrocatalytic cycle and highest activity of the enzyme.

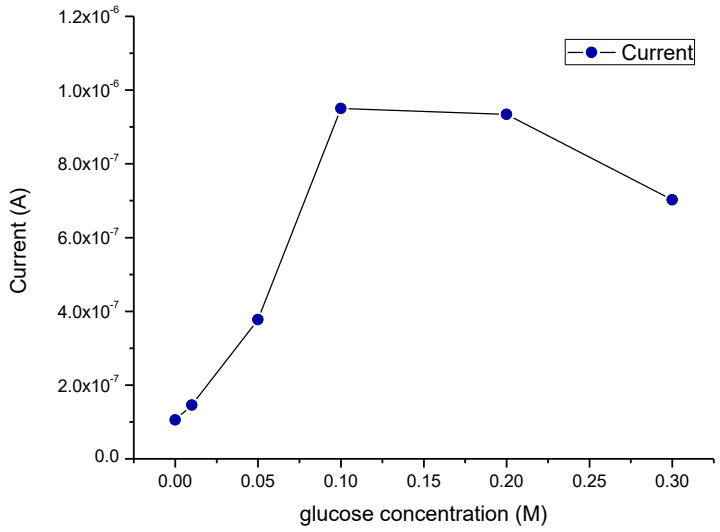

Fig 3.6: Plot of the electrocatalytic current values as a function of the substrate concentration.

3.3.3_Optimisation of the blocking step

To avoid nonspecific interaction that could decrease the selectivity of the immunosensor, the blocking of the electrode surface is necessary. The primary antibody anti-OVA proposed for this immunosensor is polyclonal, in order to ensure the identification of the protein also in degraded samples, that is an important aspect in the application to samples from cultural heritage, such as old painting samples. This choice was made to the slight detriment of the specificity of the test. BSA is one of the most used blocking agent[76,77,91], however, in this case, BSA could lead to some nonspecific interaction due to a partial recognition of the protein by the polyclonal anti-OVA primary antibody. To this aim, two other blocking agents were studied: polyvinyl alcohol and soymilk. According to literature, PVA is often used as blocking agent, with a good blocking efficiency[92,93]. Soymilk does not contain any animal protein, but contains proteins in high concentration, that can block the electrode surface[94]. BSA was also tested, to check if the supposed interaction actually occurs.

In this study, the bare electrodes were directly immersed in 1 mL of each blocking solution for 30 minutes, without the previous step of capture of the analyte. Following, the primary and secondary antibody were incubated on the electrodes.

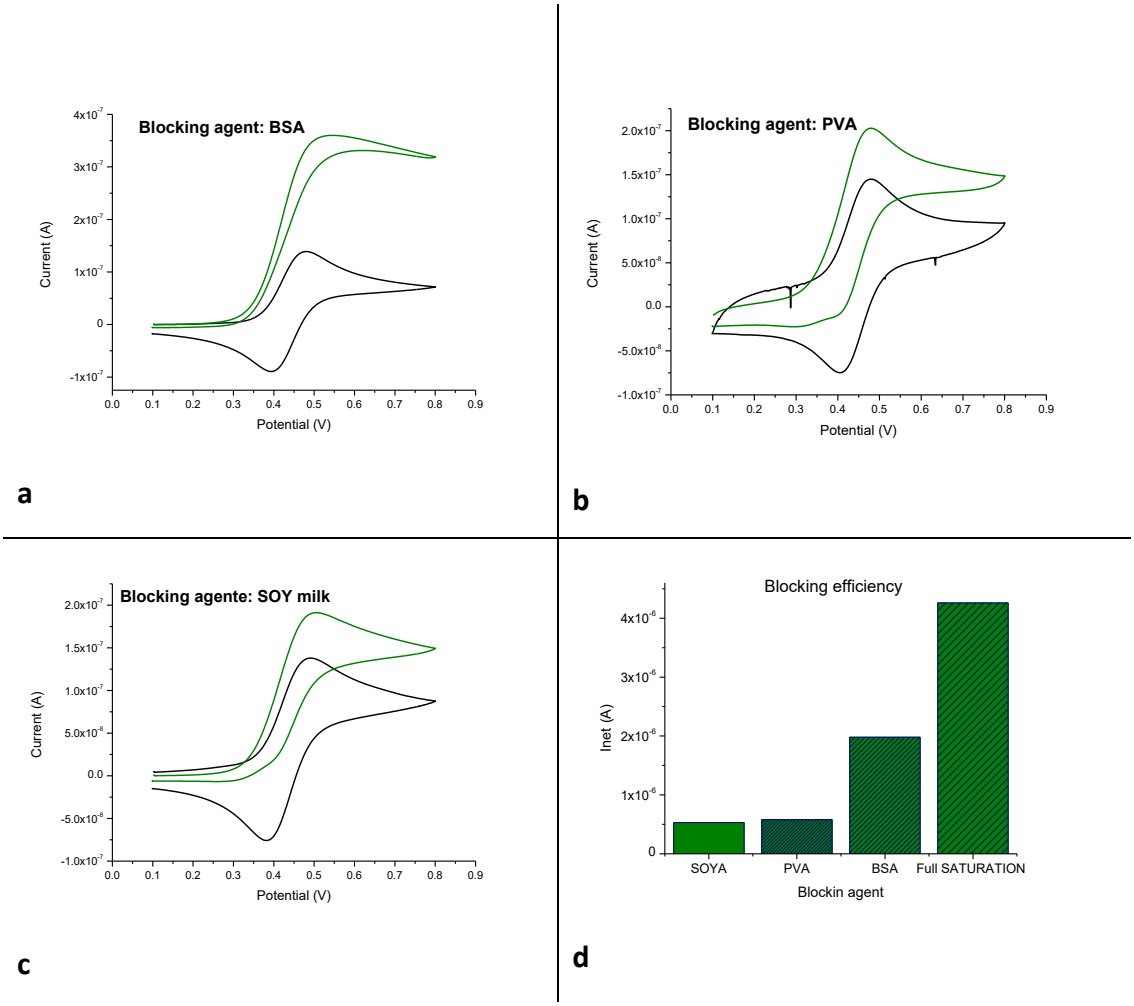

Fig 3.7: CVs FA^+ in 10 mM PBS before (black line) and after (green line) the addition of 0.1 M glucose for the different blocking agent tests: a) BSA 5%, b) PVA 2.5%, c) Soymilk 5%. Section d) of the figure shows a bar graph that reports the current values recorded after the addition of the substrate, compared with a current value obtain after the saturation of the substrate.

Fig. 3.7a shows the results obtained when blocking with BSA was tested. The catalytic current value observed ($4*10^{-7}$ A) is much lower than the one recorded when OVA is present on the electrode (usually electrocatalytic current reached when OVA is present is 10^{-6} A ca – Fig. 3.9). This suggests that the surface of the NEE was partially blocked since the electrocatalytic signal was detected. A different behaviour can be observed when PVA and soymilk were tested, since in both cases, the catalytic peak was not completely developed by the system, the anodic peaks are still present for both PVA and soymilk and a small cathodic peak can be appreciated in both cases see Fig. 3.7b and Fig. 3.7 c, respectively). The anodic current values are $1.5*10^{-7}$ A ÷ $2*10^{-7}$ A, similar

to the values recorded at the NEEs before the addition of the substrate (1.25^{-7} A–$1.5*10^{-7}$ A – black lines in Fig. 3.7).

Fig. 3.7 d reports the current values of the blocking tests compared with the current recorded when OVA was captured on the NEE (see below, Fig. 3.8). Clearly, BSA blocking efficiency is lower than PVA and soymilk. For the following tests, soymilk was chosen as blocking agent, because it is the agent that most successfully blocks the nonspecific interactions.

3.3.4_Test on egg samples

With the optimised immunosensing procedure (0.1 M glucose as the substrate and 5% soymilk as blocking agent), ovalbumin was identified in egg samples containing different amount of egg white and egg yolk. As done previously for the IgY-immunosensor, three samples (described in section 2.2.3) with a different amounts of egg white were analysed: a sample of pure egg yolk, a sample of pure egg white and a mixture 1:1 egg white and egg yolk were captured on the electrodes. Fig. 3.8 shows the CVs of the redox mediator recorded after the complete immunosensing procedure (black line for all the samples) and after the addition of the substrate (0.1 M glucose – red for egg yolk, purple for the mixture and blue for egg white) to each of the samples analysed. As shown in Fig. 3.8 red line CV, the sample containing only yolk presents a catalytic cycle with a small increase of the anodic current. This result can be related to the presence of a serum albumin in yolk that is partially recognised by the polyclonal nature of the primary antibody[95]. Nevertheless, the catalytic current value is slightly higher than the anodic current of the redox mediator recorded at the NEE after the complete immunosensing procedure. This result indicate the presence of a very low amount of protein linked with the primary antibody. The second sample analysed contained 50% of egg yolk and 50% of egg white. The CV recorded (Fig. 3.8 purple line CV) after the addition of the substrate cause the formation of a complete electrocatalytic cycle with a considerable increment of the catalytic current value. Same behaviour can be observe when only egg white was present in the sample (Fig. 3.8 blue line CV), but in this case the current increases considerably.

The inset in this figure reports the electrocatalytic current net (calculated as in the following equation) as a function of the sample analysed.

$$I_{net} = I_{pa} - I_{catal}$$

where I_{pa} is current of the anodic peak and I_{catal} is the electrocatalytic current. From the inset of Fig. 3.8, it is possible to observe that the electrocatalytic current increase with a slight linear trend.

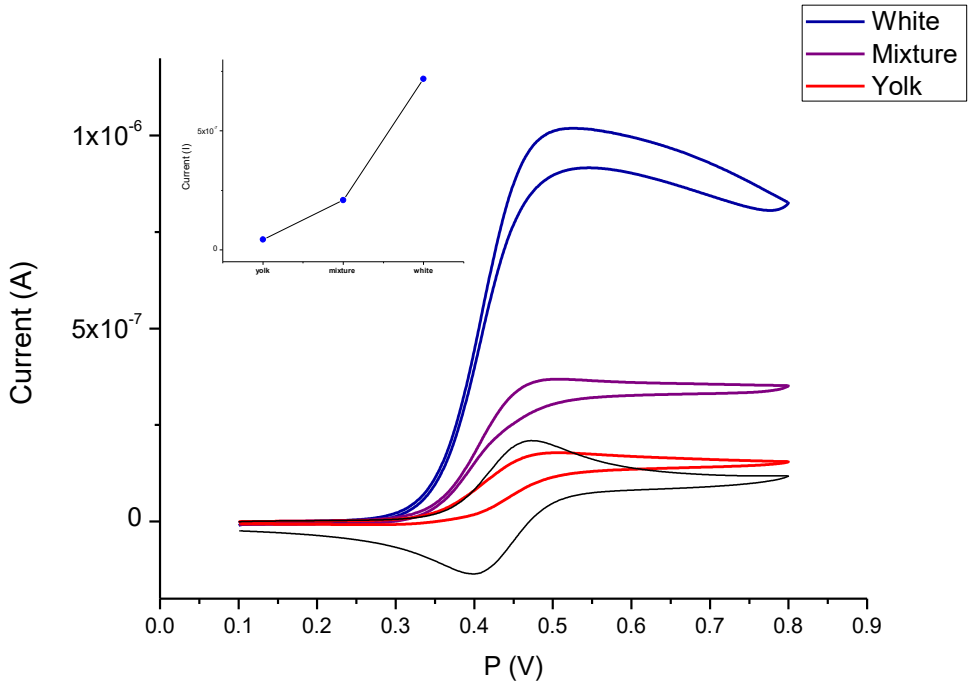

Fig 3.8: CVs recorded after the addition of 0.1 M glucose for the analysed samples: blue line – egg white; purple line – 1:1 mixture; red line – egg yolk. Insert: trend of the electrocatalytic increment as a function of the analysed samples.

3.4_Conclusion

An OVA- immunosensor was developed and the immunosensing procedure optimised. A polyclonal primary antibody was chosen for the detection of the protein in degraded samples, but this parameter does not affects the selectivity of the sensors, thanks to the proper blocking agent used: 5% soymilk. 0.1 M glucose was determined as the optimal concentration of the substrate to ensure the development of a full

electrocatalytic cycle. With the optimised conditions, the immunosensing procedure was applied on samples from egg. It was possible to identify OVA in egg white and in a 1:1 mixture prepared with egg white and egg yolk.

4_Application to cultural heritage

To test the efficiency of the IgY- and OVA- immunosensors presented in chapters two and three in the field of cultural heritage, mock-up samples were analysed with the proposed optimised sensors. These samples represent a complete and complex multilayer painting; indeed different proteinaceous binders were used, in the presence of oil, arabic gum and three inorganic pigments. Complexity of the samples is one of the most important parameters to check the applicability of the immunosensors. Considerations about the extracting procedure and the analysis on samples not containing the target proteins are presented in the chapter, besides the main results of the developed immunosensors on the mock-up samples.

4.1_Introduction

Identification of the materials used to produce a work of art is one of the critical step in the formulation of a preventive conservation project or in the choice of restoration products. To this aim, many classical analytical methods have been proposed (See 1.1.2), nevertheless researchers are still developing new and fast methods for the identification of organic and proteinaceous components in pieces of art.

Electrochemical techniques are widely used for the identification of pigments[96,97] and, most recently, to understand the stability of the pigments and to study pigments degradation[98]. On the other hand, despite their characteristic selectivity, high sensitivity and low costs, electrochemical immunosensors have been applied to this field only in the last three years, but their employment is improving. The first immunosensor for the identification of temperas was proposed by Bottari in 2014[59]. Egg yolk tempera was identified by an electrochemical immunosensor based on NEEs with IgY as the marker. A secondary antibody labelled with HRP was used for the antigen-antibody bound and to promote an electrocatalytic cycle after addition of the substrate and in presence of methylene blue as the redox mediator.

Another publication from the same year by Sciutto[99], reports the use of another electrochemical technique, scanning electrochemical microscopy (SECM), for the identification of ovalbumin in multilayer samples; this protein was chosen due to its abundance in egg white, as a target analyte for egg-based temperas and egg white based varnishes. As for the previous case, the secondary antibody used was labelled with HRP, but hydroquinone was proposed as the mediator.

The most recent work about the application of biosensor for protein recognition was published by Scarano in 2016[100]. In this case, a biosensor based on surface plasmon resonance (and not electrochemistry) was used for the detection of egg white and egg yolk in temperas; the method was also used to monitor the efficiency of novel cleaning method, with water-based highly viscous polymeric dispersions (HVPD).

In the present work, we applied the optimised immunosensor developed by Bottari (chapter 2) and the new electrochemical immunosensor based on gold nanoelectrodes ensemble for the identification of ovalbumin (chapter 3), for the

complementary identification of egg yolk and/or egg white based complex cross sections simulating tempera paintings.

4.2_Experimental

4.2.1_The samples

Twelve mock-up samples were kindly provided by KIK-IRPA (*Koninklijk Instituut voor het Kunstpatrimonium - Institut royal du Patrimoine artistique*), previously prepared by Ph.D. Stepanka Kuckova, inside her project: "*A bioanalytical view on artwork analysis: comparison of immunochemical techniques used for identification and localization of protein binders in paint cross-sections obtained from artworks – 2015*". All the main proteinaceous binders used in the production of a piece of art coexist in all the samples: egg white, egg yolk and whole egg, casein and collagen from four different animal glues (rabbit, fish, cow and gelatine). Each proteinaceous binder was separately mixed with three inorganic pigments: azurite ($Cu_3(CO_3)_2(OH)_2$, Kremer pigmente), chalk ($CaCO_3$, Janssen Chimica, Belgium) and cinnabar (HgS, s.a. UCB N.V. Belgium) and finally mixed with oil or arabic gum in different ratios (see below), as commonly prepared in the past[101]. From 5 to 6 layers were applied on a wood panel and each layer isolated with a 10% solution of Paraloid B72 (Rohm+Haas/Dow) in ethanol (Scheme 4.1). A small piece of each sample was taken from the wooden support and embedded in twelve cross-sections. The different layers were prepared as follows:

WHOLE EGG layer: whole egg was mixed with polymerised linseed oil in different whole egg/oil v/v ratios 3:1, 2:1, 1:1 and 1:2.

EGG YOLK layer: after accurate separation from egg white, egg yolk was mixed with linseed oil with the following yolk/oil v/v ratios: 2:1, 1.5:1, 1:1 and 1:2.

EGG WHITE layer: beaten egg white was mixed with arabic gum in the following egg white/arabic gum v/v ratios: 8:1, 4:1, 1:1 and 1:10.

CASEIN layer: pure casein (dissolved in a water/borax solution) was mixed with polymerised linseed oil in the following casein/oil v/v ratios: 2:1, 1:1, 1:5 and 1:10.

ANIMAL GLUES layer: animal glues were dissolved in hot water and applied pure.

OIL layer: polymerised linseed oil was mixed with previously prepared mixtures of azurite and animal glues or azurite and egg white in a 1:1 oil/glue or oil/egg white v/v ratio.

The protein content was calculated from the composition of each layer (on a dry base) considering for each proteinaceous binder the following protein content: casein and glue 100%, egg white 10%, egg yolk 16% and whole egg 12.5% (6.4% from egg white and 6.1% from egg yolk). Protein and oil contents are listed in Scheme 4.1, where all the samples are presented.

Samples are disposed on four (1-2-3-4) different wooden support and each support divided in three different zones (A-B-C). The samples are identified with a double code, considering both the bar (numeric code) and the zone in the bar (alfa code). Disposition of the samples on the bars is presented in Fig. 4.1.

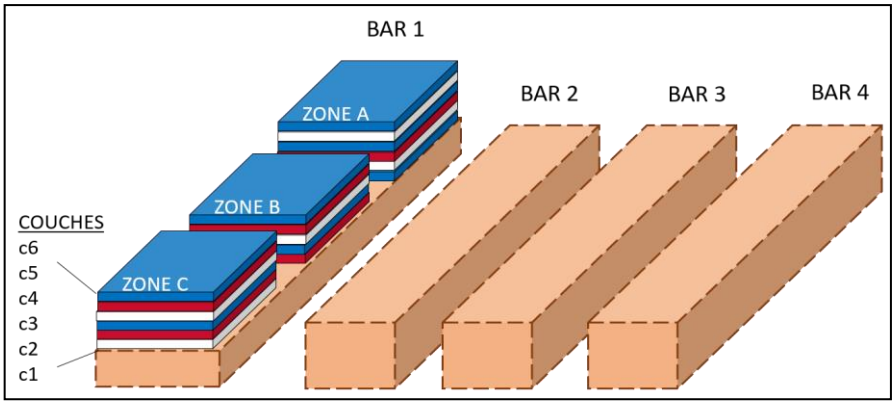

Fig 4.1: Disposition of the samples on wood support.

The amount of the egg components and whole egg is different for each sample. The trend of variation of these components in the table can be identified as follows.

Egg white: from Scheme 4.1, it is possible to observe that the amount of egg white decreases from Zone A to Zone C and from Bar 1 to Bar 4 (as indicated by arrow “egg white” in Fig. 4.2). This means that sample 1A has the highest amount of egg white, and sample 4C the lowest content.

	Layer	BAR 1 Organic binder	Pigment	% Prot	% Oil	BAR 2 Organic binder	Pigment	% Prot	% Oil	BAR 3 Organic binder	Pigment	% Prot	% Oil	BAR 4 Organic binder	Pigment	% Prot	% Oil
Zone A	6	OIL	AZU + rabbit g	0.6	55	OIL	AZU + fish g	0.5	46	OIL	AZU + beef g	0.6	48	OIL	AZU + egg whit	1	52
	5	Egg white (8:1)	$CaCO_3$	4.2	0	Egg white (1:1)	$CaCO_3$	3.1	0	Egg white (4:1)	$CaCO_3$	5	50	Egg white (1:10	$CaCO_3$	0.6	0
	4	Casein (2:1)	AZURITE	6.5	6	Casein (1:1)	AZURITE	6.1	11	Casein (1:5)	AZURITE	2.2	0	Casein (1:10)	AZURITE	0.7	48
	3	Egg yolk (2:1)	HgS	3.5	19	Egg yolk (1.5:1)	HgS	2.9	20	Egg yolk (1:1)	HgS	3.3	33	Egg yolk (1:2)	HgS	2.2	30
	2	Glue (rabbit)	$CaCO_3$	6.3	0	Glue (gelatin)	$CaCO_3$	3.2	0	Glue (beef)	$CaCO_3$	8.3	29	Glue (fish)	$CaCO_3$	6.9	0
	1	Whole egg (3:1)	AZURITE	5.7	20	Whole egg (2:1	AZURITE	5.9	25	Whole egg (1:1)	AZURITE	5.5	35	Whole egg (1:2	AZURITE	5.8	51
Zone B	5	Egg white (8:1)	AZURITE	2.2	0	Egg white (1:1)	AZURITE	1.4	0	Egg white (4:1)	AZURITE	2.8	0	Egg white (1:10	AZURITE	0.4	0
	4	Casein (2:1)	HgS	7.8	7	Casein (1:1)	HgS	11.1	22	Casein (1:5)	HgS	2	31	Casein (1:10)	HgS	0.6	41
	3	Egg yolk (2:1)	$CaCO_3$	6	32	Egg yolk (1.5:1)	$CaCO_3$	5.2	36	Egg yolk (1:1)	CaCO3	5.4	47	Egg yolk (1:2)	$CaCO_3$	3.3	45
	2	Glue (rabbit)	AZURITE	8.6	0	Glue (gelatin)	AZURITE	2.7	0	Glue (beef)	AZURITE	3.9	0	Glue (fish)	AZURITE	4.6	0
	1	Whole egg (3:1)	HgS	5	16	Whole egg (2:1	HgS	4.1	18	Whole egg (1:1)	HgS	5,8	36	Whole egg (1:2	HgS	3.3	36
Zone C	6	OIL	AZURITE + gel	0.2	44												
	5	Egg white (8:1)	HgS	2.5	0	Egg white (1:1)	HgS	1.9	0	Egg white (4:1)	HgS	2.9	0	Egg white (1:10	HgS	0.4	0
	4	Casein (2:1)	$CaCO_3$	12.5	11	Casein (1:1)	$CaCo_3$	11.6	22	Casein (1:5)	$CaCO_3$	4.3	65	Casein (1:10)	$CaCO_3$	1.1	77
	3	Egg yolk (2:1)	AZURITE	4.4	21	Egg yolk (1.5:1)	AZURITE	2.8	19	Egg yolk (1:1)	AZURITE	3.2	28	Egg yolk (1:2)	AZURITE	2.6	37
	2	Glue (rabbit)	HgS	2.7	0	Glue (gelatin)	HgS	1.5	0	Glue (beef)	HgS	2	0	Glue (fish)	HgS	1.6	0
	1	Whole egg (3:1)	$CaCO_3$	8.2	29	Whole egg (2:1	$CaCO_3$	9.1	37	Whole egg (1:1)	$CaCO_3$	12	59	Whole egg (1:2	$CaCO_3$	11	0.69

Egg white (Egg white : arabic gum)
Casein (Casein : Oil)
Egg yolk (Egg yolk : Oil)
Glue
Whole egg (Whole egg : oil)
OIL (Azurite coated with egg white / rubbit guee and then bonded oil)

Insulation between layers 10% PARALOID

Scheme 4.1: Schematic representation of the samples and their position in Bars and Zones. Enlightened rows show the layers with highest or lowest content of egg yolk, egg white, or whole egg.

Egg yolk: the amount of egg yolk decreases from Bar 1 to Bar 4, but it is constant in each bar from Zone A to Zone C (see arrow “egg yolk” in Fig. 4.2).

Whole egg: samples were prepared with the same structure as egg yolk, so the amount of egg yolk decreases from Bar 1 to Bar 4, but it is constant from Zone A to Zone C (as indicated by arrow “whole egg” in Fig. 4.2).

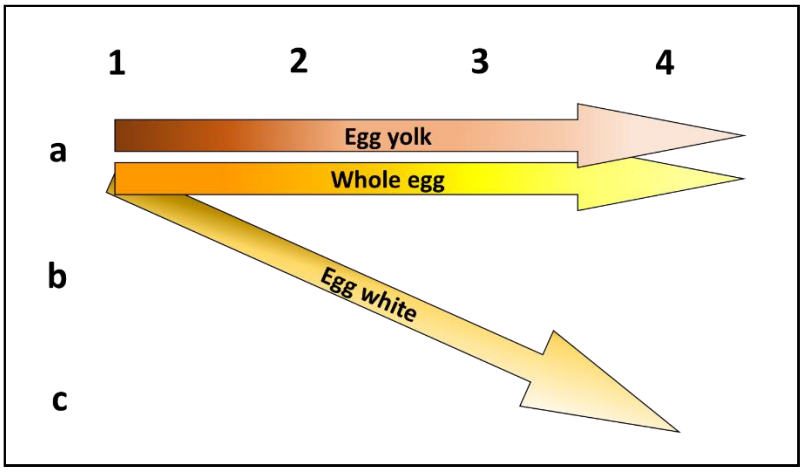

Fig 4.2: Decrease trend of egg white, egg yolk and whole egg in the samples. Arrows show the decrease direction. If not indicated, the egg component content is constant.

The total amount of egg white and egg yolk has to be considered as the summation of the contribute from the layers containing the single component and whole egg layer. A complete overview of the samples and the amount of protein contained in each sample composition is extensively presented in Scheme 4.1.

4.2.2_Materials

NEEs (prepared as described in chapter 2.1), FA^{+}, MB, 10 mM PBS, TWEEN 20, BSA, H_2O_2 and glucose were from sigma Aldrich. The secondary antibody goat anti-IgY (HRP conjugated) was from Immunology Consultants Laboratory (USA), diluted 1:10 for the immunosensing procedure. Primary and secondary antibody anti-OVA were affinity purified Rabbit anti-chicken Ovalbumin from Immunology Consultants Laboratory Inc. diluted 1:10 in 10 mM PBS as suggest by the producer; secondary antibody: goat-anti-Rabbit IgG H&L (Glucose Oxidase) from Abcam diluted 1:50 in 10mM PBS as suggested by the producer. Soymilk was achieved from a local supermarket.

Measurements were carried in a typical thee electrodes cell, NEEs as working electrodes, Ag/AgCl KCl saturated reference electrode and Pt wire as counter electrode. Autolab pgstat 101 controlled with the software NOVA 1.1 and CH1000a instrument were used for electrochemical measurements.

4.2.3_Procedure

The cross sections were initially polished with polishing paper (Silicon Carbide 1200/4000) before protein extraction. 10 µL of 10 mM PBS were added on the cross-section surface and left for two hours to extract the proteins from the samples (See below for details).

4.3_Results and discussion

4.3.1_Extraction of IgY and OVA

Few considerations on the extraction procedure are initially presented. First of all, egg white and egg yolk an high solubility in water medium at a neutral pH[102], in particular, IgY is part of the water-soluble portion of egg yolk proteins[12], and ovalbumin can be easily solubilised with pH values from 6 to 9[103]; for these reasons we chose pH 7 to conduct the protein extraction step.

The pigments present in these mock-up samples, azurite – $Cu_3(CO_3)_2(OH)_2$, chalk – $CaCO_3$ and cinnabar – HgS, are all water-insoluble inorganic pigments[104,105], so the extraction medium used does not dissolve the pigments that are not transferred in the solution.

Oil and arabic gum used in mixture with the proteinaceous binders are also water insoluble. For this reason, the extracted solution should not contain any other organic material except for the water-soluble yolk and white from eggs.

Casein is soluble in water only when borax, ethanol or other chemicals are added in high percentage, therefore, casein can be considered not soluble in PBS at pH 7[106–108].

Animal glue is water-soluble only under heating conditions; at room temperature, it is not solubilised.

Despite all these considerations, we could not completely exclude that a low amount of non-water soluble materials and small amounts of the inorganic pigments were transferred in some extent with the soluble proteins in the extracting medium, especially due to the complexity of the samples and the close contact among all the components in the dried mixture. This factor may mainly affect the shape of the voltammograms (see 4.3.4.3) that can reflect in an increase of the ohmic resistance, if these compounds adsorb on the electrodes surface.

On these bases, 10 mM PBS at pH 7 was chosen as extracting medium. 10 µL were enough both to completely cover the exposed portion of the cross-sections and to obtain adequate amount of solution to perform the following step of capture of the protein on the electrode surface. After two hours, the drop was collected (usually 9 µL out of 10 were recovered) and centrifuged for 10 minutes to deposit eventual pigment powder present in the drop. After centrifugation, 5 µL were taken from the extract and incubated on the NEE. All the mock-up samples in cross-section were analysed twice with both immunosensors, and after each extraction, the cross-sections were re-polished. The immunosensing analytical procedures for IgY and OVA are the same as those presented in chapter 2 and 3, however they are briefly summarised in Tab. 4.1.

Tab 4.1: Brief summary of the analytical procedures.

NEEs Geometric area	**0.022 cm^2**	**0.022 cm^2**
Capture of the protein	5 µL, 30 min	5 µL, 30 min
Washing step	4 rinsing with 1% TWEEN 20 in 10 mM PBS pH 7	4 rinsing with 1% TWEEN 20 in 10 mM PBS pH 7
Blocking step	blocking solution, BSA 1%, 30 min	blocking solution, soymilk 5%, 30 min
Washing step	4 rinsing with 1% TWEEN 20 in 10 mM PBS pH 7	4 rinsing with 1% TWEEN 20 in 10 mM PBS pH 7
Incubation I ab	//	5 µL of anti-OVA (diluted 1:10), 30 min

Washing step	4 rinsing with 1% TWEEN 20 in 10 mM PBS pH 7	4 rinsing with 1% TWEEN 20 in 10 mM PBS pH 7
Incubation II ab	5 µL of 0.01 mg/mL anti-IgY HRP	5 µL of II ab (diluted 1:50), 30 min
Washing step	4 rinsing with TWEEN 20 in 10 mM PBS pH 7	4 rinsing with TWEEN 20 in 10 mM PBS pH 7
EC parameters	Mediator: 0.1 mM MB, supporting electrolyte: 10 mM PBS pH 7; substrate: 0.5 mM H_2O_2; scan rate: 10 mV/s.	Mediator: 0.1 mM FA^+, supporting electrolyte: 0.1 M PBS pH 7; substrate 0.1 M glucose; scan rate: 10 mV/s.

4.3.2_Cyclic voltammetric results

The redox mediators for each immunosensor were chosen on the basis of the two different enzymes labelled to the secondary antibodies. As shown in Fig. 4.3, the cyclic voltammetric behaviour of the two redox mediators present the typical peak-to-peak shape with $E_{1/2}$ values of -0.18 V and 0.43 V for MB and for FA^+ respectively. It is evident that there is not overlay in the potential windows and, in particular, the reduction peak of MB (-0.2 V) and the oxidation peak of FA (+0.47 V) are very well separated.

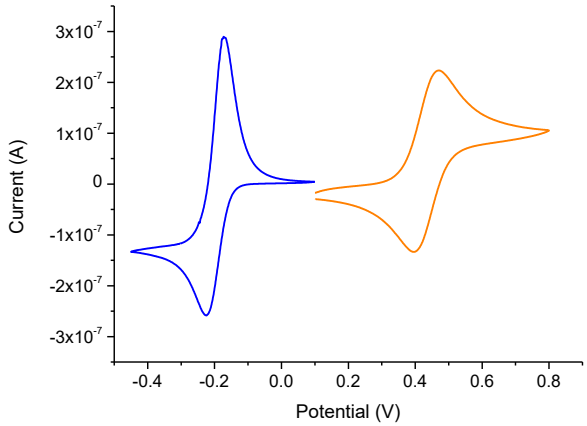

Fig 4.3: Cyclic voltammograms of the two redox mediators used for the immunosensors: MB (blue) and FA^+ (orange). Concentration of both mediators: 0.1 mM in 10 mM PBS. Scan rate 10 mV/s.

A similar situation is obtained when the substrates that produce the electrocatalytic cycle are added. As shown in Fig. 4.4, the electrocatalytic current develops in two different directions, one in the oxidation (MB and H_2O_2) and the other in the reduction (FA^+ and glucose) region. This behaviour is a premise of a possible development of a multianalyte electrochemical immunosensor.

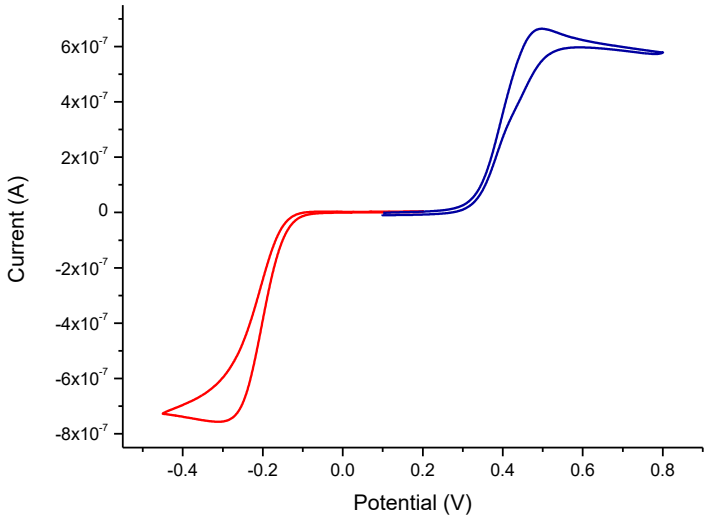

Fig 4.4: Cyclic voltammograms of the two redox mediators used for the immunosensor after the addition of the substrates 0.5 mM H_2O_2 (red line) for IgY immunosensor, and 0.1 M glucose (blue line) for OVA immunosensor.

4.3.3_Preliminary tests on samples without IgY and OVA

In order to verify the possible role of nonspecific interactions, at first some "negative" samples were analysed using oil or animal glue or casein alone as the binder. In principle, none of these constituents should be recognised by anti-IgY or anti-OVA, however, these expectations need to be confirmed by experimental evidences. To this aim, oil, casein and animal glue were mixed with azurite, cinnabar and chalk respectively. The resulting samples were incubated on a NEE, washed and incubated again according to the procedure in Tab. 4.1. Finally, the CV responses were recorded in electrolyte solutions containing for IgY first MB and after MB + H_2O_2; and for OVA first FA^+ and after FA^+ + glucose. Results are shown in Fig. 4.5.

Sample	IgY-immunosensor	OVA-immunosensor
Oil azurite	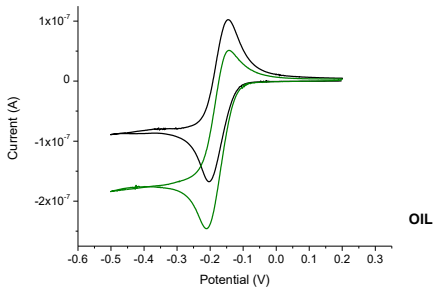	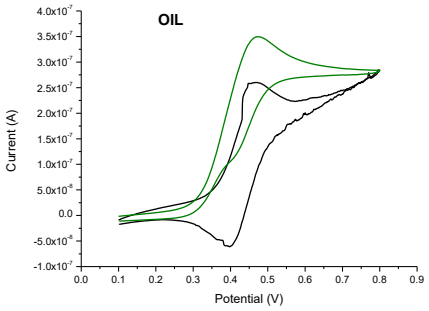
Glue cinnabar	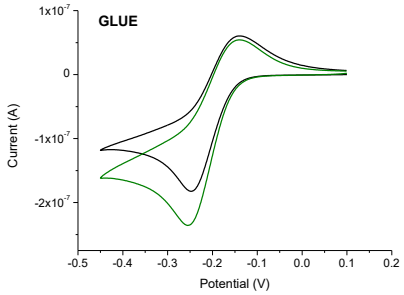	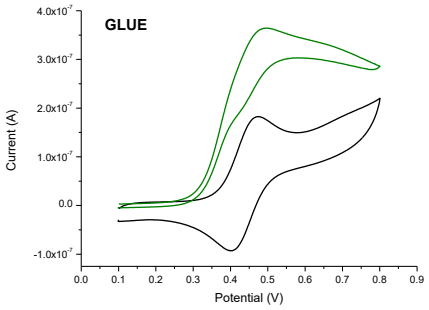
Casein chalk	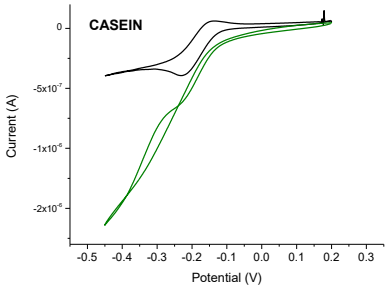	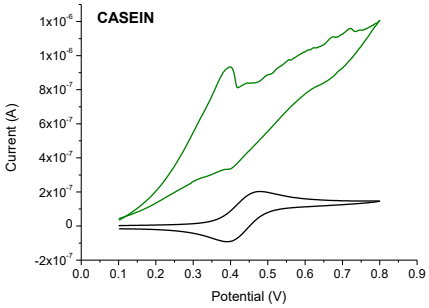

Fig 4.5: Results of the "negative" tests performed on representative samples. Black CVs were recorded after the complete immobilisation procedure, while green CVs were recorded after the addition of the relevant substrate.

For the oil/azurite case, only minor changes were observed in the CVs after the addition of the relevant substrates (H_2O_2 for IgY and glucose for OVA). This suggests that only minor nonspecific interactions occurred between the anti-IgY or anti-OVA antibodies with the water extract obtained from these samples.

For the glue/cinnabar case, the addition of H_2O_2 causes a slight increase of the MB reduction peak, while the oxidation peak remains practically unchanged. This indicates only minor interactions not related to the binding of the labelled anti-IgY-HRP with the extract. A different situation is observed for the anti-OVA antibodies, since the addition of glucose causes the partial appearance of an electrocatalytic process, suggesting that “some” nonspecific interactions could occur in this case, however we can point out that the electrocatalytic increase in the oxidation current is much lower than the one detected for OVA containing samples (see below).

For the casein/chalk case, the addition of the substrate caused an increase of the cathodic current; however, these changes are very different from those expected in the case of a pure electrocatalytic process.

We can conclude that even if we cannot exclude the occurrence of nonspecific interactions between anti-IgY and anti-OVA with oil, glue or casein, the effects observed in the voltammograms are negligible with respect to those expected for really “positive” samples.

4.3.4_Results on the mock-up samples

The immunosensing tests were performed twice on each of the 12 cross-sections. Following, only representative results will be extensively shown and discussed, while all the CVs recorded relevant to the 24 tests will be presented in appendix A.

4.3.4.1_Egg yolk

At first, we focused on the determination of IgY in the cross sections where a layer very rich or very poor of egg yolk is present. In particular, we present here the results for IgY extracted from the samples listed in Tab. 4.2, where the amount of proteins from egg yolk ranges from 2.2% (sample 4A) to 6% (sample 1B) of the total protein content of the dried mixtures. Difference between maximum and minimum is not so relevant, and the contribution from the layer prepared with whole egg was considered, as shown in Tab. 4.2 where the estimation of egg protein contents are indicated.

Tab 4.2: Protein percentage content in egg yolk and whole egg in the listed samples.

Sample	Egg yolk (%)	Whole egg (%)	Yolk + whole	Total yolk
1B	6 (max)	5 (2.3 % yolk)	8.3	High
4C	2.6	11 (5.1 % yolk)	7.7	High
4A	2.2 (min)	5.8 (2.7 % yolk)	5.9	Average
4B	3.3	3.3 (min) (1.5 % yolk)	4.8	Low

The voltammetric responses recorded with the IgY-immunosensor for samples 4C and 4B are shown in Fig. 4.6 a and b, respectively.

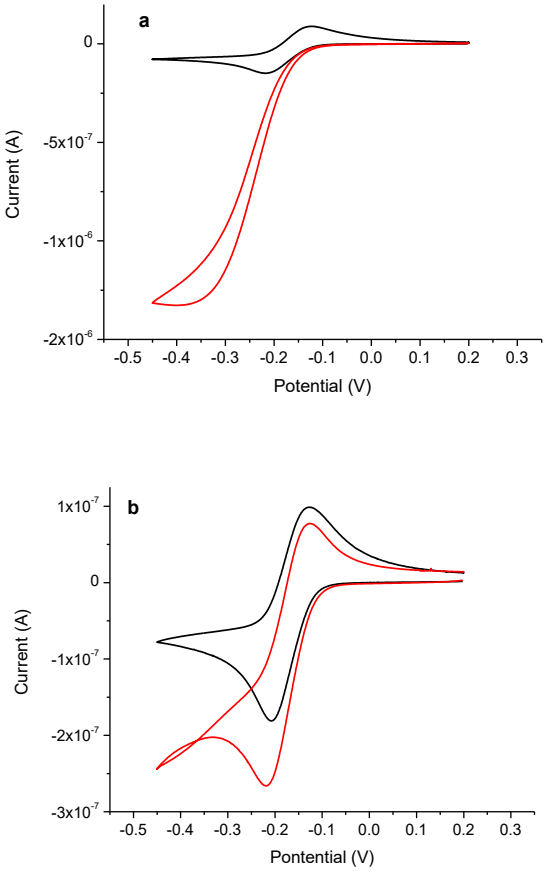

Fig 4.6: CVs recorded for samples 4C (a) and 4B (b) before (black line) and after the addition of the substrates (red lines).

The CV reported in Fig. 4.6a shows that a high cathodic electrocatalytic current was observed when H_2O_2 was added to the extract from sample 4C (high yolk content). Electrocatalytic current recorded for sample 4C is $1.5*10^{-6}$, indicating not only the

presence of the protein, but also that it is present in high concentration. On the other hand, when sample 4B was analysed, the addition of the substrate did not cause any electrocatalytic cycle (Fig. 4.6b, being the sample with the lowest overall amount of yolk. These evidences are in agreement with what expected, indeed the immunosensor response is proportional to the amount of IgY content in the extract from the cross-sections.

We report Tab. 4.4 the general results achieved for both the repetitions of the IgY-immunosensing procedure applied for the 12 samples. In this table results are represented as (+) a positive response and (-) the negative one.

The analysis of the results presented in this table evidence that for 7 of the 12 samples it was possible to obtain a double positive results, indicating the presence of egg yolk in the cross-sections. For 3 of the 12 samples it was possible to identify egg yolk only in one of the two repetitions of the test, and only for 2 samples it was not possible to recognise the target protein. As previously said, sample 4B is the one with the lowest amount of yolk (egg yolk + whole egg); sample 2C is another sample poor of egg yolk (Scheme 4.1 or Appendix A). It has to be considered that egg yolk and whole egg layers were prepared mixed with polymerised linseed oil, and even if does not cause any nonspecific interaction (see 4.3.2), the oil can affect the CVs pattern, that are then considered as a negative result. Similar evidence are in agreement with those previously observed by Bottari.

Tab 4.4: Results achieved for the immunosensing of IgY.

Sample	TEST 1	TEST 2	Sample	TEST 1	TEST 2
1A	+	+	**3A**	+	+
1B	+	+	**3B**	+	-
1C	-	+	**3C**	-	+
2A	+	+	**4A**	+	+
2B	+	+	**4B**	-	-
2C	-	-	**4C**	+	+

4.3.4.2_Egg white

Following, we focused on the determination of OVA in the cross sections where a layer very reach or very poor of egg white is present. In particular, we present here the results for OVA extracted from the samples listed in Tab. 4.5 where the amount of proteins from egg white ranges from 0.4% (samples 4B and 4C) to 5% (sample 3A) of the total protein content of the dried mixtures. To have a complete overview of the egg white content, it is necessary to consider also the contribution of the layers prepared with whole egg. Tab. 4.5 shows the samples that contain the highest and lowest amount of egg white, considering both the contributions.

Tab 4.5: Protein percentage in egg white and whole egg in the listed samples.

Sample	Egg white (%)	Whole egg (%)	white + whole	Total white
3A	5 - max	5.5 (3 % white)	8	High
3C	2.9	12 (6.5 % white)	9.4	High
4B	0.4 - min	3.3 - min (1.8 % white)	2.2	Very low
4C	0.4 - min	11 (5.9 % white)	6.3	Low

The voltammetric responses recorded with the OVA-immunosensor for samples 3A and 4B are shown in Fig. 4.7 a and b, respectively.

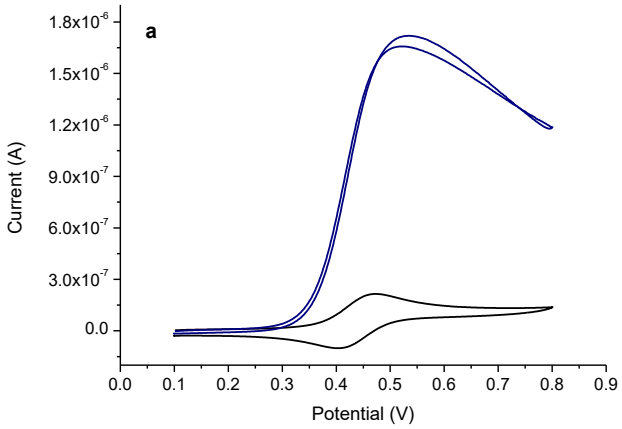

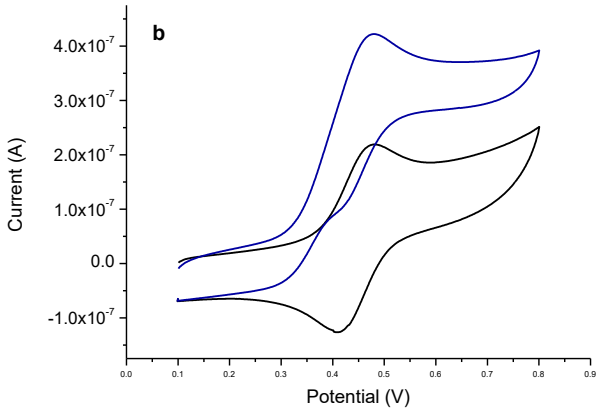

Fig 4.7: CVs of FA recorded after the complete procedure of preparation of the OVA immunosensor (black line) and after the addition of 0.1 M glucose (blue line) for sample 3A(a) and 4B(b).

From Fig. 4.7a, it is possible to observe that in the case of sample 3A, the electrocatalytic cycle is well developed, the cathodic peak is absent and the anodic current presents a remarkable increment. This result supports the presence of egg white in high quantity in the cross section and so, a high quantity of the target protein. Electrocatalytic current value is $1.5*10^{-6}$ A. Similar electrocatalytic current values (in the order of magnitude of 10^{-6} A) were recorded also for samples 3C (CVs of this sample are presented in appendix A). When the immunosensing procedure was performed on samples extracted from cross section 4B, the electrocatalytic cycle is not completely developed. As shown in Fig 4.6b, there is an increase in the anodic peak, however, the cathodic peak did not disappeared completely.

We report Tab. 4.6 the general results achieved for both the repetitions of the OVA-immunosensing procedure applied for the 12 samples. Positive results are presented as (+), while negative results are presented as (-).

The analysis of the results presented in this table, confirms that OVA from egg white can be easily identified both when it is present in layers prepared with pure egg white or as a component of whole egg tempera, even in samples containing an overall very low amount of the target protein. Indeed, the high sensitivity of the OVA-immunosensor allowed the identification of OVA in both or at least in one of the two tests for all the samples except for sample 4B, that is the one with the very lowest amount of egg white in the layers.

Tab 4.6: Results achieved for the immunosensing of OVA.

Sample	TEST 1	TEST 2	Sample	TEST 1	TEST 2
1A	+	+	**3A**	+	+
1B	+	+	**3B**	+	+
1C	+	+	**3C**	+	+
2A	+	+	**4A**	+	+
2B	-	+	**4B**	-	-
2C	+	+	**4C**	+	+

Considering the results obtained with both immunosensors, it can be noticed that OVA-immunosensor could recognize the target protein in more cases than the IgY-immunosensor. This result can be associated with the composition of the egg white layer, since egg white is mixed with arabic gum, instead of linseed oil as in layers of egg yolk.

4.3.5_Casein and glue effect

Casein and animal glues are present in the cross sections in different concentrations. As discussed in 4.3.1, casein is not water-soluble and animal glue is soluble only in heated water. Nevertheless, due to the complexity of the samples, it is possible that these two components are transferred in the extracting solution even in some small extent. In this case, a small amount of these two proteins can be captured by the NEEs and the CVs patterns before and after the addition of the substrate are considerably different with respect to the ones shows until now. This behaviour is evidenced in Fig. 4.15, where the CVs recorded with the IgY and OVA-immunosensors applied on sample 1A are presented. This sample is characterized by a high content of these two proteins, indeed casein content is 6.5% and animal glue content is 6.3%.

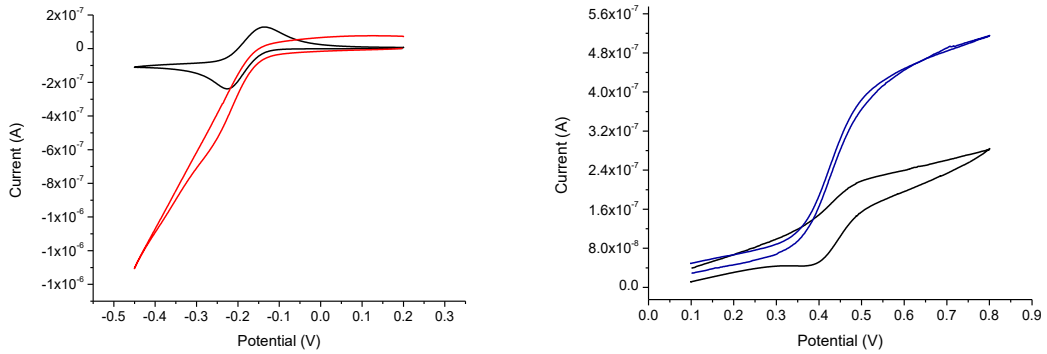

Fig 4.8: Effect of casein in the CVs, (left: CVs before and after the addition of 0.5mM H_2O_2 and right: CVs before and after the addition of 0.1M glucose for samples taken from cross section 1A.

It is possible to observe that the shape of the CVs is characterized by a great resistance that evolves in the same direction of the electrocatalytic current. Such effect is observed both for IgY or OVA detection. Recognition of the target proteins is not inhibited by the presence of casein or glue, preserving the reliability and selectivity of the immunosensors, but quantitative or semi-quantitative information cannot be achieved by these CVs. The resistance can be associated to the intrinsic sticky nature of these two proteins that adsorbs to the NEEs surface modifying its electrochemical behaviour. It is worth to note that casein and animal glue are used pure for the samples preparation, and as specified in 4.1, casein and collagen layers contain 100% of protein. This “casein and glue effect” is present in some of the samples taken from BAR 1 and 2, where their content is very high. Samples taken from BAR 3 and 4 never showed this behaviour.

4.4_Conclusion

The electrochemical immunosensors developed and optimised for the identification of relevant egg proteins used in the production of artworks were successfully applied to complex mock-up samples simulating egg-based temperas. An extracting procedure of two hours carried out with 10 mM PBS at pH 7. Only water-soluble proteins, such as IgY and OVA were extracted from the cross-section and in principle no other components of the samples were extracted. Tests on samples not containing the target proteins were carried out, to investigate possible nonspecific

interaction between other proteins in the samples and the primary antibodies. Lastly, the application of both the immunosensors furnished complete information about the composition of the samples. It was possible to detect IgY in 10 of the 12 samples, despite egg yolk and whole egg are in a mixture with polymerised linseed oil. One of the samples with a negative result contained the lowest amount of egg yolk + whole egg. With the OVA-immunosensor, it was possible to identify the protein in 11 of the 12 samples and also in this case the sample that gave a negative result is the one containing the lowest amount of egg white + whole egg. The main influence of casein and glue was studied and reflects in an increase of the resistance, without hindering completely the response.

5_Application to food supplements

IgY is an interesting protein that can find application in many fields, such as health and food. Its determination can be of medical and food industry interest. In the present chapter, we present the application of the IgY-immunosensor described in chapter 2 to the monitoring of an IgY extracting procedure present in literature, to evaluate its efficiency. Following we propose the application of the sensor in the identification of the analyte in food supplements that undergone an industrial treatment such as freeze-drying. In both cases, the results were compared (and confirmed) with electrophoresis and western blot assays.

Results shown in this chapter were partially published in "Chiara Gaetani, Emmanuele Ambrosi, Paolo Ugo, Ligia M. Moretto: Electrochemical Immunosensor for Detection of IgY in Food and Food Supplements. Chemosensors 2017, 5(1), 10".

5.1_Introduction

Due to its importance and wide range of application fields, many IgY-extracting procedures were studied and can be found in literature[12,18]. Purification methods can be divided into three groups based on: 1) precipitation[18], 2) chromatographic[109] and c) ultrafiltration[110]. All of them ensure a high yield, but the costs are different. The most common and less expensive methods for the extraction of IgY are those based on precipitation. Monitoring the IgY-isolation procedure can be useful in order to understand the function and the efficiency of the methods. In this work we present the systematic analysis one of the most common procedure, carried out with three PEG precipitations and followed by two dialysis, proposed by Pauly[67].

With the purpose to further study the stability of IgY, we investigated the protein in food that undergone an industrial treatment. Among the treatments used in food preparation, freeze-drying is one of the most common, used for eggs since the second half of the past century[111]. Most of the papers in literature regards the preservation of the rheological properties of egg yolk, due to the necessity of using the freeze-dried product in the production of food supplements, but they are not focused on preserving the protein structures and functionalities[112,113]. We had the chance to investigate stability of IgY that undergone a freeze-drying treatment in food supplements for sportsmen.

In this chapter, to better evaluate the results, we compare the results obtained with the IgY-immunosensor with those obtained with sodium dodecyl sulphate polyacrylamide gel electrophoresis, a typical methods used to separate proteins and western blot, that is based on the same bases of the immunosensor.

5.2_Experimental

5.2.1_Materials

NEEs were prepared as described in chapter 2.1; MB, PBS, TWEEN 20, BSA, H_2O_2, PEG 6000 and dialysis membrane were from Sigma Aldrich. The secondary antibody goat anti-IgY (HRP conjugated) was from Immunology Consultants Laboratory (USA), diluted 1:10 for the immunosensing procedure.

Freeze-dried eggs (egg white and egg yolk, separately) were from a sport-related company specialized in the production of freeze-dried products and proteins for sportsmen.

Measurements were carried out in a typical three electrodes cell, NEE as working electrodes, Ag/AgCl in KCl saturated as reference electrode and Pt wire as counter electrode. CH1000a with its CHI software was the instrument was used for electrochemical measurements.

5.2.2_Extraction procedure

The IgY extraction procedure, proposed by Pauly in 2011[67], was followed step by step with the IgY-immunosensor, electrophoresis and western blot. The procedure consists of three precipitation steps with PEG and two dialysis as presented in scheme 5.1. In the first step of the procedure egg yolk was separated from egg white and mixed with PEG at 3.5 % in weight in 10 mM PBS. It causes the precipitation of the lipid portion (pellet A) of egg yolk and the solubilisation of IgY and other soluble proteins in PBS (supernatant A). In the second precipitation step, PEG 8.5% is added to the supernatant A with the aim to separate soluble and not soluble proteins from egg yolk. The insoluble portion of the proteins is in the supernatant (supernatant B), while IgY and other soluble proteins precipitate with PEG in a white pellet (pellet B). This pellet is dissolved in PEG 12% in PBS. Also in this case, IgY precipitates (pellet C), while the other soluble portion of egg yolk proteins is in the supernatant (supernatant C). Following, two steps of dialysis have the aim to further purify IgY, the first in NaCl is carried out overnight, while the second in PBS takes three hours.

The products of all the steps (except pellet A) were analysed with the electrochemical immunosensor and SDS-PAGE and WB. Two samples of the saline solutions from the dialysis membrane were analysed, as well as the final solution containing IgY, in total 7 samples were collected during the extraction-purification procedure.

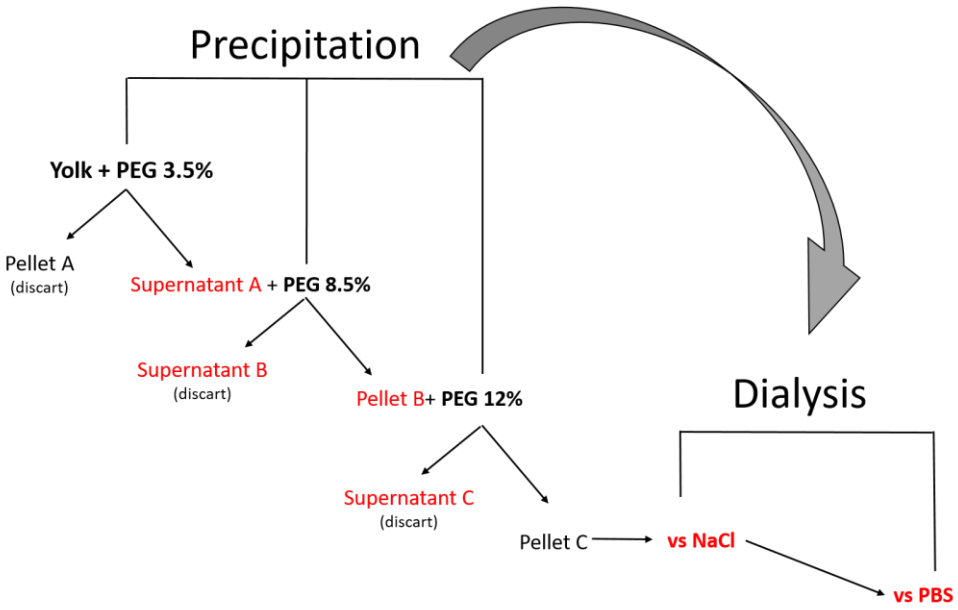

Scheme 5.1: Schematic representation of the IgY extracting procedure.

5.2.2_Industrial samples preparation

Freeze-dried egg samples were prepared following indications provided by the company, that were the mixing of 15–45 g of powder in 150–200 mL of water or milk. For our purposes, the proteins were extracted in acetate buffer 0.2 M at pH 5, as proposed for the immunosensor analysis, directly from the freeze-dried product instead of using water or milk. The preparation of the samples is summarized in Tab. 5.1. One sample of freeze-dried egg white and two samples of freeze-dried egg yolk at different concentrations were analysed with the IgY-electrochemical immunosensor. For each sample, 1.5 g of powder was dissolved in 25 mL of acetate buffer; the sample containing egg yolk was further diluted to obtain a lower concentration value. Yolk concentration was calculated considering the dilution factor. Percentage of the protein contents in the samples declared by the company are reported in column 5 of Tab. 5.1.

Table 5.1: Description of the freeze-dried samples.

Sample	Powder (g)	Acetate Buffer pH 5 (mL)	Egg Yolk g/mL	Protein Content* (%)
Egg white powder	1.5	25	0	79
Egg yolk powder	1.5	25	0.06	35

"	1.5	250	0.006	35

* Protein content declared by the producer.

5.2.3_SDS PAGE and WB

SDS-PAGE and Western blot (WB) analysis were performed according to the following procedure. Samples were loaded on 12% polyacrylamide discontinuous gels[114] under reducing condition, and separation occurred using a constant voltage of 180 V. Proteins were stained using Commassie Blue. A broad range protein standard (Bio-Rad 161-0317) from 6.5 kDa to 200 kDa was used as the marker. Proteins were also blotted on a polyvinyl diene difluoride (PVDF) membrane with a Mini Trans-Blot® Electrophoretic Transfer Cell (instruments settings: 100 V and 350 mA, Bio-Rad, Hercules, CA, USA). IgY detection was carried out with the same secondary antibody anti-IgY HRP-conjugated used for the immunosensor. HRP detection was done with 4-chloronaphthol and hydrogen peroxide.

5.3_Results and discussion

5.3.1_Monitoring the IgY extracting procedure

Each step of the extraction procedure is here discussed in detail and CVs recorded, the relevant SDS-PAGE and WB assays are compared step by step.

1) Precipitation with 3.5% PEG

Aim of this step is to separate egg yolk proteins from the lipid content. In the presence of 3.5% PEG solution lipid precipitate, while proteins get dissolved in the supernatant A. The overall IgY content should be present in this solution. The discarded lipid pellet was not analysed. Fig. 5.1a show the CV recorded at the IgY immunosensor. In this figure it is possible to observe that the electrocatalytic cycle generated after the addition of the enzyme substrate is complete and that the electrocatalytic current is in the order of magnitude $3*10^{-6}$ A, indicating the presence of the analyte at high concentration. Fig. 5.1b presents the results achieved with SDS-PAGE and WB assays. From SDS-PAGE at first, it is not possible to correlate the relevant bands to IgY, due to the complexity of the samples and so the large numbers of bands obtained. On the

other hand, western blot assay results in two bands, one for the heavy chains and one for the light chains associated to IgY. These bands are also present in SDS-PAGE, where is now possible to correlate the bands to IgY.

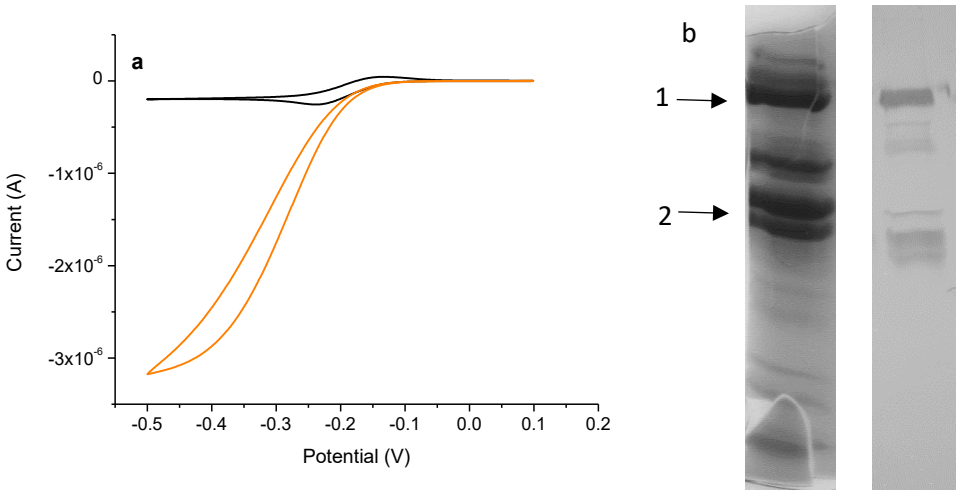

Fig 5.1: a) CVs relevant sample supernatant A, recorded before (black line) and after (orange line) the addition of the substrate. b) SDS-PAGE (left) and western blot (right) of the same sample. Bands correlated with IgY are indicated with number 1 and 2.

2) Precipitation with 8.5% PEG

Second precipitation with 8.5% PEG is needed to separate the water-soluble proteins from the water insoluble ones. Two samples were collected from this step: pellet B, which contains IgY and other soluble proteins (as α and β livetins), and the supernatant B, where the water insoluble proteins are dispersed. Fig. 5.2 a shows the CV recorded at the immunosensor, . In this figure dark blue CV is the one obtained after the addition of the substrate when a sample from pellet B was captured on the electrode. The electrocatalytic cycle is complete with a current value in the order of magnitude of $3*10^{-6}$, similar to the one obtained when supernatant A was analysed. This indicates that all the IgY obtained with the first precipitation with PEG was preserved also during the second precipitation. When a sample from supernatant B was analysed (CV light blue in Fig. 5.2a, an electrocatalytic cycle was also obtained, but the current recorded is lower. This result can be related to the presence of fragments of IgY, detected by the sensor, or to some nonspecific interaction of some of the insoluble proteins content in the sample. The results of SDS-PAGE and western blot relevant to

the two samples are shown in Fig. 5.2b, on the left the results of sample pellet B and on the right of supernatant B. As in the previous case, it is possible to determine the IgY bands in the SDS-PAGE gel thanks to the comparison with WB assay. In the electrophoresis gel, the bands are complementary to the bands of the ones present on the left, indicating absence of IgY, result confirmed also with WB, since no bands are visible on the membrane.

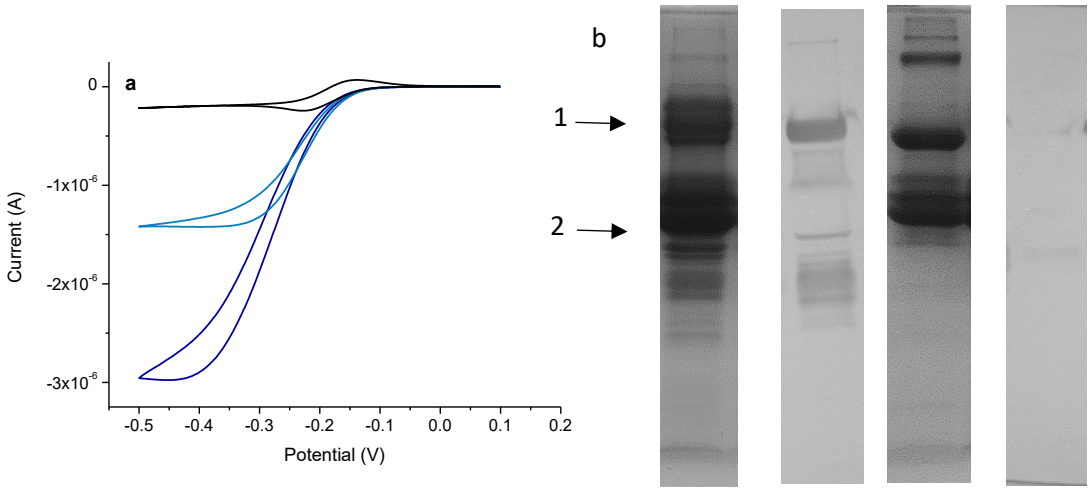

Fig 5.2: a) CVs relevant samples supernatant and pellet B, recorded before (black line) and after the addition of the substrate, light blue is for supernatant B, while dark blue is for pellet B. b) SDS-PAGE and western blot of the samples pellet B (on the left) and supernatant B (on the right). Bands correlated with IgY are indicated with number 1 and 2.

3) Precipitation with PEG 12%

This step is necessary to separate IgY from the other soluble proteins. Only one sample was collected from this step, supernatant C, that should not contain IgY. Fig. 5.3a shows the CVs recorded before (black) and after (yellow) the addition of the substrate for the relevant sample. It is possible to observe that a small electrocatalytic cycle is generated after the addition of the substrate, but the electrocatalytic current is three times lower than the one recorded in presence of the analyte. This low electrocatalytic current can be related to a very low amount of IgY that is not separated; this result was confirmed by WB, where the two IgY bands were detected.

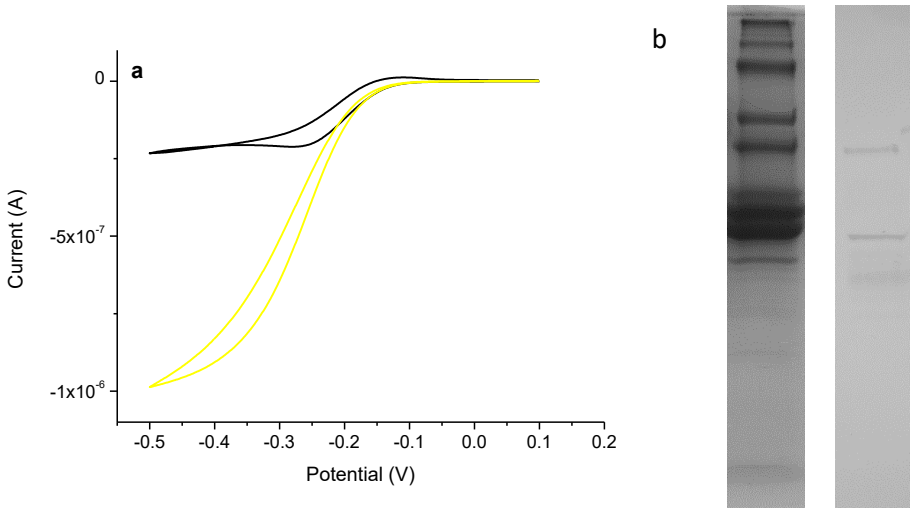

Fig 5.3: a) CV of the sample supernatant C, recorded before (black line) and after (yellow line) the addition of the substrate. b) SDS-PAGE and western blot of the same sample.

4) Dialysis vs NaCl and PBS

After the precipitation of IgY, two dialysis were needed to further purify the IgY. The two solutions out of the dialysis that are NaCl (the first overnight dialysis) and PBS (the second one) were analysed. These samples should not contain IgY. Fig. 5.4a shows the CVs recorded at the IgY immunosensor after the addition of the substrate (green lines). The values of the catalytic currents are similar, order of magnitude $1*10^{-6}$. This small electrocatalytic cycle can be related to a low concentration of IgY or its fragments in the samples, as in the previous case. This result is not confirmed by SDS-PAGE or WB, were no bands were detected (Fig. 5.4b). This data indicates that the immunosensor is more sensitive than SDS-PAGE or WB.

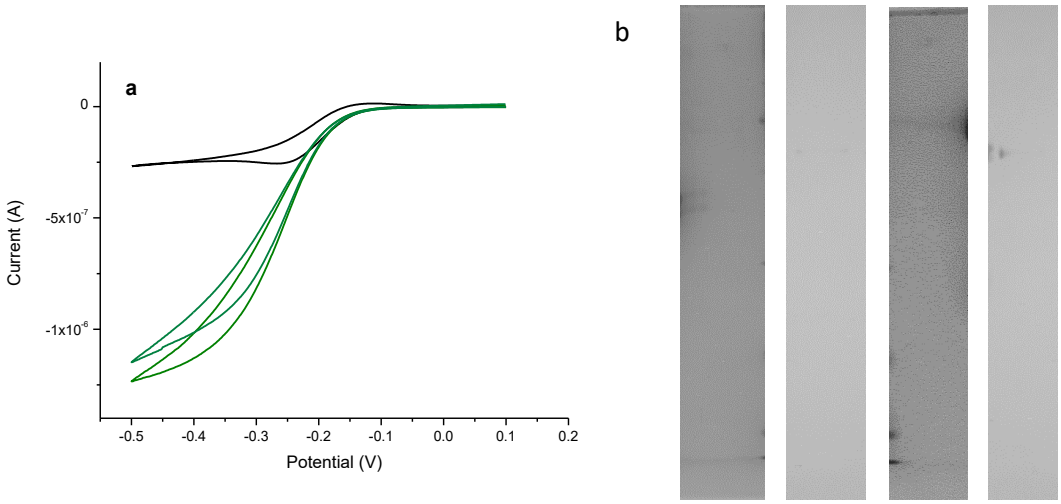

Fig 5.4: a) CVs relevant to samples collected from the dialysis solution, recorded before (black line) and after (green lines) the addition of the substrate, b) SDS-PAGE and western blot of the samples.

5) IgY obtained with the extracting procedure

IgY obtained with the extracting procedure was analysed with the IgY-immunosensor and SDS-PAGE and WB. This sample should contain pure IgY. Fig. 5.5a shows the CV recorded when IgY was captured by the electrode surface. The electrocatalytic current generated after the addition of the substrate (red line) is order of magnitude $3*10^{-6}$, similar to the values obtained for supernatant A and pellet B, the other two samples that contain IgY. This result indicates that IgY was preserved during the whole extracting procedure. Fig. 5.5b shows the results relevant to SDS-PAGE and WB. IgY heavy and light chains bands (indicated with 1 and 2) are present both on the electrophoretic gel and on the WB membrane. Many other bands were detected with both the techniques and can be related to some IgY fragments, since there is a good correspondence of the bands present on the electrophoretic gel and the WB membrane.

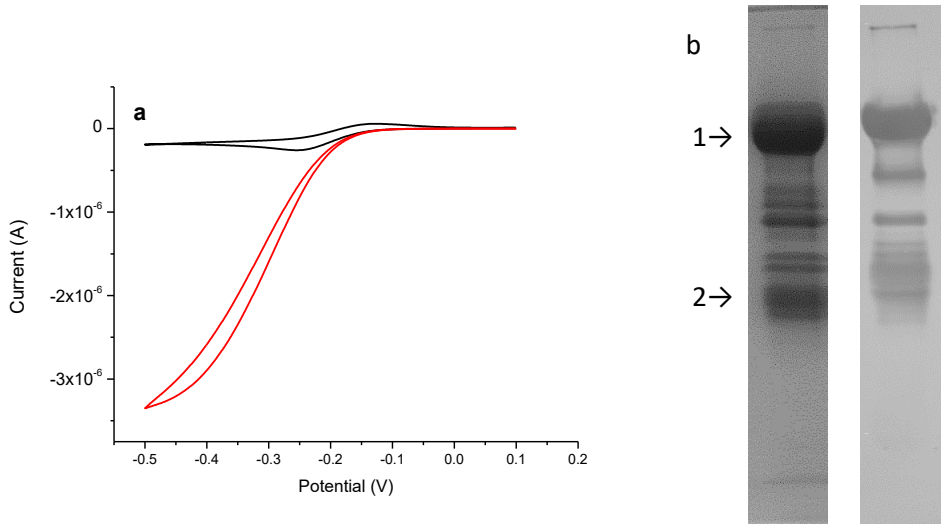

Fig 5.5: Fig 5.2: a) CV of the sample supernatant containing pure IgY, recorded before (black line) and after (red line) the addition of the substrate. b) SDS-PAGE and western blot of the same sample. Bands correlated with IgY are indicated with number 1 and 2.

Fig. 5.6 reports the overlay of all the CVs recorded during the monitoring of the procedure. CVs of Pellet B, supernatant A and the purified IgY have a similar electrocatalytic current ($3*10^{-6}$ A), indicating that the IgY obtained with the first

precipitation with PEG was preserved during the following steps. Supernatant C, dialysis one and two, and supernatant B have similar electrocatalytic current values, much lower than the ones recorded for the other samples. In the cases of dialysis 1 and 2, supernatant C and supernatant B, electrocatalytic currents are lower than those recorded in presence of the analyte. These signals can be related to a low concentration of IgY in the samples, or the presence of some fragments that cannot be identified with SDS-PAGE. Despite the amount of IgY detected after the first extraction step generates an electrocatalytic cycle similar to the amount of IgY detected at the end of the procedure, we cannot completely exclude that part of the antibody gets lost during the procedure, as suggested by the electrocatalytic currents recorded for the samples supernatant C and B.

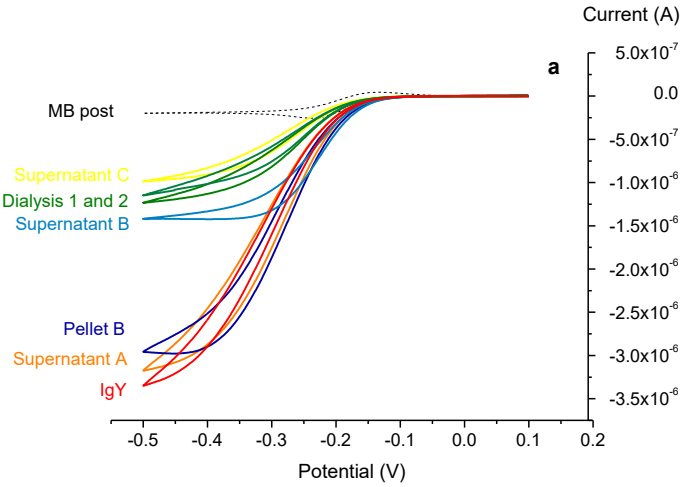

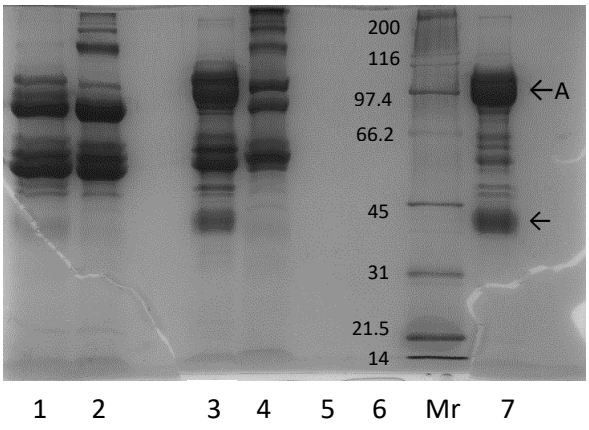

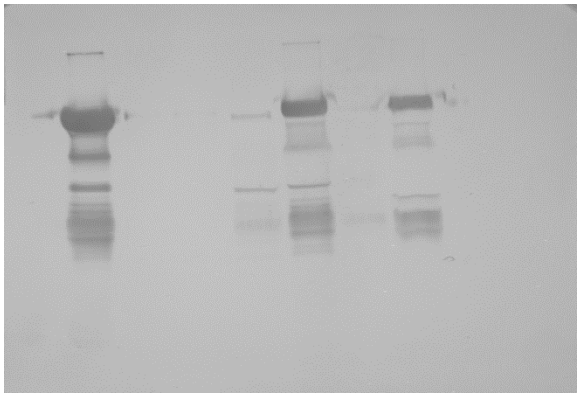

7 6 5 4 3 2 1

Fig 5.6: a) CVs recorded during the IgY extracting procedure, b) SDS-PAGE and c) WB results. The numbers in SDS-PAGE and WB are relevant to the same sample: 1) supernatant A, 2) pellet B, 3) supernatant B, 4) supernatant C, 5-6) dialysis and 7) IgY obtained with the procedure.

5.3.2_Analysis of food supplements

The cyclic voltammograms recorded after the complete procedure of preparation of the IgY-immunosensor with the three samples containing egg white 0.06 g/mL, egg yolk 0.006 g/mL and 0.06 g/mL and described in Tab. 5.1 are shown in Fig. 5.7. In all the cases, a typical electrocatalytic process is observed. The catalytic current recorded in the presence of only egg white (Fig. 5.7 solid-yellow line) is very low and can be ascribed to aspecific adsorption. On the other hand, the same parameter increases dramatically for egg yolk powder (Fig. 5.7 orange and red lines voltammograms), scaling with the amount of food supplement analysed.

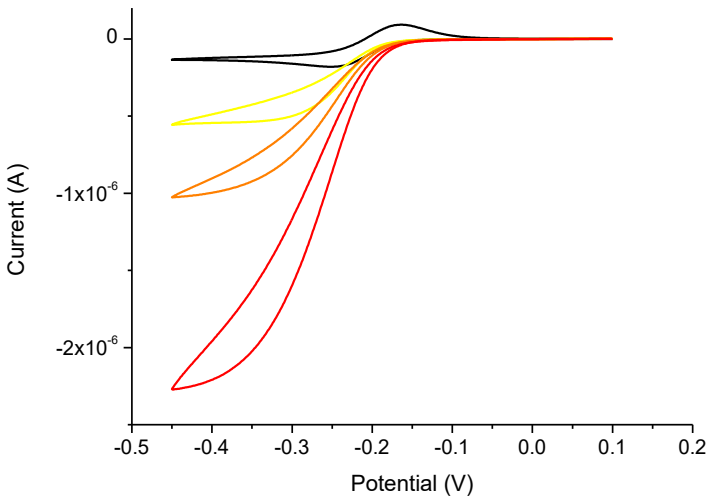

Fig 5.7: CVs of 0.1 mM MB in 0.01 M PBS recorded at 10 mV/s before (full black line) and after addition (solid lines) of 0.5 mM H_2O_2 for the following samples: 0.06 g/mL egg white powder (full-yellow line), 0.006 g/mL egg yolk powder (full-orange line) and 0.06 g/mL egg yolk powder (full-red line).

By combining electrophoresis (see below) and voltammetric data, it has been possible to estimate the amount of IgY detected by the immunosensor. Calculations carried out on the most diluted samples suggest a concentration of IgY close to 0.4 mg/mL, correlated to 0.005 g/mL of yolk, while the experimental concentration of the analysed sample is 0.006 g/mL of yolk. The industrial treatments of the eggs probably cause a little damage to the protein structure that involves 20% of the material.

5.3.2.1_SDS-PAGE and WB Analysis

The validation of the results obtained with the electrochemical immunosensor was carried out with SDS-PAGE and WB assays. Fig. 5.8a,b show the SDS-PAGE and WB results, respectively, for the sample containing the lowest concentration of yolk from the freeze-dried product and the sample containing egg white, prepared as described in Tab. 5.1. Electrophoresis carried out in reducing conditions should provide two bands that can be correlated with IgY, one corresponding to the heavy chain (HC) and the other to the light chain (LC). Molecular weight of HC and LC of IgY according to literature are 68 and 27 kDa respectively[16]. Due to the complexity of egg yolk and the large amount of water-soluble proteins, it is difficult to correlate and identify IgY bands (Fig. 5.8a). In order to obtain specific results, a WB assay was performed. Secondary antibody anti-IgY identified three IgY bands, as shown in Fig. 5.8, lane 1. The first band is relevant to the heavy IgY chains and the third one is relevant to the light chains. The band that is intermediate to the first and third ones has not been associated to any fragment or chain of IgY, but is previously observed in the literature[115]. Verifying the correlation between WB and SDS-PAGE bands, it is possible to ascribe a molecular weight to these bands: the HC bands in WB correspond to the 67 kDa band in SDS-PAGE, the LC band corresponds to 28.6 kDa, in good agreement with literature data. The intermediate band corresponds to a Mw of 44kDa, previously observed but not completely explained in the literature[67].

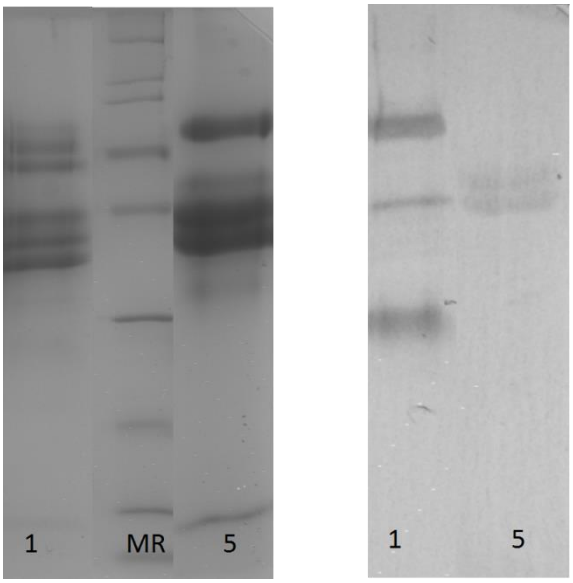

Fig 5.8: (a) SDS-PAGE results for the following samples: (1) freeze-dried yolk, 0.006 g/mL; (5) freeze-dried egg white; Mr = marker; (b) Results of the WB, with the samples in the same order as in (a).

The freeze-dried egg white was analysed by SDS-PAGE and WB as well. The results are shown in lane 5 in Figure 5.8b. The SDS-PAGE presents at least five bands (Fig. 5.8 a), but none of these can be correlated to IgY, indicating the absence of IgY in egg white. Despite this, the secondary antibody recognised two bands at Mw around 45 kDa (Fig. 5.8 b, lane 5) that can be ascribed to an aspecific interaction between the antibody and an egg white protein present in high concentration in the samples. It is worth noting that this aspecific interaction was observed also with the immunosensor (Fig 5.7).

5.4_Conclusion

An IgY extracting procedure was monitored step by step with the IgY immunosensor, SDS-PAGE and WB. The results obtained with the different techniques are in agreement, confirming the reliability and high sensitivity of the sensor. This agreement was also obtained when freeze-dried samples containing egg yolk were analysis.

The combination of NEEs' high sensitivity and selectivity of the enzyme–substrate interaction allows the detection of IgY in low concentration both in simple and complex matrices. Other advantages of the proposed method concern the time-

consumption and costs of the techniques: the electrochemical procedure is, in fact, shorter than ELISA and definitively shorter than SDS-PAGE and WB procedures. Moreover, thanks to the low amount of chemicals required, the electrochemical immunosensor has a lower cost.

6_General conclusion

In this thesis we demonstrated the suitability and feasibility of electrochemical nanostructured biosensors to detect different proteins, with focus on proteins used as binders in works of art. With respect to previous studies, here it is demonstrated that this approach can be successful to detect immunoglobulin from egg yolk and from very small amounts of samples. The immunosensing recognition has been implemented towards the sensitive detection of ovalbumin from egg white, so allowing the independent detection of one or both egg white and egg yolk in a micro sample. In principle, the developed sensors constitutes a component of a low cost analytical device which is relatively simple to use and which can evolve in the future in a portable instrumentation manageable also for non-specialists.

The study is focused on the detection of the two proteins used in the binders of tempera paintings, however it is demonstrated that this approach can be extended also for samples of different nature, such as for instance food and food supplements.

The studied sensors required the use of an enzymatic label to generate enzymatic amplified signals. The careful choice of the label allows the detection of IgY and OVA in two well separated potential ranges: cathodic for IgY, and anodic for OVA. This can open important prospects for future studies towards the development of multiplexed sensing devices, based on the use of the same physical platform. Indeed, one can think to develop a dual-electrode system on the same platform where one electrode is used to detect IgY and the other OVA from the same extract. To achieve this goal the avoidance of interferences between the two immunosensors must be carefully studied and evaluated.

In this thesis many mock-ups of paintings have been analysed to evaluate the OVA and IgY sensors performances. The results obtained in these very complex samples containing several different pigments as well as binders from different nature are very promising. In the future, more work is required to further validate the applicability of the sensors to a large number of samples from real paintings.

7_Bibliography

1. Casoli, A., Berzioli, M. & Cremonesi, P. The Chemistry of Egg Binding Medium and Its Interactions with Organic Solvents and Water. *Smithson. Contrib. TO MUSEUM Conserv. fraction* **3,** 39–44 (2012).
2. Bonaduce, Ilaria, Carlyle, L. & Colombini, Maria Perla, Duce, Celia, Ferrari, Carlo, Ribechini, Erika, Selleri, Paola, Tine, M. R. A multi-analytical approach to studying binding media in oil paintings: Characterisation of differently pre-treated linseed oil by DE-MS, TG and GC/MS. *J. Therm. Anal. Calorim.* **107,** 1055–1066 (2012).
3. James C. Shearer, David C. Peters, .Gerald Hoeplner Travers Newton. FTIR in the Service of Art Conservation. *Anal. Chem.* **55,** 874–880 (1983).
4. Vetter, W. & Schreiner, M. Characterization of pigment-binding media systems: comparison of non-invasive in-situ reflection FTIR with transmission FTIR microscopy. *e-Preservation Sci.* **8,** 10–22 (2011).
5. Pelagotti, a., Mastio, a. Del, Rosa, a. De & Piva, a. Multispectral imaging of paintings. *IEEE Signal Process. Mag.* **25,** 27–36 (2008).
6. Bisulca, C., Picollo, M., Bacci, M. & Kunzelman, D. Uv-Vis-Nir Reflectance Spectroscopy of Red Lakes in Paintings. *9th Int. Conf. NDT Art, Jerusalem, Isr. 25-30 May 2008* 1–7 (2008).
7. Romani, A., Clementi, C., Miliani, C. & Favaro, G. Fluorescence spectroscopy: A powerful technique for the noninvasive characterization of artwork. *Acc. Chem. Res.* **43,** 837–846 (2010).
8. Chiavari, G., Gandini, N., Russo, P. & Fabbri, D. Characterisation of standard tempera painting layers containing proteinaceous binders by pyrolysis (/Methylation)-gas chromatography-mass spectrometry. *Chromatographia* **47,** 420–426 (1998).
9. Colombini, M. P. & Modugno, F. Characterisation of proteinaceous binders in artistic paintings by chromagtographic techniques. *J. Sep. Sci.* **27,** 147–160 (2004).
10. Cartechini, L., Palmieri, M., Vagnini, M. & Pitzurra, L. Immunochemical methods applied to art-historical materials: Identification and localization of proteins by ELISA and IFM. *Top. Curr. Chem.* **374,** 1–21 (2016).
11. Potenza Mariangela, Sabatino Giuseppina, G. F., Rosi Luca, P. A. M. & Dei, L. Analysis of egg-based model wall paintings by use of an innovative combined dot-ELISA and

UPLC-based approach. *Anal. Bioanal. Chem.* **405,** 691–701 (2013).

12. Fallis, A. . *Bioactive egg compounds*. *Journal of Chemical Information and Modeling* **53,** (2013).
13. Bernardi, G. & Cook, W. H. Separation and Characterization of the Two High Density Lipoproteins of Egg Yolk, α- and β-Lipovitellin. *Biochim. Biophys. Acta* **44,** 96–105 (1960).
14. Munhoz, L. S. *et al.* Avian IgY antibodies: characteristics and applications in immunodiagnostic. *Cienc. Rural* **44,** 153–160 (2014).
15. Nguyen, S. Van, Umeda, K. & Kodama, Y. Oral passive immunotherapeutics. 1–10 (2013).
16. Spillner, E. *et al.* Avian IgY antibodies and their recombinant equivalents in research, diagnostics and therapy. *Biologicals* **40,** 313–322 (2012).
17. Dias da Silva, W. & Tambourgi, D. V. IgY: A promising antibody for use in immunodiagnostic and in immunotherapy. *Vet. Immunol. Immunopathol.* **135,** 173–180 (2010).
18. Schade, R. *et al.* Chicken Egg Yolk Antibodies (IgY-technology): A Review of Progress in Production and Use in Research and Human and Veterinary Medicine. *ATLA* **33,** 1–26 (2005).
19. Huntington, J. A. & Stein, P. E. Structure and properties of ovalbumin. *J. Chromatogr. B Biomed. Sci. Appl.* **756,** 189–198 (2001).
20. Walsh, B. J., Hill, D. J., Macoun, P., Cairns, D. & Howden, M. E. H. Detection of four distinct groups of hen egg allergens binding IgE in the sera of children with egg allergy. *Allergol. Immunopathol. (Madr).* **33,** 183–191 (2005).
21. Azarnia, S., Boye, J. I., Mongeon, V. & Sabik, H. Detection of ovalbumin in egg white, whole egg and incurred pasta using LC-ESI-MS/MS and ELISA. *Food Res. Int.* **52,** 526–534 (2013).
22. Turin, L. & Bonomi, F. Immunochemical detection of ovalbumin in dairy-based foods. *J. Sci. Food Agric.* **64,** 39–45 (1994).
23. Thevenot, D. R. ELECTROCHEMICAL BIOSENSORS: RECOMMENDED Electrochemical biosensors: Recommended definitions and classification (Technical Report). *Pure Appl. Chem.* **71,** 2333–2348 (1999).
24. Monošík, R., Streďanský, M. & Šturdík, E. Biosensors - classification, characterization

and new trends. *Acta Chim. Slovaca* **5,** 109–120 (2012).

25. Fan, X. *et al.* Sensitive optical biosensors for unlabeled targets: A review. *Anal. Chim. Acta* **620,** 8–26 (2008).
26. Přibyl, J., Hepel, M., Halámek, J. & Skládal, P. Development of piezoelectric immunosensors for competitive and direct determination of atrazine. *Sensors Actuators, B Chem.* **91,** 333–341 (2003).
27. Ramanathan, K. & Danielsson, B. Principles and applications of thermal biosensors. *Biosens. Bioelectron.* **16,** 417–423 (2001).
28. Länge, K., Rapp, B. E. & Rapp, M. Surface acoustic wave biosensors: A review. *Anal. Bioanal. Chem.* **391,** 1509–1519 (2008).
29. Wang, J. Glucose Biosensors : 40 Years of Advances and Challenges. *Eletroanalysis* **1312,** 983–988 (2001).
30. Wang, J. Electrochemical glucose biosensors. *Electrochem. Sensors, Biosens. their Biomed. Appl.* 57–69 (2008). doi:10.1016/B978-012373738-0.50005-2
31. Chen, C. *et al.* Recent advances in electrochemical glucose biosensors: a review. *RSC Adv.* **3,** 4473 (2013).
32. Song, S., Xu, H. & Fan, C. Potential diagnostic applications of biosensors: Current and future directions. *Int. J. Nanomedicine* **1,** 433–440 (2006).
33. Mehrotra, P. Biosensors and their applications - A review. *J. Oral Biol. Craniofacial Res.* **6,** 153–159 (2016).
34. Patel, S., Nanda, R., Sahoo, S. & Mohapatra, E. Biosensors in health care: The milestones achieved in their development towards lab-on-chip-analysis. *Biochem. Res. Int.* **2016,** (2016).
35. Thakur, M. S. & Ragavan, K. V. Biosensors in food processing. *J. Food Sci. Technol.* **50,** 625–641 (2013).
36. Gaetani, C., Ambrosi, E., Ugo, P. & Moretto, L. Electrochemical Immunosensor for Detection of IgY in Food and Food Supplements. *Chemosensors* **5,** 10 (2017).
37. Palchetti, I. & Mascini, M. Nucleic acid biosensors for environmental pollution monitoring. *Analyst* **133,** 846–854 (2008).
38. Barton, J. *et al.* Screen-printed electrodes for environmental monitoring of heavy metal ions: a review. *Microchim. Acta* **183,** 503–517 (2016).
39. Goldberg, R. J. A Theory of Antibody-Antigen Reactions. II. Theory for Reactions of

Multivalent Antigen with Multivalent Antibody. *J. Am. Chem. Soc.* **75,** 3127–3131 (1953).

40. Johnson, S. & Krauss, T. F. Label-free affinity biosensor arrays: novel technology for molecular diagnostics. *Expert Rev. Med. Devices* **14,** 177–179 (2017).
41. Distefano, M. D. NIH Public Access. **19,** 213–223 (2015).
42. Farka, Z., Juřík, T., Kovář, D., Trnková, L. & Skládal, P. Nanoparticle-Based Immunochemical Biosensors and Assays: Recent Advances and Challenges. *Chem. Rev.* **117,** 9973–10042 (2017).
43. Kašná, A. & Skládal, P. A Four-Channel Electrochemical Immunosensor for Detection of Herbicides Based on Phenoxyalkanoic Acids. *Int. J. Environ. Anal. Chem.* **83,** 101–109 (2003).
44. Clark, L. C. & Lyons, C. Electrode systems for continuous monitoring in cardiovascular surgery. *Ann. N. Y. Acad. Sci.* **102,** 29–45 (1962).
45. Karyakin, A. A., Gitelmacher, O. V. & Karyakina, E. E. Prussian Blue-Based First-Generation Biosensor. A Sensitive Amperometric Electrode for Glucose. *Anal. Chem.* **67,** 2419–2423 (1995).
46. Putzbach, W. & Ronkainen, N. J. Immobilization techniques in the fabrication of nanomaterial-based electrochemical biosensors: A review. *Sensors (Switzerland)* **13,** 4811–4840 (2013).
47. Bourdillon, C., Demaille, C., Moiroux, J. & Savéant, J.-M. From Homogeneous Electroenzymatic Kinetics to Antigen−Antibody Construction and Characterization of Spatially Ordered Catalytic Enzyme Assemblies on Electrodes. *Acc. Chem. Res.* **29,** 529–535 (1996).
48. Lee, K. J., Elgrishi, N., Kandemir, B. & Dempsey, J. L. Electrochemical and spectroscopic methods for evaluating molecular electrocatalysts. *Nat. Rev. Chem.* **1,** (2017).
49. Menon, V. P. & Martin, C. R. Fabrication and Evaluation of Nanoelectrode Ensembles. *Anal. Chem.* **67,** 1920–1928 (1995).
50. Brunetti, B., Ugo, P., Moretto, L. M. & Martin, C. R. Electrochemistry of phenothiazine and methylviologen biosensor electron-transfer mediators at nanoelectrode ensembles. *J. Electroanal. Chem.* **491,** 166–174 (2000).
51. Hopg, G. & Penner, R. M. and Microstructures on Highly Oriented Pyrolytic. *Handb.*

Electrochem. Pretreat. Act. 661–676 (2007). doi:10.1016/B978-0-444-51958-0.50029-X

52. Henry, M., Dupont-Gillain, C. & Bertrand, P. Conformation change of albumin adsorbed on polycarbonate membranes as revealed by ToF-SIMS. *Langmuir* **19,** 6271–6276 (2003).
53. Henry, M. & Bertrand, P. Influence of polymer surface hydrophilicity on albumin adsorption. *Surf. Interface Anal.* **36,** 729–732 (2004).
54. Mucelli, S. P., Zamuner, M., Tormen, M., Stanta, G. & Ugo, P. Nanoelectrode ensembles as recognition platform for electrochemical immunosensors. *Biosens. Bioelectron.* **23,** 1900–1903 (2008).
55. Silvestrini, M., Fruk, L. & Ugo, P. Functionalized ensembles of nanoelectrodes as affinity biosensors for DNA hybridization detection. *Biosens. Bioelectron.* **40,** 265–270 (2013).
56. Habtamu, H. B. *et al.* A Sensitive Electrochemiluminescence Immunosensor for Celiac Disease Diagnosis Based on Nanoelectrode Ensembles. *Anal. Chem.* **87,** 12080–12087 (2015).
57. De Leo, M. *et al.* Towards a better understanding of gold electroless deposition in track-etched templates. *Chem. Mater.* **19,** 5955–5964 (2007).
58. Mardegan, A., Scopece, P., Ugo, P. & Moretto, L. M. Ensembles of Gold Nanowires for the Anodic Stripping Voltammetric Determination of Inorganic Arsenic. *J. Nanosci. Nanotechnol.* **15,** 3417–3422 (2015).
59. Bottari, F., Oliveri, P. & Ugo, P. Electrochemical immunosensor based on ensemble of nanoelectrodes for immunoglobulin IgY detection: Application to identify hen's egg yolk in tempera paintings. *Biosens. Bioelectron.* **52,** 403–410 (2014).
60. Moretto, L. M., Pepe, N. & Ugo, P. Voltammetry of redox analytes at trace concentrations with nanoelectrode ensembles. *Talanta* **62,** 1055–1060 (2004).
61. Habtamu, H. B. & Ugo, P. Miniaturized Enzymatic Biosensor via Biofunctionalization of the Insulator of Nanoelectrode Ensembles. *Electroanalysis* **27,** 2187–2193 (2015).
62. Coutouli-Argyropoulou, E., Kelaidopoulou, A., Sideris, C. & Kokkinidis, G. Electrochemical studies of ferrocene derivatives and their complexation by β-cyclodextrin. *J. Electroanal. Chem.* **477,** 130–139 (1999).
63. Kelley, S. O., Barton, J. K., Jackson, N. M. & Hill, M. G. Electrochemistry of methylene

blue bound to a DNA-modified electrode. *Bioconjug. Chem.* **8,** 31–37 (1997).

64. Pheeney, C. G. & Barton, J. K. DNA electrochemistry with tethered methylene blue. *Langmuir* **28,** 7063–7070 (2012).
65. Ye, J. & Baldwin, R. P. Catalytic Reduction of Myoglobin and Hemoglobin at Chemically Modified Electrodes Containing Methylene Blue. *Anal. Chem.* **60,** 2263–2268 (1988).
66. Gee, S. C., Bate, I. M., Thomas, T. M. & Rylatt, D. B. The purification of IgY from chicken egg yolk by preparative electrophoresis. *Protein Expr. Purif.* **30,** 151–155 (2003).
67. Pauly, D., Chacana, P., Calzado, E., Brembs, B. & Schade, R. IgY Technology: Extraction of Chicken Antibodies from Egg Yolk by Polyethylene Glycol (PEG) Precipitation. *J. Vis. Exp.* **51,** 3–7 (2011).
68. Kohji Kitaguchi, Masato Minoura, Miho Noritake, Makoto Mizutani, Keiji Kinoshita, Fumihiko Horio, and A. M. Determination of immunoglobulin Y concentration in yolk extract prepred by water dilution method: comparisons among three strains chickens. *J. Poult. Sci.* **45,** 82–87 (2008).
69. Wang, Q. *et al.* A rapid triple-mode fluorescence switch assay for immunoglobulin detection by using quantum dots-gold nanoparticles nanocomposites. *Sensors Actuators, B Chem.* **231,** 779–786 (2016).
70. Liu, H., Malhotra, R., Peczuh, M. W. & Rusling, J. F. Electrochemical immunosensors for antibodies to peanut allergen Ara h2 using gold nanoparticle-peptide films. *Anal. Chem.* **82,** 5865–5871 (2010).
71. Figueiredo, A. *et al.* Electrical Detection of Dengue Biomarker Using Egg Yolk Immunoglobulin as the Biological Recognition Element. *Sci. Rep.* **5,** 7865 (2015).
72. Sadhasivam, S. *et al.* A real time detection of the ovarian tumor associated antigen 1 (OVTA 1) in human serum by quartz crystal microbalance immobilized with anti-OVTA 1 polyclonal chicken IgY antibodies. *Mater. Sci. Eng. C* **32,** 2073–2078 (2012).
73. Jiang, B. *et al.* Aptamer pseudoknot-functionalized electronic sensor for reagentless and single-step detection of immunoglobulin e in human serum. *Anal. Chem.* **87,** 3094–3098 (2015).
74. He, Y. N., Chen, H. Y., Zheng, J. J., Zhang, G. Y. & Chen, Z. L. Differential pulse voltammetric enzyme-linked immunoassay for the determination of Helicobacter

pylori specific immunoglobulin G (IgG) antibody. *Talanta* **44,** 823–830 (1997).

75. Reimhult, K., Petersson, K. & Krozer, A. QCM-D Analysis of the Performance of Blocking Agents on Gold and Polystyrene Surfaces QCM-D Analysis of the Performance of Blocking Agents on Gold and Polystyrene Surfaces. *Society* **24,** 8695–8700 (2008).
76. Jeyachandran, Y. L., Mielczarski, J. A., Mielczarski, E. & Rai, B. Efficiency of blocking of non-specific interaction of different proteins by BSA adsorbed on hydrophobic and hydrophilic surfaces. *J. Colloid Interface Sci.* **341,** 136–142 (2010).
77. Jeyachandran, Y. L., Mielczarski, E., Rai, B. & Mielczarski, J. A. Quantitative and qualitative evaluation of adsorption/desorption of bovine serum albumin on hydrophilic and hydrophobic surfaces. *Langmuir* **25,** 11614–11620 (2009).
78. Vasilescu, A., Nunes, G., Hayat, A., Latif, U. & Marty, J. L. Electrochemical affinity biosensors based on disposable screen-printed electrodes for detection of food allergens. *Sensors (Switzerland)* **16,** (2016).
79. Kilshaw, P. J., McEwan, F. J., Baker, K. C. & Cant, a J. Studies on the specificity of antibodies to ovalbumin in normal human serum: technical considerations in the use of ELISA methods. *Clin. Exp. Immunol.* **66,** 481–9 (1986).
80. Peng, J. *et al.* Development of a monoclonal antibody-based sandwich ELISA for the detection of ovalbumin in foods. *Food Agric. Immunol.* **25,** 1–8 (2014).
81. Zhang, S., Lai, X. & Yang, G. Enzyme-linked FAB fragment based competitive immunoassay for ovalbumin in hot-processed food. *J. Immunoass. Immunochem.* **34,** 393–403 (2013).
82. S. Eissaa, L. L'Hocineb, M. Siajc, M. Z. Graphene-based label-free voltammetric immunosensor for sensitive detection of the egg allergen ovalbumin. *Analyst* **138,** 4378–4384 (2013).
83. Pilolli, R., Visconti, A. & Monaci, L. Rapid and label-free detection of egg allergen traces in wines by surface plasmon resonance biosensor. **407,** (2015).
84. Purushothama, S., Kradtap, S., Wijayawardhana, C. A., Halsall, H. B. & Heineman, W. R. Small volume bead assay for ovalbumin with electrochemical detection. *Analyst* **126,** 337–341 (2001).
85. Čadková, M. *et al.* Magnetic beads-based electrochemical immunosensor for monitoring allergenic food proteins. *Anal. Biochem.* **484,** 4–8 (2015).

86. Korecká, L., Šálek, P., Metelka, R. & Bílková, Z. Voltammetric detection of Ovalbumin at Screen-Printed electrodes in combination with immunomagnetic particles. *Sens. Electroanal.* **6,** 347–356 (2011).

87. Kuramitz, H., Halsall, H. B. & Heineman, W. R. Magnetic microbead-based enzyme immunoassay for ovalbumin using hydrodynamic voltammetry and fluorometric detection. *Anal. Methods* **4,** 1783–1789 (2012).

88. Carter, T. C. The Hen's Egg: Density of Egg Shell and Egg Contents. *Br. Poult. Sci.* **9,** 265–271 (1968).

89. Albery, W. J. & Knowles, J. R. Evolution of enzyme function and the development of catalytic efficiency. *Biochemistry* **15,** 5631–40 (1976).

90. Teipel, J. & Koshland, D. E. The Significance of Intermediary Plateau Regions in Enzyme Saturation Curves. *Biochemistry* **8,** 4656–4663 (1969).

91. Kim, J. & Somorjai, G. A. Molecular Packing of Lysozyme , Fibrinogen , and Bovine Serum Albumin on Hydrophilic and Hydrophobic Surfaces Studied by Infrared - Visible Sum Frequency Generation and Fluorescence Microscopy. *Jacs* **125,** 3150–3158 (2003).

92. Sharma, P., Sablok, K., Bhalla, V. & Suri, C. R. A novel disposable electrochemical immunosensor for phenyl urea herbicide diuron. *Biosens. Bioelectron.* **26,** 4209–4212 (2011).

93. Investigations, I., Alcohol, N. Y. L., Agentenzyme, B. & David, I. 421-428 (1994). **3,** (1994).

94. Galva, C., Gatto, C. & Milanick, M. Soymilk: An effective and inexpensive blocking agent for immunoblotting. *Anal. Biochem.* **426,** 22–23 (2012).

95. Rose, M. E., Orlans, E. & Buttress, N. Immunoglobulin classes in the hen's egg: Their segregation in yolk and white. *Eur. J. Immunol.* **4,** 521–523 (1974).

96. Doménech, A., Doménech-Carbó, M. T. & Vázquez De Agredos Pascual, M. L. Chemometric study of Maya Blue from the voltammetry of microparticles approach. *Anal. Chem.* **79,** 2812–2821 (2007).

97. Moretto, L. M., Montagner, F., Ganzerla, R. & Ugo, P. Nafion® as advanced immobilisation substrate for the voltammetric analysis of electroactive microparticles: The case of some artistic colouring agents. *Anal. Bioanal. Chem.* **405,** 3603–3610 (2013).

98. Anaf, W. *et al.* Electrochemical photodegradation study of semiconductor pigments: Influence of environmental parameters. *Anal. Chem.* **86,** 9742–9748 (2014).

99. Sciutto, G. *et al.* Localization of proteins in paint cross-sections by scanning electrochemical microscopy as an alternative immunochemical detection technique. *Anal. Chim. Acta* **831,** 31–37 (2014).

100. Scarano, S., Carretti, E., Dei, L., Baglioni, P. & Minunni, M. Coupling non invasive and fast sampling of proteins from work of art surfaces to surface plasmon resonance biosensing: Differential and simultaneous detection of egg components for cultural heritage diagnosis and conservation. *Biosens. Bioelectron.* **85,** 83–89 (2016).

101. Bohuslav, S. *Technika malby*. (2003).

102. Fernandez-Diaz, M. D., Barsotti, L., Dumay, E. & Cheftel, J. C. Effects of pulsed electric fields on ovalbumin solutions and dialyzed egg white. *J. Agric. Food Chem.* **48,** 2332–2339 (2000).

103. Ferreira Machado, F. *et al.* Solubility and density of egg white proteins: Effect of pH and saline concentration. *LWT - Food Sci. Technol.* **40,** 1304–1307 (2007).

104. Odlyha, M., Cohen, N. S. & Foster, G. M. Dosimetry of paintings: Determination of the degree of chemical change in museum exposed test paintings (smalt tempera) by thermal analysis. *Thermochim. Acta* **365,** 35–44 (2000).

105. Feller, L. 7 Vermilion. **17,** 45–69 (1972).

106. Smiddy, M. A., Martin, J.-E. G. H., Kelly, A. L., de Kruif, C. G. & Huppertz, T. Stability of Casein Micelles Cross-Linked by Transglutaminase. *J. Dairy Sci.* **89,** 1906–1914 (2006).

107. Samir, M., Patrick, B. & Józef, K. Original article Solubility of α S1 - , β - and κ -casein in water-ethanol solutions. **88,** 313–325 (2008).

108. Ye, R. & Harte, F. Casein maps: Effect of ethanol, pH, temperature, and CaCl2 on the particle size of reconstituted casein micelles Ran. *J diary Sci.* **96,** 799–805 (2015).

109. Verdoliva, Basile, F. Affinity purification of immunoglobulins from chicken egg yolk using a new synthetic ligand. *J. Chromatogr. B Biomed. Sci. Appl.* **749,** (2000).

110. Kim, H. & Nakai, S. Simple Separation of Immunoglobulin from Egg Yolk by Ultrafiltration. *J. Food Sci.* **63,** 485–490 (1998).

111. Harper, J. C. & Tappel, A. L. Freeze-Drying of Food Products. *Adv. Food Res.* **7,** 171–234 (1957).

112. Jaekel, T., Dautel, K. & Ternes, W. Preserving functional properties of hen's egg yolk

during freeze-drying. *J. Food Eng.* **87,** 522–526 (2008).

113. Kitabatake, N., Indo, K. & Doi, E. Changes in Interfacial Properties of Hen Egg Ovalbumin Caused by Freeze-Drying and Spray-Drying. *J. Agric. Food Chem.* **37,** 905–910 (1989).
114. LAEMMLI, U. K. Cleavage of Structural Proteins during the Assembly of the Head of Bacteriophage T4. *Nature* **227,** 680–685 (1970).
115. Borhani, K., Mobarez, A. M., Khabiri, A. R., Behmanesh, M. & Khoramabadi, N. Production of specific IgY Helicobacter pylori recombinant OipA protein and assessment of its inhibitory effects towards attachment of H. pylori to AGS cell line. *Clin. Exp. Vaccine Res.* **4,** 177–83 (2015).

Appendix A

We present here all the CVs recorded during the analysis of the cross-sections. For each samples, a table with the composition is presented and four cyclic voltammograms, two for the IgY-immunosensor and two for the OVA-immunosensor.

Sample 1A

Organic binder	Pigment	% Prot	% Oil
OIL	AZU + rabbit g.	0.6	55
Egg white (8:1)	CaCO3	4.2	0
Casein (2:1)	AZURITE	6.5	6
Egg yolk (2:1)	HgS	3.5	19
Glue (rabbit)	CaCO3	6.3	0
Whole egg (3:1)	AZURITE	5.7	20

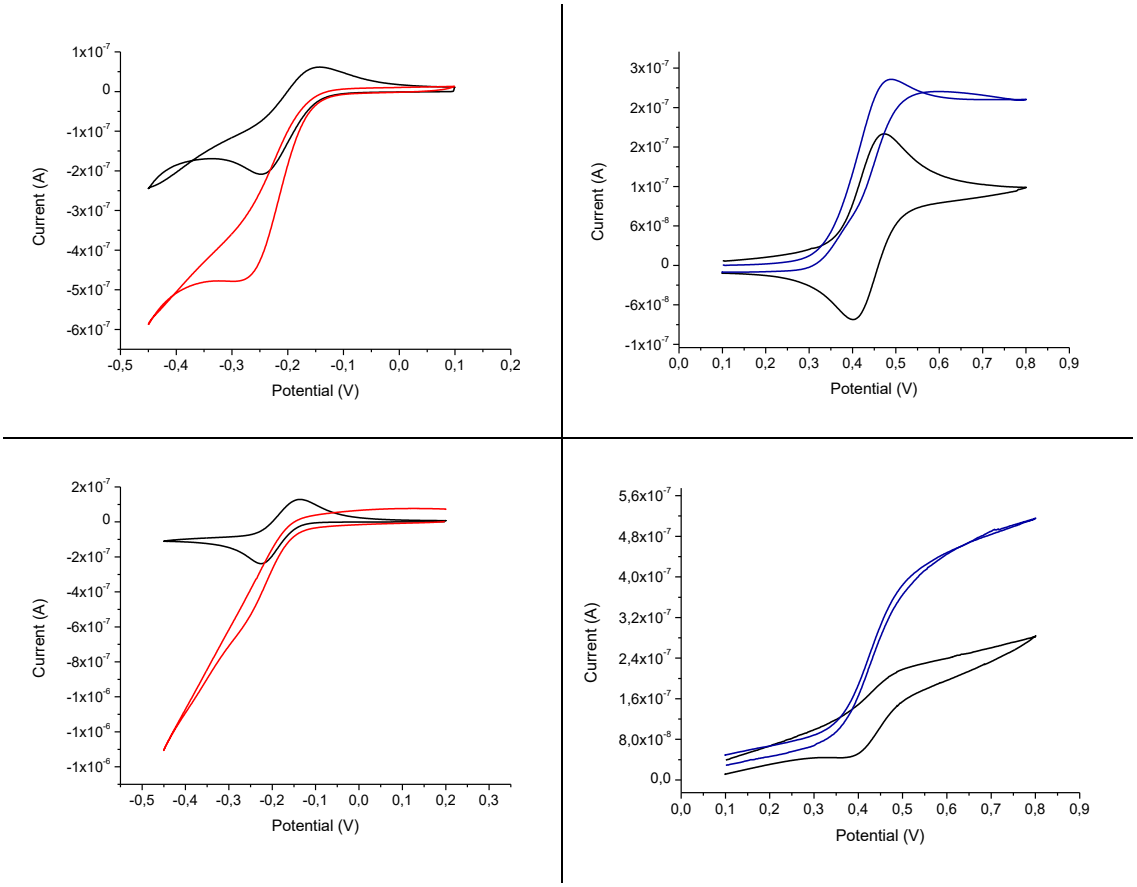

Sample 1B

Organic binder	Pigment	% Prot	% Oil
Egg white (8:1)	AZURITE	2.2	0
Casein (2:1)	HgS	7.8	7
Egg yolk (2:1)	CaCO3	6	32
Glue (rabbit)	AZURITE	8.6	0
Whole egg (3:1)	HgS	5	16

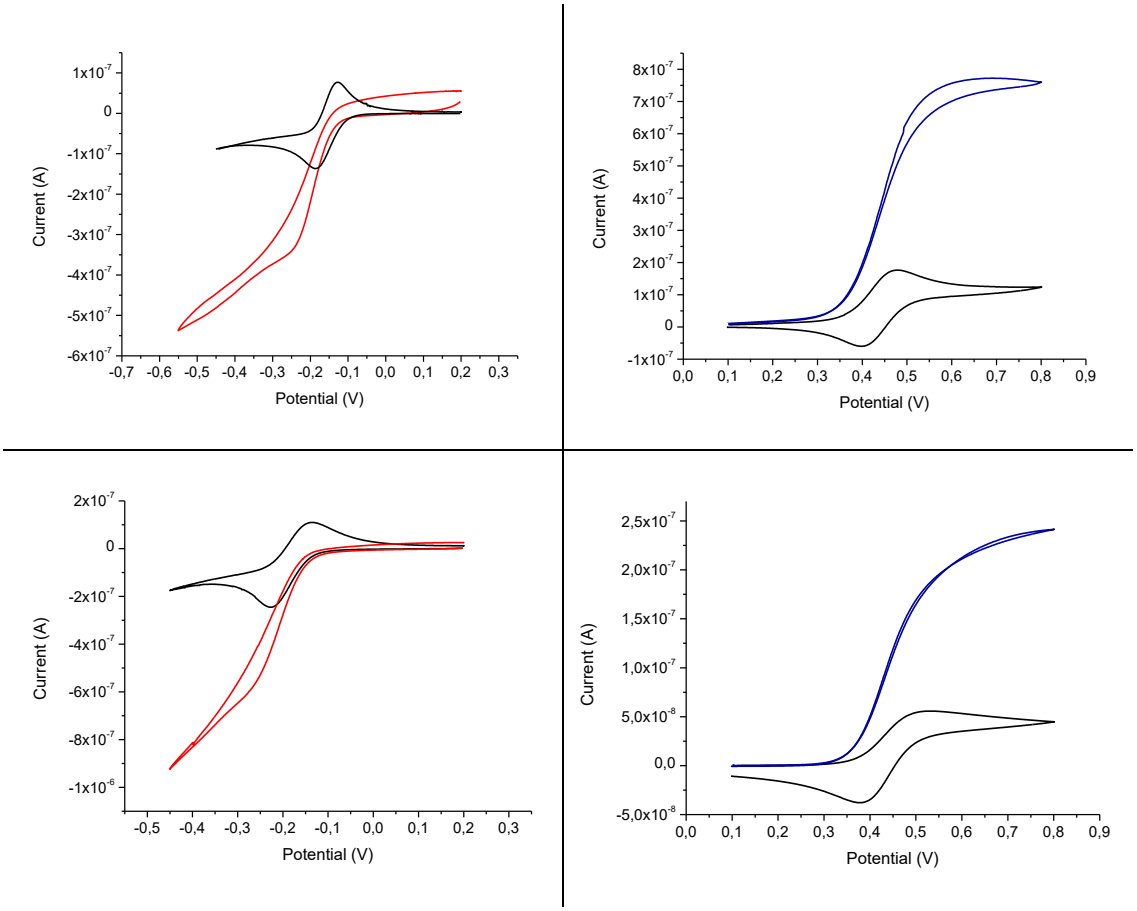

Sample 1C

Organic binder	Pigment	% Prot	% Oil
OIL	AZURITE + gel	0.2	44
Egg white (8:1)	HgS	2.5	0
Casein (2:1)	CaCO3	12.5	11
Egg yolk (2:1)	AZURITE	4.4	21
Glue (rabbit)	HgS	2.7	0
Whole egg (3:1)	CaCO3	8.2	29

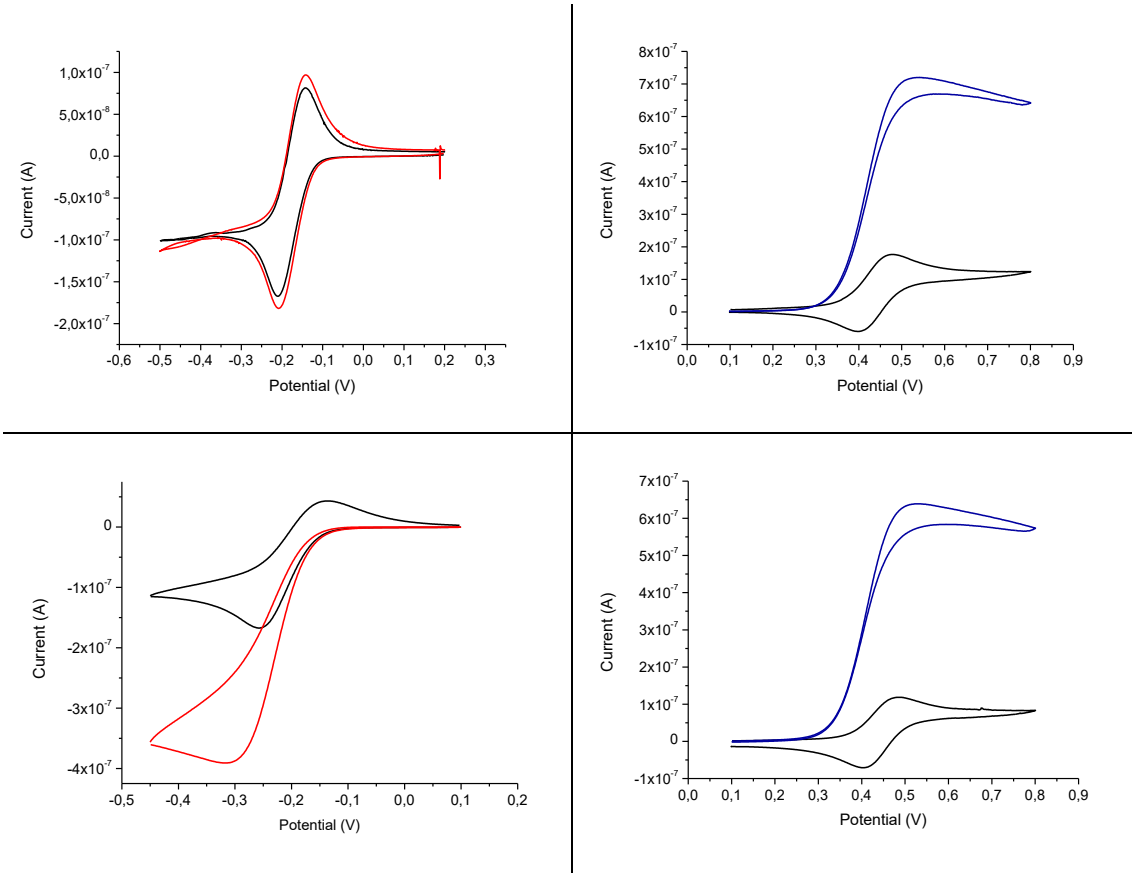

Sample 2A

Organic binder	Pigment	% Prot	% Oil
OIL	AZU + fish g.	0.5	46
Egg white (1:1)	CaCO3	3.1	0
Casein (1:1)	AZURITE	6.1	11
Egg yolk (1.5:1)	HgS	2.9	20
Glue (gelatin)	CaCO3	3.2	0
Whole egg (2:1)	AZURITE	5.9	25

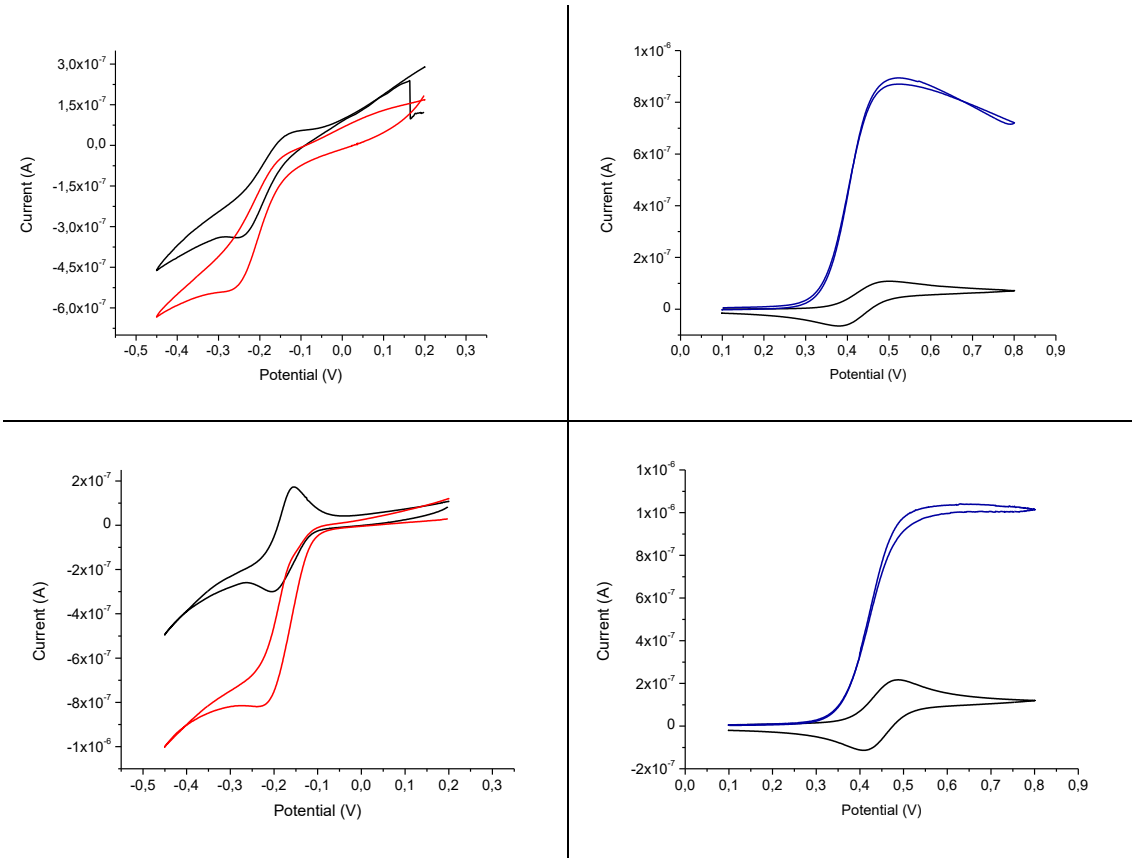

Sample 2B

Organic binder	Pigment	% Prot	% Oil
Egg white (1:1)	AZURITE	1.4	0
Casein (1:1)	HgS	11.1	22
Egg yolk (1.5:1)	CaCO3	5.2	36
Glue (gelatin)	AZURITE	2.7	0
Whole egg (2:1)	HgS	4.1	18

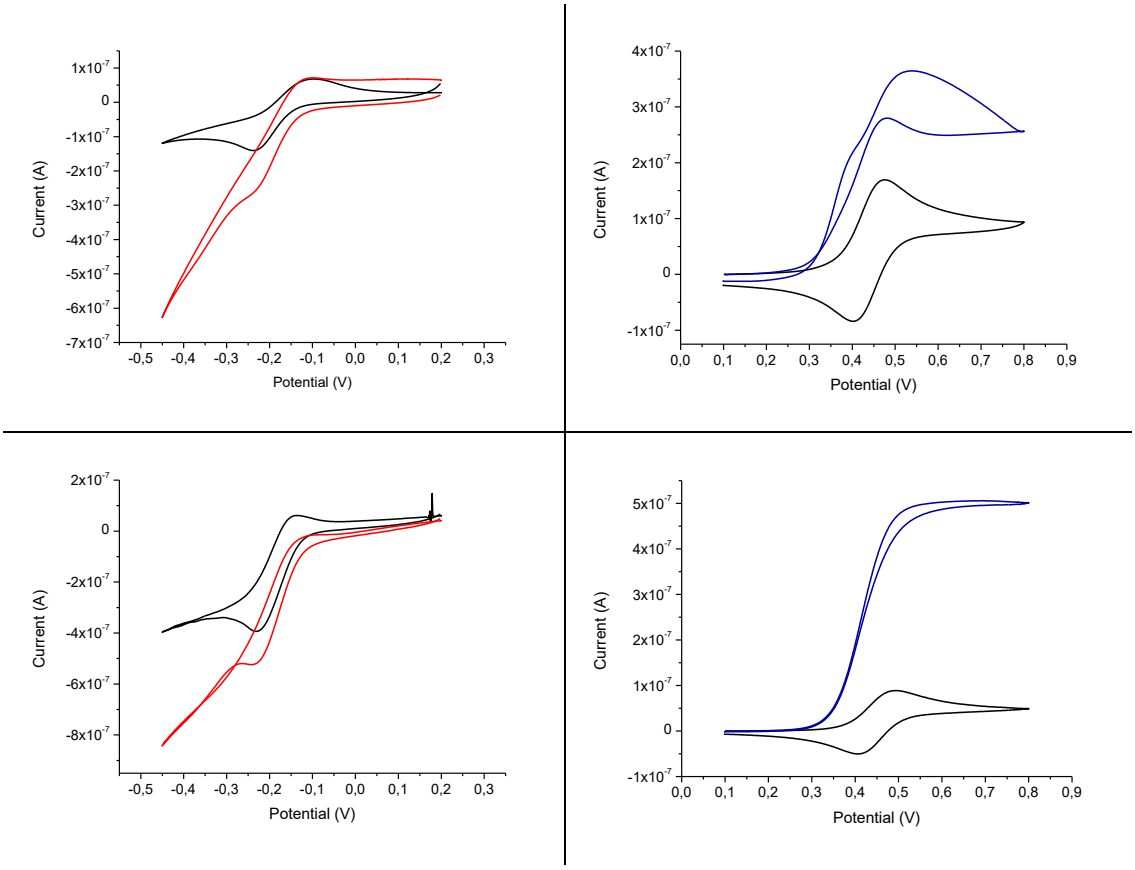

Sample 2C

Organic binder	Pigment	% Prot	% Oil
Egg white (1:1)	HgS	1.9	0
Casein (1:1)	CaCO3	11.6	22
Egg yolk (1.5:1)	AZURITE	2.8	19
Glue (gelatin)	HgS	1.5	0
Whole egg (2:1)	CaCO3	9.1	37

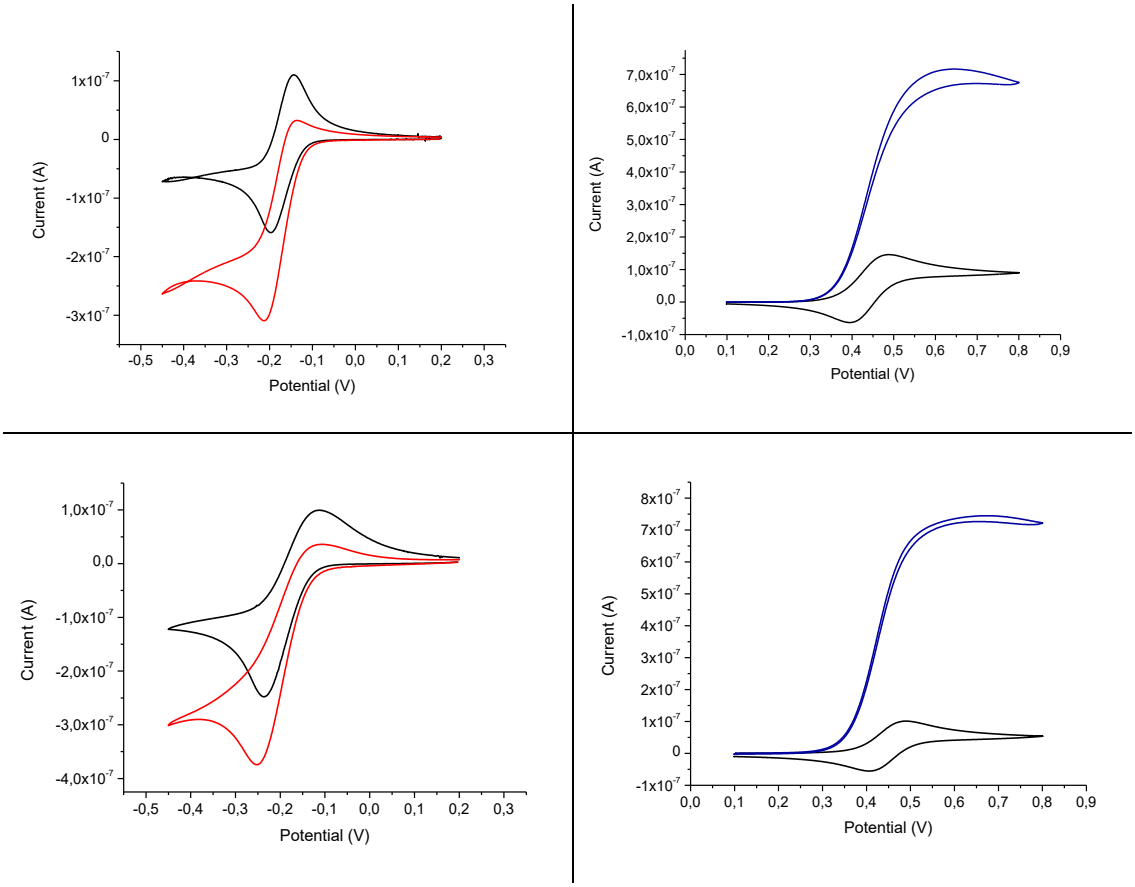

Sample 3A

Organic binder	Pigment	% Prot	% Oil
OIL	AZU + beef g.	0.6	48
Egg white (4:1)	CaCO3	5	50
Casein (1:5)	AZURITE	2.2	0
Egg yolk (1:1)	HgS	3.3	33
Glue (beef)	CaCO3	8.3	29
Whole egg (1:1)	AZURITE	5.5	35

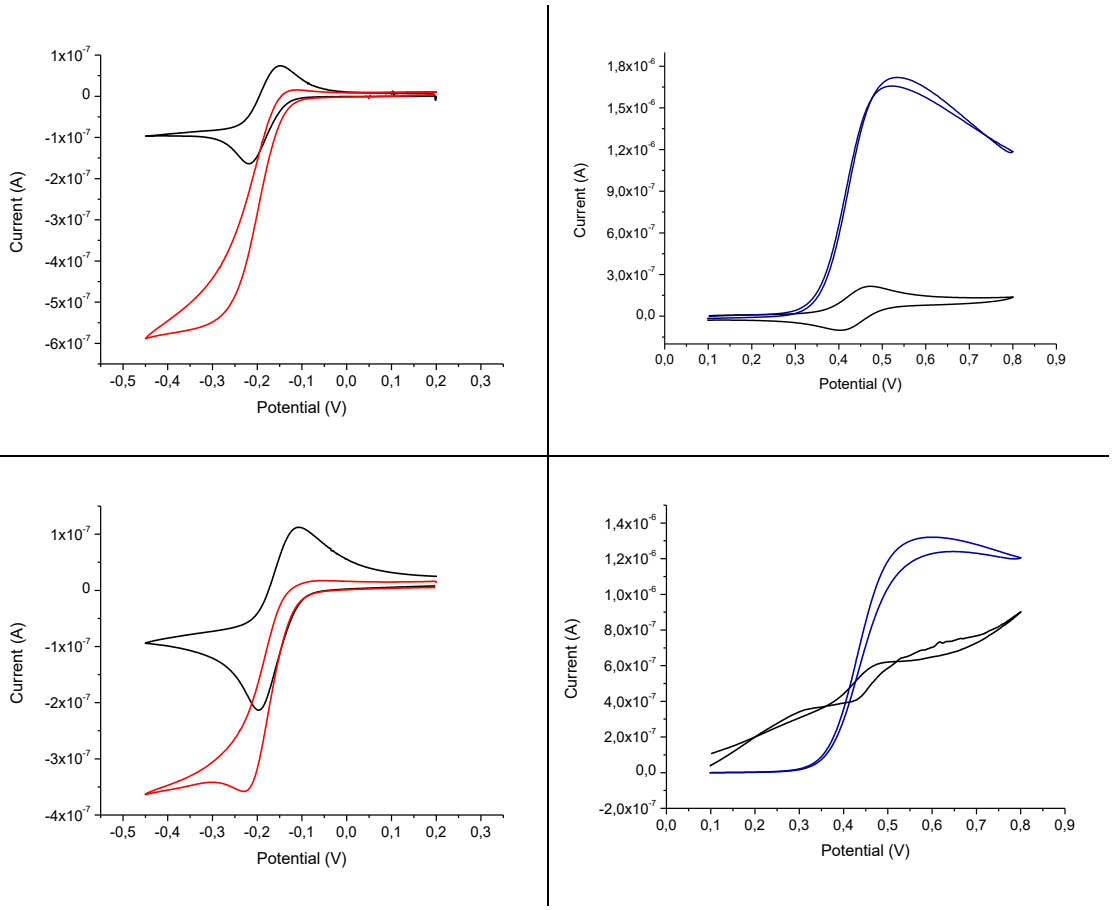

Sample 3B

Organic binder	Pigment	% Prot	% Oil
Egg white (4:1)	AZURITE	2.8	0
Casein (1:5)	HgS	2	31
Egg yolk (1:1)	CaCO3	5.4	47
Glue (beef)	AZURITE	3.9	0
Whole egg (1:1)	HgS	5,8	36

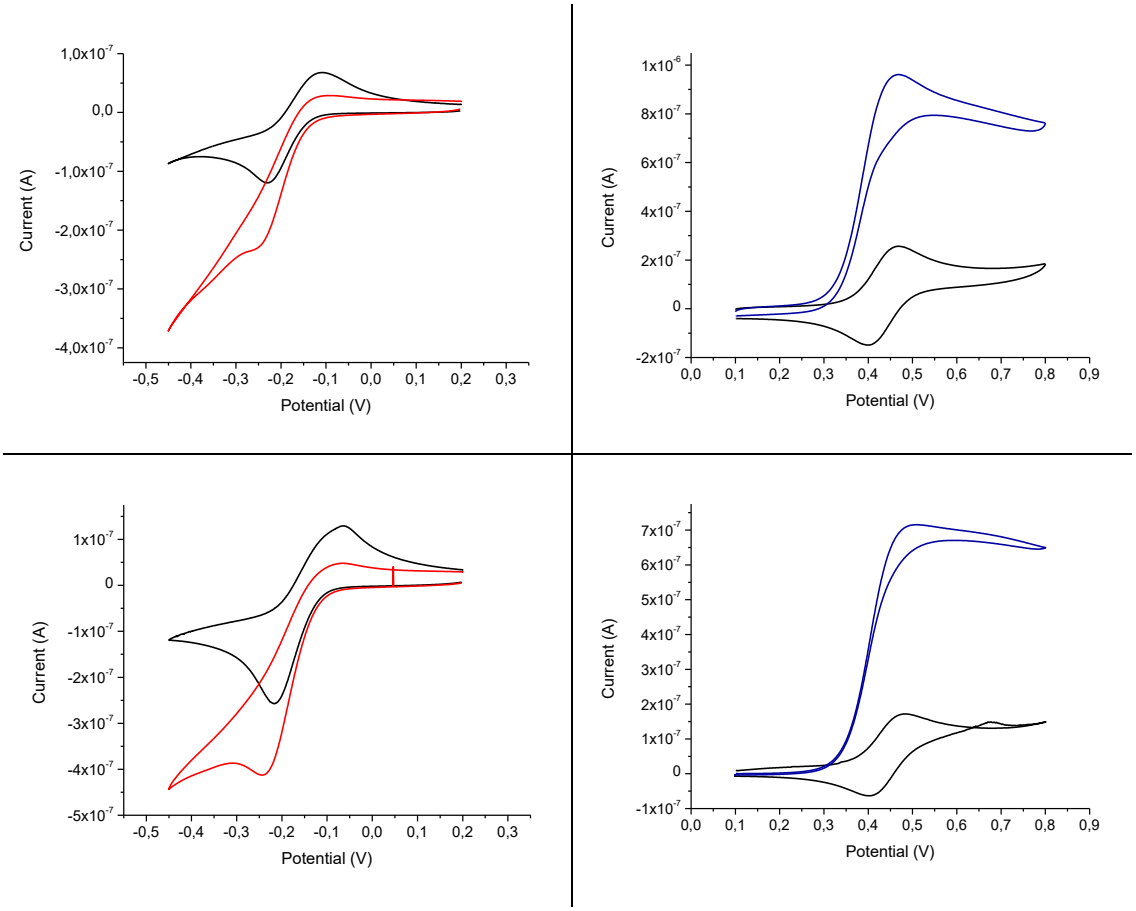

Sample 3C

Organic binder	Pigment	% Prot	% Oil
Egg white (4:1)	HgS	2.9	0
Casein (1:5)	CaCO3	4.3	65
Egg yolk (1:1)	AZURITE	3.2	28
Glue (beef)	HgS	2	0
Whole egg (1:1)	CaCO3	12	59

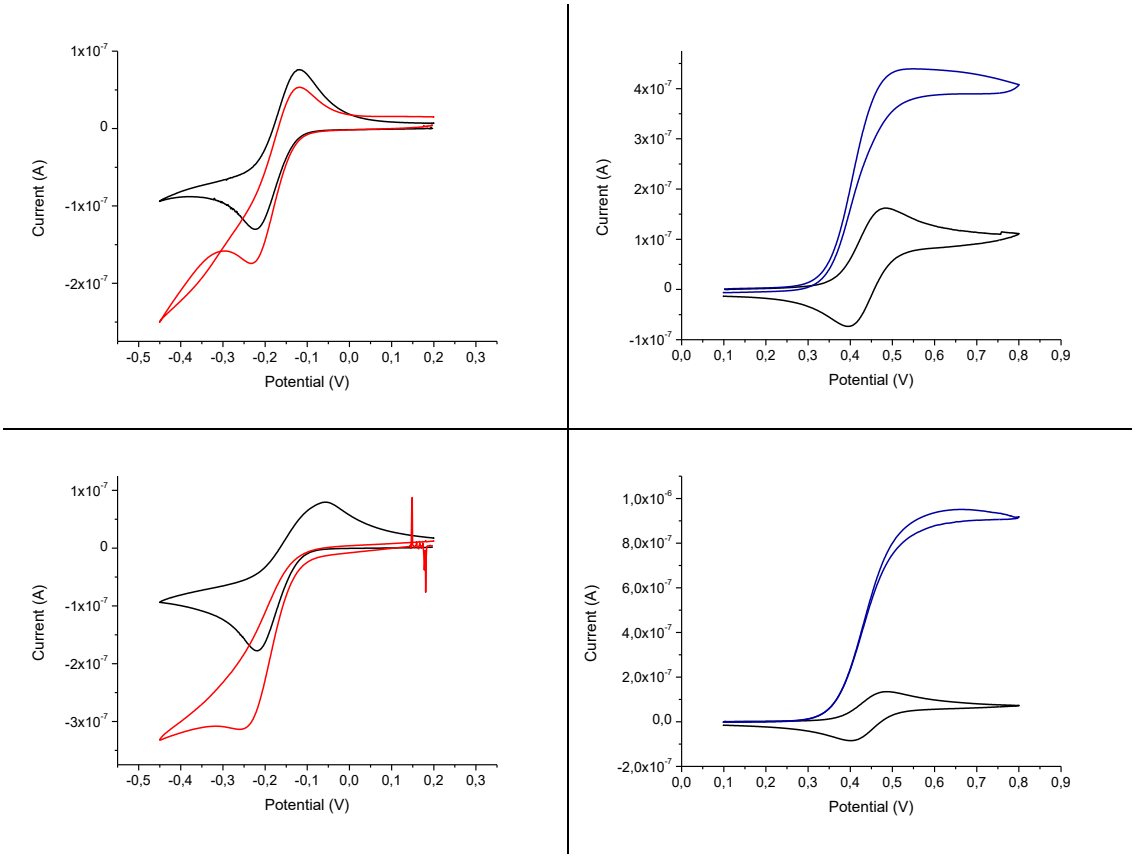

Sample 4A

Organic binder	Pigment	% Prot	% Oil
OIL	AZU + egg white	1	52
Egg white (1:10)	CaCO3	0.6	0
Casein (1:10)	AZURITE	0.7	48
Egg yolk (1:2)	HgS	**2.2**	30
Glue (fish)	CaCO3	6.9	0
Whole egg (1:2)	AZURITE	5.8	51

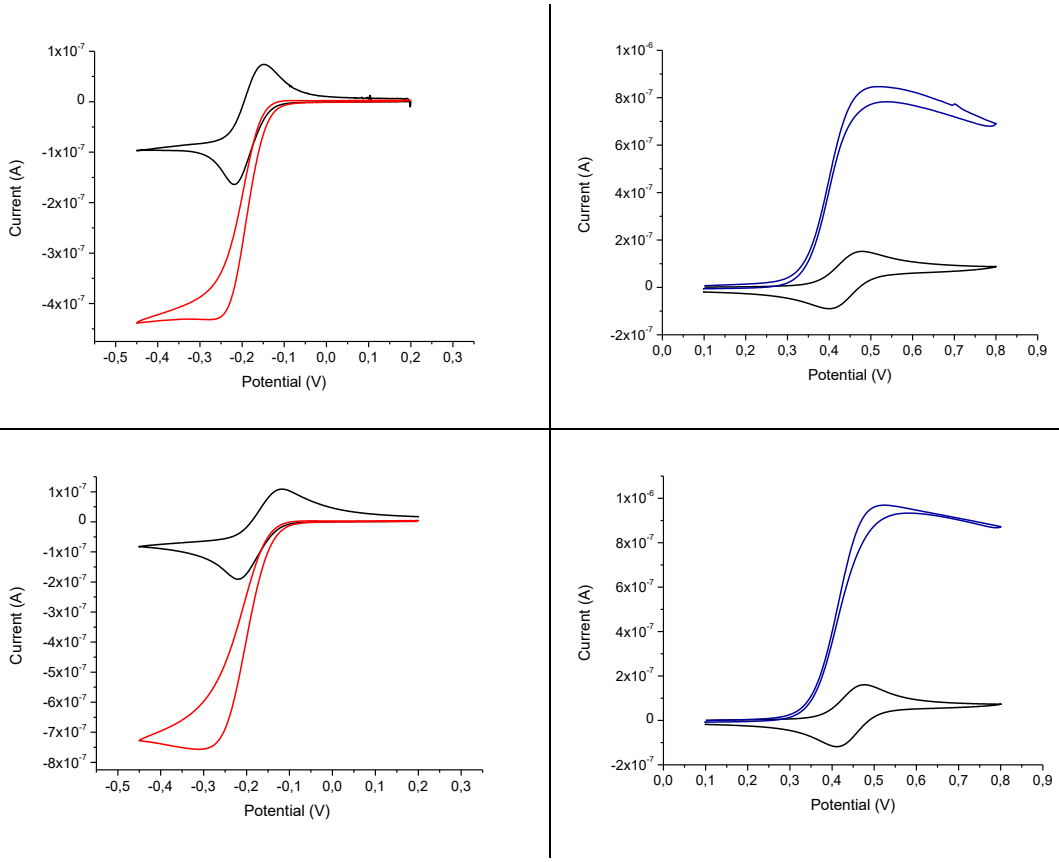

Sample 4B

Organic binder	Pigment	% Prot	% Oil
Egg white (1:10)	AZURITE	**0.4**	0
Casein (1:10)	HgS	0.6	41
Egg yolk (1:2)	CaCO3	3.3	45
Glue (fish)	AZURITE	4.6	0
Whole egg (1:2)	HgS	**3.3**	36

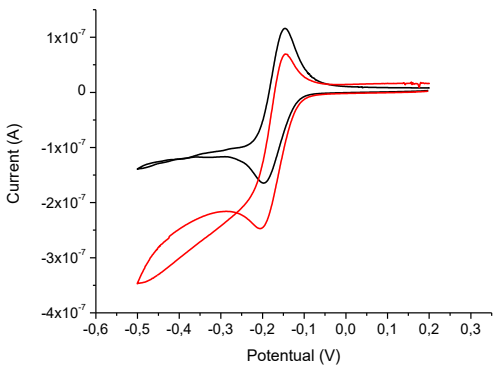

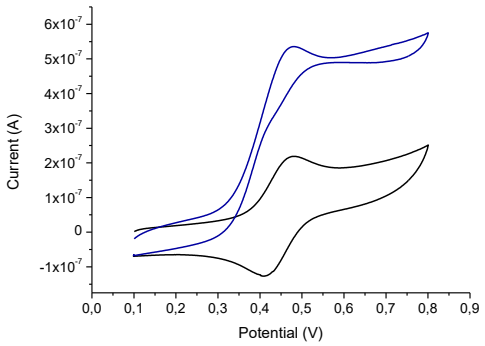

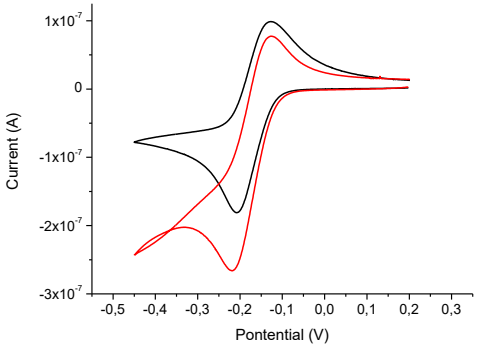

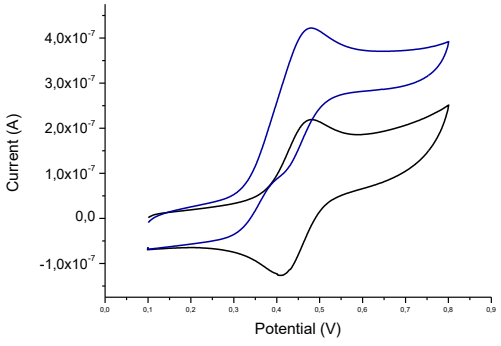

Sample 4C

Organic binder	Pigment	% Prot	% Oil
Egg white (1:10)	HgS	**0.4**	0
Casein (1:10)	CaCO3	1.1	77
Egg yolk (1:2)	AZURITE	2.6	37
Glue (fish)	HgS	1.6	0
Whole egg (1:2)	CaCO3	11	0.69